2006

Structural and functional studies on SNAREs-mediated membrane fusion

Yong Chen
Iowa State University

Structural and functional studies on SNAREs-mediated membrane fusion

by

Yong Chen

A dissertation submitted to the graduate faculty

in partial fulfillment of the requirements for the degree of

DOCTOR OF PHILOSOPHY

Major: Biophysics

Program of Study Committee:
Yeon-Kyun Shin (Major Professor)
Herbert Fromm
Richard Honzatko
Amy Andreotti
Diane Bassham

Iowa State University

Ames, Iowa

2006

UMI Number: 3243567

ProQuest Information and Learning Company
300 North Zeeb Road
P.O. Box 1346
Ann Arbor, MI 48106-1346

TABLE OF CONTENTS

LIST OF FIGURES

CHAPTER 1: INTRODUCTION

CHAPTER 2: PROBING DOMAIN SWAPPING FOR THE NEURONAL SNARE COMPLEX WITH ELECTRON PARAMAGNETIC RESONANCE

CHAPTER 3: CONSTITUTIVE VERSUS REGULATED SNARE ASSEMBLY: A STRUCTURAL BASIS

CHAPTER 4: YKT6 IS A CORE CONSTITUENT OF MEMBRANE FUSION MACHINERIES AT THE ARABIDOPSIS TRANS-GOLGI NETWORK

LIST OF TABLES

ABSTRACT

Membrane fusion is an essential biological process for vesicle trafficking in eukaryotic cells. Soluble N-ethylmaleimide-sensitive factor attachment protein receptors (SNAREs) are a family of proteins that have been recognized as key components of protein complexes that drive membrane fusion. The SNARE proteins localized in opposite membranes form a SNARE complex, which bridges the two membranes into close proximity and promotes fusion. Despite considerable sequence divergence among SNARE proteins, this fusion machinery is conserved structurally, mechanistically and evolutionally from yeast to human.

Site-directed spin labeling (SDSL) and electron paramagnetic resonance (EPR) are well established techniques to study the structures of membrane proteins. Fluorescent labeled lipids allow us to test the function of SNARE proteins by lipid mixing assay. With these techniques, we are able to study the structures and functions of SNAREs in vitro. In this dissertation, three sets of SNARE proteins coming from yeast, plant and mammalian sources have been investigated. The information gathered from these systems will help to understand the molecular mechanism of SNARE-induced membrane fusion.

CHAPTER 1: INTRODUCTION

One important feature of eukaryotic cells is the presence of biochemically distinct intracellular organelles. Exchanges and communications among these membrane-enclosed compartments, or to and from the cell surface, are mediated by trafficking vesicles. Membrane-bound transport vesicles carry cargos from one compartment to another, and discharge them into a specific space by fusing with the target membrane. However, the fusion of two membranes does not occur spontaneously because of the extraordinary stability of the lipid bilayer structure. In eukaryotic cells, soluble *N*-ethylmaleimide-sensitive factor attachment protein receptors (SNAREs) are generally accepted to be the central players of the cellular fusion machinery (Brunger, 2001; Chen and Scheller, 2001; Jahn et al., 2003; Jahn and Scheller, 2006; Rizo and Sudhof, 2002). There are remarkable sequence similarities among SNARE families, implying conserved functions of these proteins (Weimbs et al., 1997). Generally, the SNARE molecules share a highly conserved coiled-coil domain called the SNARE motif composed of 60-70 amino acids, and are anchored to the membrane by a C-terminal hydrophobic transmembrane domain (TMD) or post-translational lipid attachment (Figure 1-1). Functionally, SNARE proteins can be classified into vesicle associated (v-) SNAREs and target membrane (t-) SNAREs. The v-SNARE must interact with the cognate target membrane SNARE (t-SNARE) to form a SNARE complex (McNew et al., 2000), which brings the two membranes into close proximity, merging them into one continuous bilayer (Weber et al., 1998). The objective of this research is to investigate the structure and function of SNARE proteins during liposome

fusion. The study focused on SNARE proteins from mammalian (*Rattus norvegicus*) sources, plant (*Arabidopsis thaliana*) sources and yeast (*Saccharomyces cerevisiae*) sources, respectively.

1.1 Mammalian SNARE Proteins

At least 36 SNARE genes have been identified and expressed in mammalian species and the major features of the human SNAREs are summarized in Table 1-1 (Bock et al., 2001; Hong, 2005). The most well represented ones are the synaptic SNAREs, including the synaptic vesicle protein synaptobrevin-2 (also referred to vesicle-associated membrane protein 2 or VAMP2), the presynaptic plasma membrane protein syntaxin-1A and SNAP-25 (synaptosome-associated protein of molecular weight 25kD) (Sollner et al., 1993a; Sollner et al., 1993b). They are involved in neurotransmitter release in neuroendocrine cells (Figure 1-2). Synaptobrevin-2 and syntaxin-1A are membrane integral proteins. They contain a single transmembrane domain at the C-terminus and one SNARE motif in the membrane proximal region. SNAP-25 contains two SNARE motifs at both N-terminus and C-terminus with a linker loop in between. Although SNAP-25 does not have a transmembrane domain, it associates with the plasma membrane through post-translational lipid modification on the cysteines in the linker region. These three proteins are able to form ternary complexes with 1:1:1 stoichiometry, called SNARE complexes. The formation of SNARE complexes is required for synaptic vesicle fusion with the plasma membrane and consequent release of neurotransmitters (Broadie et al., 1995; Hayashi et al., 1994; Niemann et al., 1994). The minimal interacting region of SNARE complexes (the soluble core fusion complex region)

has been identified (Chapman et al., 1994; Hayashi et al., 1994; Kee et al., 1995; Poirier et al., 1998a) and the structure of this core region has been solved by electron paramagnetic resonance (EPR) and x-ray crystallography (Poirier et al., 1998b; Sutton et al., 1998). In the core complex, one SNARE motif from v-SNARE (synaptobrevin-2) and three SNARE motifs from t-SNAREs (one from syntaxin-1A and two from SNAP-25) assemble into a parallel four-helix bundle composed of 15 hydrophobic layers and a central ionic '0' layer (Figure 1-3). These three proteins are sufficient to promote vesicle fusion *in vitro* and thought to be the minimal fusion machinery (Weber et al., 1998).

1.2 Yeast SNARE Proteins

Genome analyses suggest 25 SNAREs are present in yeast (Burri and Lithgow, 2004; Hong, 2005). The best characterized SNAREs in yeast include Snc2p, Sso1p and Sec9. They are involved in post-Golgi vesicle trafficking toward the plasma membrane (Figure 1-2). Snc2p is the v-SNARE protein localized on secretory vesicles; it is the yeast homologue of synaptobrevin-2 in neuron (Protopopov et al., 1993). Sso1p and Sec9 are the t-SNAREs residing on the plasma membrane; they are counterparts of neuronal syntaxin-1A and SNAP-25, respectively (Aalto et al., 1993; Brennwald et al., 1994). Snc2p, Sso1p and Sec9 form a four helical bundle SNARE complex, similar to their neuronal homologues (Fiebig et al., 1999). Despite the similarity of the two SNARE complexes, yeast SNAREs may function differently with neuronal SNAREs. For example, yeast vesicles' trafficking seems to be active constitutively (Lew and Simon, 1991), while neuronal transmitter release is tightly controlled and primarily triggered by the Ca^{2+} signal (Chen et al., 1999).

1.3 Plant SNARE Proteins

The *Arabidopsis* genome encodes 54 predicted SNARE proteins based on sequence homology to yeast and mammalian SNAREs (Sanderfoot et al., 2000; Uemura et al., 2004). Previously, it was shown that SYP41 (the plant analog of neuronal syntaxin) resides in the *trans*-Golgi network (TGN), and interacts with two other TGN SNAREs, VTI12 and SYP61 (Bassham et al., 2000; Sanderfoot et al., 2001a). However, these three proteins may not simply function together as a SNARE complex to cause membrane fusion (Sanderfoot et al., 2001b; Surpin et al., 2003; Zhu et al., 2002). YKTs are potential candidates to participate in the vesicle trafficking in TGN by forming a SNARE complex with appropriate SNARE proteins. In mammals and yeast, YKT 6 is a multifunctional SNARE protein, and has been proposed to participate in the recycling from endosomes to the TGN (Dilcher et al., 2001; Tai et al., 2004). There are two homologues of YKT6 in *Arabidopsis*, YKT61 and YKT62.

1.4 SNARE Complex Assembly and Membrane Fusion

The hallmark of SNARE assembly is the formation of a four-helical bundle core complex. Many SNARE proteins have N-terminal domains besides the SNARE motifs. For example, syntaxin-1A and Sso1p have N-terminal H_{abc} domains which form three-helical bundles (Fernandez et al., 1998; Lerman et al., 2000; Munson et al., 2000). These folded domains interact intramolecularly with their SNARE motifs, and inhibit SNARE assembly by adopting a ‘closed’ conformation. An ‘open’ conformation must be achieved to form a binary complex (Figure 1-4). Another case is mammalian YKT6, which has a profilin-like

N-terminal domain that is necessary for proper compartmental localization (Hasegawa et al., 2003).

The formation of SNARE complexes is accompanied by significant conformational changes (Fasshauer et al., 1997a; Fasshauer et al., 1997b; Sutton et al., 1998). The core complexes' formation starts from the assembly of *trans*-SNARE complexes, in which the v-SNARE and t-SNAREs residing on apposed membranes engage each other and bridge the two membranes (Figure 1-4). After membrane fusion, these *trans*-complexes are converted to *cis*-complexes, in which all of the SNARE proteins are associated with the same membrane. In the case of neurotransmitter release, the *cis*-SNARE complexes are extremely stable and their disassembly requires specialized chaperons NSF (*N*-ethylmaleimide sensitive factor) and SNAP (soluble NSF attachment protein) (Fasshauer et al., 2002). The zippering model proposed that the *trans*-SNARE complexes zippered from the membrane distal terminus toward the membrane proximal terminus (Chen et al., 2001; Melia et al., 2002; Xu et al., 1999). The parallel arrangement of SNARE motifs within complexes brings their transmembrane anchors, and the two membranes, into close proximity (Hanson et al., 1997). The high stability of *cis*-SNARE complexes suggested that the SNARE complex assembly is also associated with energy release, which might provide the force to overcome the energy barrier for lipid mixing (Poirier et al., 1998a; Sutton et al., 1998).

Each membrane is composed of two monolayers (leaflets) and their mixing can pass through two different pathways, the direct fusion pathway and the fusion-through-hemifusion pathway (Chernomordik and Kozlov, 2005; Jackson and Chapman, 2006). The direct fusion model assumes that membrane fusion is initiated by protein-lined pores, which form hemichannel structures on both sides of the apposed membranes. Two hemichannels

combine together to form a fusion pore that connects two lipid bilayers, allowing lipids and contents exchange. In this model, both leaflets of the membranes mix at the same time. The fusion-through-hemifusion pathway proposes a sequential merging of the membranes. First, the two outer leaflets merge together with the inner leaflets intact, forming a lipid stalk intermediate called a hemifusion state. Then, the inner leaflets start to mix and lead to the formation of a fusion pore. The fusion of two membranes results in the mixing of the lipid and protein components residing in membranes, as well as the mixing of the contents initially bound by those bilayers (Figure 1-5).

Site-directed spin labeling (SDSL) and electron paramagnetic resonance (EPR) spectroscopy are established techniques for investigation of structures and topologies of membrane associated proteins in the phospholipids bilayer (Figure 1-6). In this method, native amino acid residues are substituted with cysteines and subsequently modified with a MTSL nitroxide spin label. Distances between pairs of nitroxides in the range of 7-25 Å can be determined by analyzing the electron-electron dipolar interaction. Nitroxide-scanning EPR utilizes the power saturation method to yield information on the secondary structure and topology of membrane-bound proteins such as SNAREs.

The lipids mixing assay is a powerful tool to study membrane fusion. This method is based on the dequenching of two fluorescent dyes (NBD and Rhodamine) labeled on the head group of phospholipids (Figure 1-7). When these two dye-labeled lipids are put into a lipid vesicle together and excited with the donor (NBD) wavelength, the emission of NBD will be quenched by acceptor (Rhodamine) and the emission of Rhodamine will be observed. After fusion with non-fluorescent vesicles, dequenching occurs due to the dilution of the dyes in the membrane, which increases the emission of NBD. Thus, by monitoring the

fluorescence intensity of NBD during the liposome fusion, we are able to track SNARE-induced lipid mixing in real time. Also, by selectively reducing the donor (NBD) to a non-fluorescent ABD, we can separate the inner and outer leaflets mixing (McIntyre and Sleight, 1991).

1.5 References

Aalto, M.K., Ronne, H., and Keranen, S. (1993). Yeast syntaxins Sso1p and Sso2p belong to a family of related membrane proteins that function in vesicular transport. EMBO J *12*, 4095-4104.

Bassham, D.C., Sanderfoot, A.A., Kovaleva, V., Zheng, H., and Raikhel, N.V. (2000). AtVPS45 complex formation at the trans-Golgi network. Mol Biol Cell *11*, 2251-2265.

Bock, J.B., Matern, H.T., Peden, A.A., and Scheller, R.H. (2001). A genomic perspective on membrane compartment organization. Nature *409*, 839-841.

Brennwald, P., Kearns, B., Champion, K., Keranen, S., Bankaitis, V., and Novick, P. (1994). Sec9 is a SNAP-25-like component of a yeast SNARE complex that may be the effector of Sec4 function in exocytosis. Cell *79*, 245-258.

Broadie, K., Prokop, A., Bellen, H.J., O'Kane, C.J., Schulze, K.L., and Sweeney, S.T. (1995). Syntaxin and synaptobrevin function downstream of vesicle docking in Drosophila. Neuron *15*, 663-673.

Brunger, A.T. (2001). Structure of proteins involved in synaptic vesicle fusion in neurons. Annu Rev Biophys Biomol Struct *30*, 157-171.

Burri, L., and Lithgow, T. (2004). A complete set of SNAREs in yeast. Traffic *5*, 45-52.

Chapman, E.R., An, S., Barton, N., and Jahn, R. (1994). SNAP-25, a t-SNARE which binds to both syntaxin and synaptobrevin via domains that may form coiled coils. J Biol Chem *269*, 27427-27432.

Chen, Y.A., Scales, S.J., Jagath, J.R., and Scheller, R.H. (2001). A discontinuous SNAP-25 C-terminal coil supports exocytosis. J Biol Chem *276*, 28503-28508.

Chen, Y.A., Scales, S.J., Patel, S.M., Doung, Y.C., and Scheller, R.H. (1999). SNARE complex formation is triggered by Ca2+ and drives membrane fusion. Cell *97*, 165-174.

Chen, Y.A., and Scheller, R.H. (2001). SNARE-mediated membrane fusion. Nat Rev Mol Cell Biol *2*, 98-106.

Chernomordik, L.V., and Kozlov, M.M. (2005). Membrane hemifusion: crossing a chasm in two leaps. Cell *123*, 375-382.

Dilcher, M., Kohler, B., and von Mollard, G.F. (2001). Genetic interactions with the yeast Q-SNARE VTI1 reveal novel functions for the R-SNARE YKT6. J Biol Chem *276*, 34537-34544.

Fasshauer, D., Antonin, W., Subramaniam, V., and Jahn, R. (2002). SNARE assembly and disassembly exhibit a pronounced hysteresis. Nat Struct Biol *9*, 144-151.

Fasshauer, D., Bruns, D., Shen, B., Jahn, R., and Brunger, A.T. (1997a). A structural change occurs upon binding of syntaxin to SNAP-25. J Biol Chem *272*, 4582-4590.

Fasshauer, D., Otto, H., Eliason, W.K., Jahn, R., and Brunger, A.T. (1997b). Structural changes are associated with soluble N-ethylmaleimide-sensitive fusion protein attachment protein receptor complex formation. J Biol Chem *272*, 28036-28041.

Fernandez, I., Ubach, J., Dulubova, I., Zhang, X., Sudhof, T.C., and Rizo, J. (1998). Three-dimensional structure of an evolutionarily conserved N-terminal domain of syntaxin 1A. Cell *94*, 841-849.

Fiebig, K.M., Rice, L.M., Pollock, E., and Brunger, A.T. (1999). Folding intermediates of SNARE complex assembly. Nat Struct Biol *6*, 117-123.

Hanson, P.I., Roth, R., Morisaki, H., Jahn, R., and Heuser, J.E. (1997). Structure and conformational changes in NSF and its membrane receptor complexes visualized by quick-freeze/deep-etch electron microscopy. Cell *90*, 523-535.

Hasegawa, H., Zinsser, S., Rhee, Y., Vik-Mo, E.O., Davanger, S., and Hay, J.C. (2003). Mammalian ykt6 is a neuronal SNARE targeted to a specialized compartment by its profilin-like amino terminal domain. Mol Biol Cell *14*, 698-720.

Hayashi, T., McMahon, H., Yamasaki, S., Binz, T., Hata, Y., Sudhof, T.C., and Niemann, H. (1994). Synaptic vesicle membrane fusion complex: action of clostridial neurotoxins on assembly. Embo J *13*, 5051-5061.

Hong, W. (2005). SNAREs and traffic. Biochim Biophys Acta *1744*, 120-144.

Jackson, M.B., and Chapman, E.R. (2006). Fusion Pores and Fusion Machines in Ca(2+)-Triggered Exocytosis. Annu Rev Biophys Biomol Struct *35*, 135-160.

Jahn, R., Lang, T., and Sudhof, T.C. (2003). Membrane fusion. Cell *112*, 519-533.

Jahn, R., and Scheller, R.H. (2006). SNAREs - engines for membrane fusion. Nat Rev Mol Cell Biol *7*, 631-643.

Kee, Y., Lin, R.C., Hsu, S.C., and Scheller, R.H. (1995). Distinct domains of syntaxin are required for synaptic vesicle fusion complex formation and dissociation. Neuron *14*, 991-998.

Lerman, J.C., Robblee, J., Fairman, R., and Hughson, F.M. (2000). Structural analysis of the neuronal SNARE protein syntaxin-1A. Biochemistry *39*, 8470-8479.

Lew, D.J., and Simon, S.M. (1991). Characterization of constitutive exocytosis in the yeast Saccharomyces cerevisiae. J Membr Biol *123*, 261-268.

McIntyre, J.C., and Sleight, R.G. (1991). Fluorescence assay for phospholipid membrane asymmetry. Biochemistry *30*, 11819-11827.

McNew, J.A., Parlati, F., Fukuda, R., Johnston, R.J., Paz, K., Paumet, F., Sollner, T.H., and Rothman, J.E. (2000). Compartmental specificity of cellular membrane fusion encoded in SNARE proteins. Nature *407*, 153-159.

Melia, T.J., Weber, T., McNew, J.A., Fisher, L.E., Johnston, R.J., Parlati, F., Mahal, L.K., Sollner, T.H., and Rothman, J.E. (2002). Regulation of membrane fusion by the membrane-proximal coil of the t-SNARE during zippering of SNAREpins. J Cell Biol *158*, 929-940.

Munson, M., Chen, X., Cocina, A.E., Schultz, S.M., and Hughson, F.M. (2000). Interactions within the yeast t-SNARE Sso1p that control SNARE complex assembly. Nat Struct Biol *7*, 894-902.

Niemann, H., Blasi, J., and Jahn, R. (1994). Clostridial neurotoxins: new tools for dissecting exocytosis. Trends Cell Biol *4*, 179-185.

Poirier, M.A., Hao, J.C., Malkus, P.N., Chan, C., Moore, M.F., King, D.S., and Bennett, M.K. (1998a). Protease resistance of syntaxin.SNAP-25.VAMP complexes. Implications for assembly and structure. J Biol Chem *273*, 11370-11377.

Poirier, M.A., Xiao, W., Macosko, J.C., Chan, C., Shin, Y.K., and Bennett, M.K. (1998b). The synaptic SNARE complex is a parallel four-stranded helical bundle. Nat Struct Biol *5*, 765-769.

Protopopov, V., Govindan, B., Novick, P., and Gerst, J.E. (1993). Homologs of the synaptobrevin/VAMP family of synaptic vesicle proteins function on the late secretory pathway in S. cerevisiae. Cell *74*, 855-861.

Rizo, J., and Sudhof, T.C. (2002). Snares and Munc18 in synaptic vesicle fusion. Nat Rev Neurosci *3*, 641-653.

Sanderfoot, A.A., Assaad, F.F., and Raikhel, N.V. (2000). The Arabidopsis genome. An abundance of soluble N-ethylmaleimide-sensitive factor adaptor protein receptors. Plant Physiol *124*, 1558-1569.

Sanderfoot, A.A., Kovaleva, V., Bassham, D.C., and Raikhel, N.V. (2001a). Interactions between syntaxins identify at least five SNARE complexes within the Golgi/prevacuolar system of the Arabidopsis cell. Mol Biol Cell *12*, 3733-3743.

Sanderfoot, A.A., Pilgrim, M., Adam, L., and Raikhel, N.V. (2001b). Disruption of individual members of Arabidopsis syntaxin gene families indicates each has essential functions. Plant Cell *13*, 659-666.

Sollner, T., Bennett, M.K., Whiteheart, S.W., Scheller, R.H., and Rothman, J.E. (1993a). A protein assembly-disassembly pathway in vitro that may correspond to sequential steps of synaptic vesicle docking, activation, and fusion. Cell *75*, 409-418.

Sollner, T., Whiteheart, S.W., Brunner, M., Erdjument-Bromage, H., Geromanos, S., Tempst, P., and Rothman, J.E. (1993b). SNAP receptors implicated in vesicle targeting and fusion. Nature *362*, 318-324.

Surpin, M., Zheng, H., Morita, M.T., Saito, C., Avila, E., Blakeslee, J.J., Bandyopadhyay, A., Kovaleva, V., Carter, D., Murphy, A.*, et al.* (2003). The VTI family of SNARE proteins is necessary for plant viability and mediates different protein transport pathways. Plant Cell *15*, 2885-2899.

Sutton, R.B., Fasshauer, D., Jahn, R., and Brunger, A.T. (1998). Crystal structure of a SNARE complex involved in synaptic exocytosis at 2.4 A resolution. Nature *395*, 347-353.

Tai, G., Lu, L., Wang, T.L., Tang, B.L., Goud, B., Johannes, L., and Hong, W. (2004). Participation of the syntaxin 5/Ykt6/GS28/GS15 SNARE complex in transport from the early/recycling endosome to the trans-Golgi network. Mol Biol Cell *15*, 4011-4022.

Uemura, T., Ueda, T., Ohniwa, R.L., Nakano, A., Takeyasu, K., and Sato, M.H. (2004). Systematic analysis of SNARE molecules in Arabidopsis: dissection of the post-Golgi network in plant cells. Cell Struct Funct *29*, 49-65.

Weber, T., Zemelman, B.V., McNew, J.A., Westermann, B., Gmachl, M., Parlati, F., Sollner, T.H., and Rothman, J.E. (1998). SNAREpins: minimal machinery for membrane fusion. Cell *92*, 759-772.

Weimbs, T., Low, S.H., Chapin, S.J., Mostov, K.E., Bucher, P., and Hofmann, K. (1997). A conserved domain is present in different families of vesicular fusion proteins: a new superfamily. Proc Natl Acad Sci U S A *94*, 3046-3051.

Xu, T., Rammner, B., Margittai, M., Artalejo, A.R., Neher, E., and Jahn, R. (1999). Inhibition of SNARE complex assembly differentially affects kinetic components of exocytosis. Cell *99*, 713-722.

Zhu, J., Gong, Z., Zhang, C., Song, C.P., Damsz, B., Inan, G., Koiwa, H., Zhu, J.K., Hasegawa, P.M., and Bressan, R.A. (2002). OSM1/SYP61: a syntaxin protein in Arabidopsis controls abscisic acid-mediated and non-abscisic acid-mediated responses to abiotic stress. Plant Cell *14*, 3009-3028.

1.6 Figures and Captions

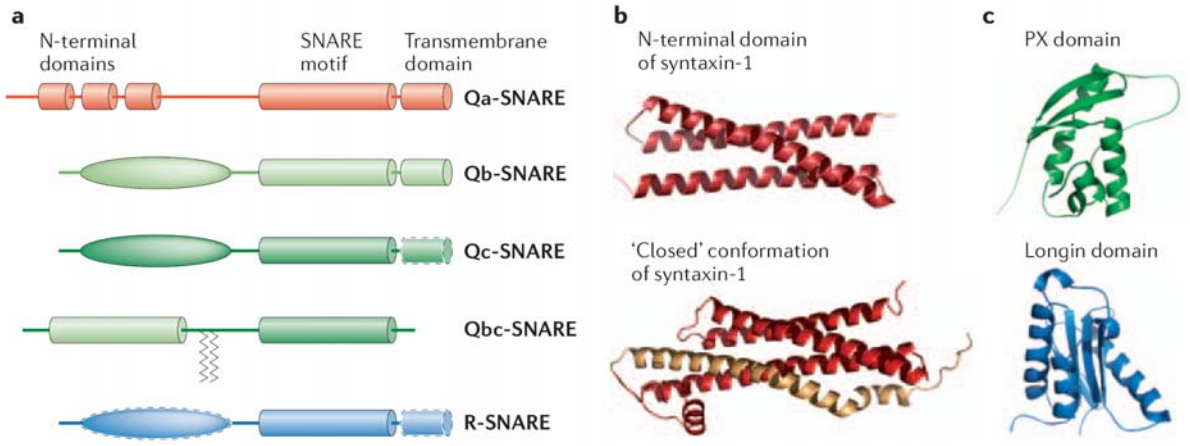

Figure 1-1. The general structures of different SNAREs.[1]

(a). The domain structure of the SNARE subfamilies. Dashed domain borders highlight domains that are missing in some subfamily members. Qa-SNAREs have N-terminal antiparallel three-helix bundles. The various N-terminal domains of Qb-, Qc- and R-SNAREs are represented by a basic oval shape. Qbc-SNAREs represent a small subfamily of SNAREs — the SNAP-25 subfamily — that contain one Qb-SNARE motif and one Qc-SNARE motif. These motifs are connected by a linker that is frequently palmitoylated (zig-zag lines in the figure). Qa-SNARE is shown in red; Qb-SNARE is in light green; Qc-SNARE is in dark green; and R-SNARE is in blue.

(b). The upper panel shows the three-dimensional structure of the isolated N-terminal domain of syntaxin-1. This structure is an N-terminal three-helix bundle that is typical of Qa-SNAREs, as well as of some Qb- and Qc-SNAREs. The lower panel shows the 'closed' conformation of syntaxin-1, in which the N-terminal domain of syntaxin-1 (red, as in the upper panel) is associated with part of its

[1] Jahn, R., and Scheller, R.H. (2006). SNAREs - engines for membrane fusion. Nat Rev Mol Cell Biol *7*, 631-643.

own SNARE motif (beige structure; absent in the upper panel). This structure was solved as part of the structure of the Munc18–syntaxin-1 complex.

(c). Three-dimensional structures of the N-terminal domains of other SNAREs, which exemplify the structural diversity that exists. The upper panel shows the Phox-homology (PX) domain of the Qc-SNARE Vam7, which seems to be unique for this particular SNARE. The lower panel shows the profilin or longin domain of the R-SNARE Ykt6.

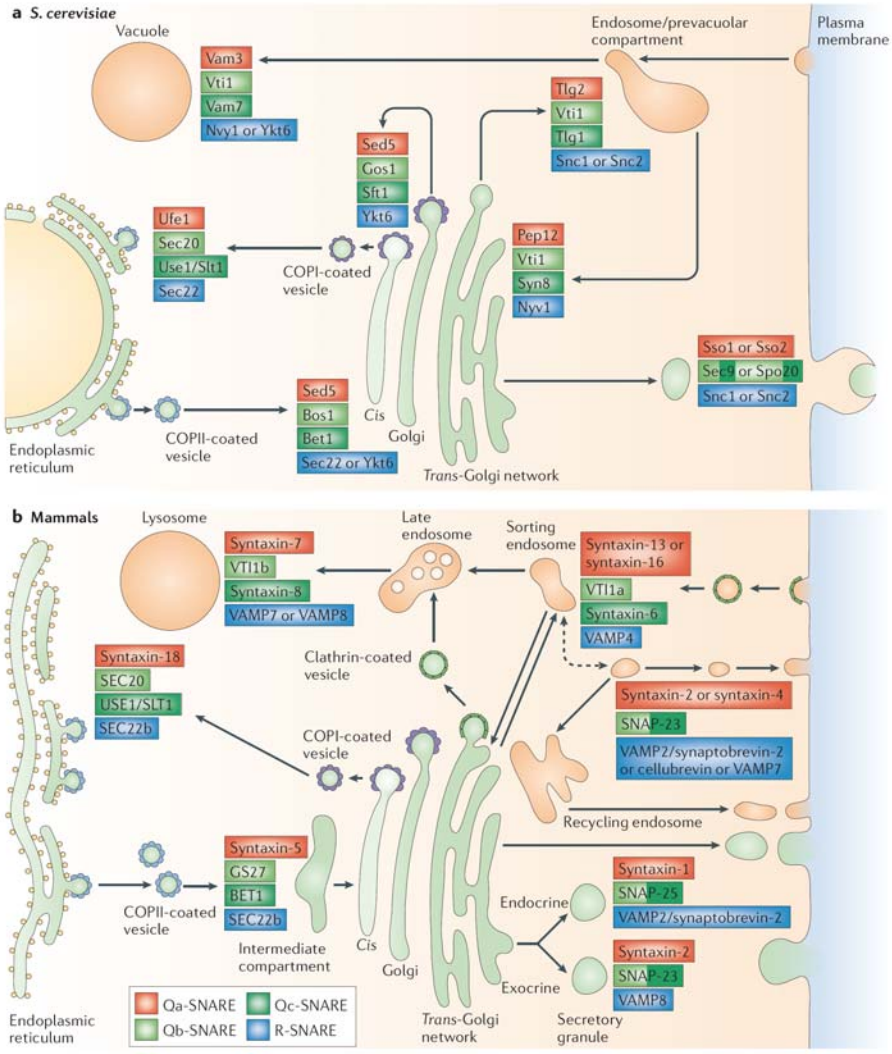

Figure 1-2. SNARE complexes in mammalian cells and yeast.[2]

(a). SNARE proteins in *Saccharomyces cerevisiae*. Snc1p, Sso1p and Sec9 can form a SNARE complex which is involved in the vesicle trafficking from the Golgi complex to the plasma membrane. Snc1 and Snc2, as well as Sso1 and Sso2, are homologous isoforms.

(b). SNAREs in mammalian cells. Synaptobrevin-2, Syntaxin-1 and SNAP-25 can form a SNARE complex that is involved in the neurotransmitter release by synaptic vesicle exocytosis.

---

[2] Jahn, R., and Scheller, R.H. (2006). SNAREs - engines for membrane fusion. Nat Rev Mol Cell Biol *7*, 631-643.

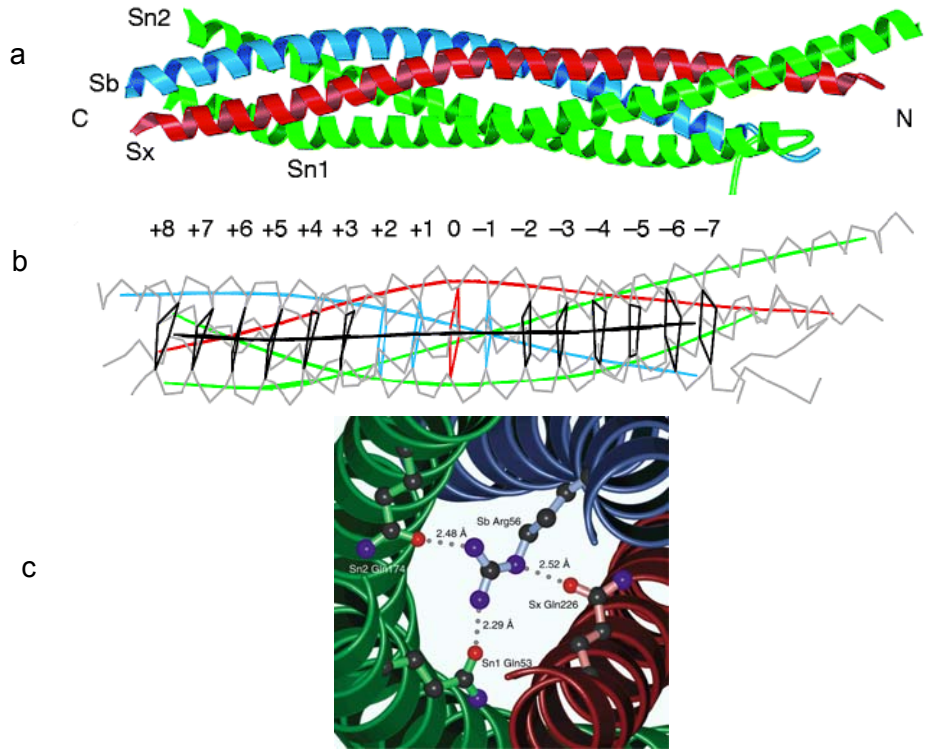

Figure 1-3. The crystal structure of neuronal SNARE complex.[3]

(a). Backbone ribbon drawing of the synaptic fusion complex. Synaptobrevin (Sb) is shown in blue; syntaxin-1 (Sx) is in red; and SNAP-25 (Sn1 and Sn2) is in green.

(b). Organization of the SNARE complex shows 15 hydrophobic layers and 1 ionic '0' layer.

(c). The structure of central ionic '0' layer.

[3] Sutton, R.B., Fasshauer, D., Jahn, R., and Brunger, A.T. (1998). Crystal structure of a SNARE complex involved in synaptic exocytosis at 2.4 A resolution. Nature *395*, 347-353.

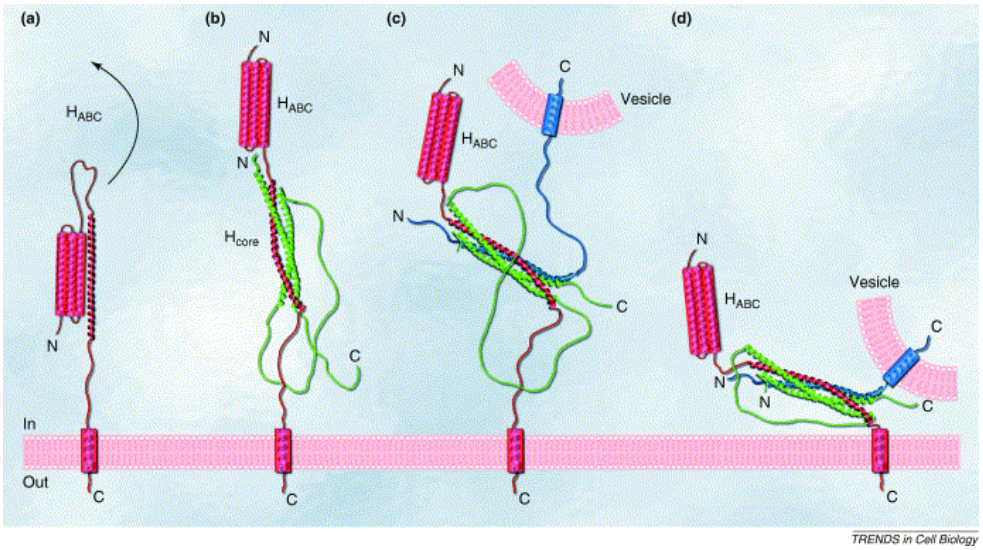

Figure 1-4. Different conformational states of the SNARE proteins assembly.[4]

(a). The N-terminal HABC domain of syntaxin 1 interacts with the H3 domain to fold into a 'closed' conformation unable to bind to SNAP 25 or synaptobrevin.

(b). The formation of the tertiary SNARE complex appears to be proceeded by a binary interaction of syntaxin 1 and SNAP 25.

(c, d). The tertiary SNARE complex is composed of four parallel helices: the syntaxin H3 domain, one coiled-coil domain from synaptobrevin and two from SNAP 25.

Color code: syntaxin 1, red; synaptobrevin, blue; SNAP 25, green.

[4] Toonen, R.F., and Verhage, M. (2003). Vesicle trafficking: pleasure and pain from SM genes. Trends Cell Biol *13*, 177-186.

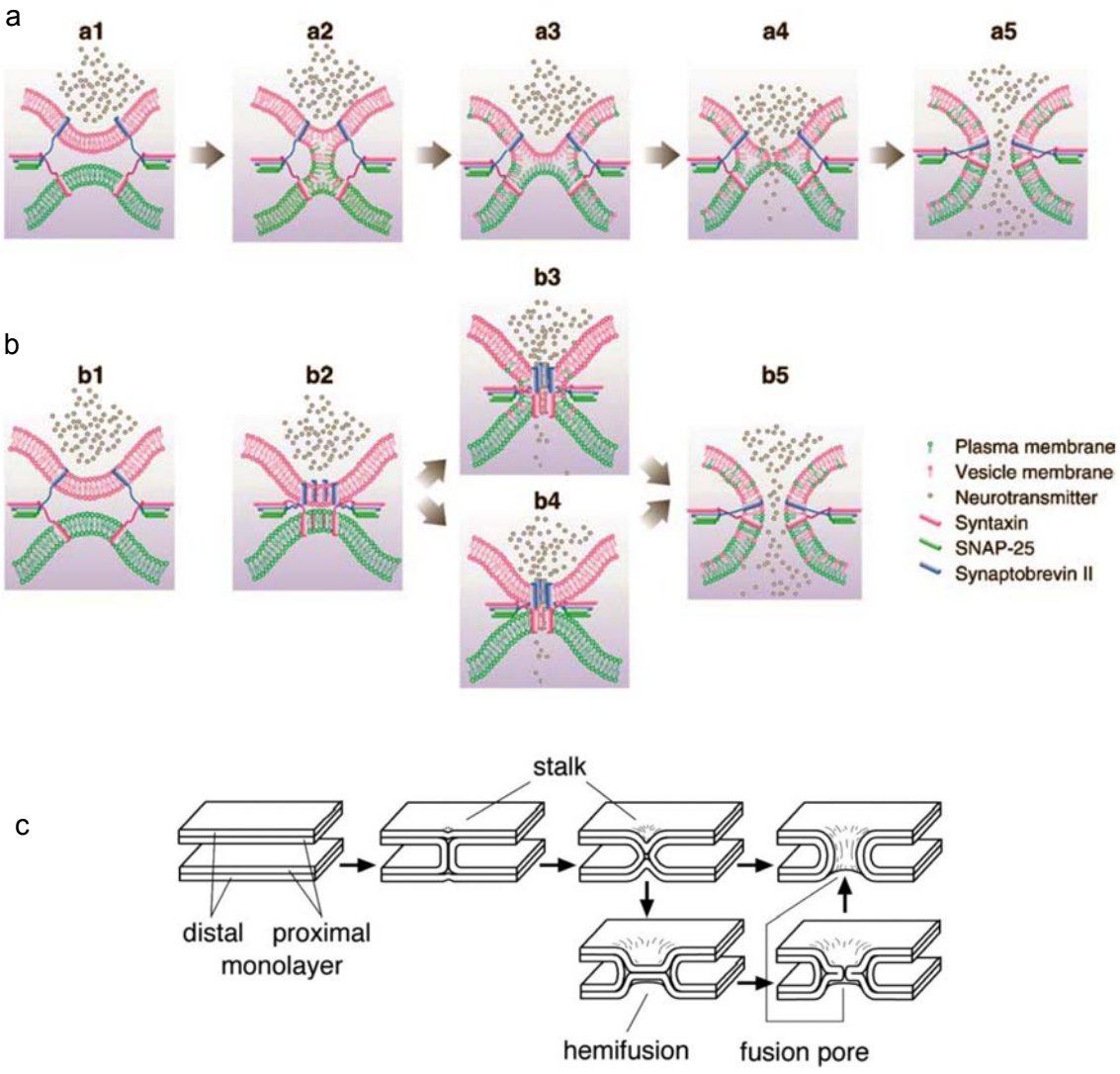

Figure 1-5. Two models of membrane fusion.[5,6]

(a). The fusion-through-hemifusion model shows a fusion pore lined by lipids.

(b). The direct fusion model shows a fusion pore formed from transmembrane domains of proteins.

(c). Transition states in membrane fusion.

---

[5] Jackson, M.B., and Chapman, E.R. (2006). Fusion Pores and Fusion Machines in Ca(2+)-Triggered Exocytosis. Annu Rev Biophys Biomol Struct *35*, 135-160.

[6] Jahn, R., Lang, T., and Sudhof, T.C. (2003). Membrane fusion. Cell *112*, 519-533.

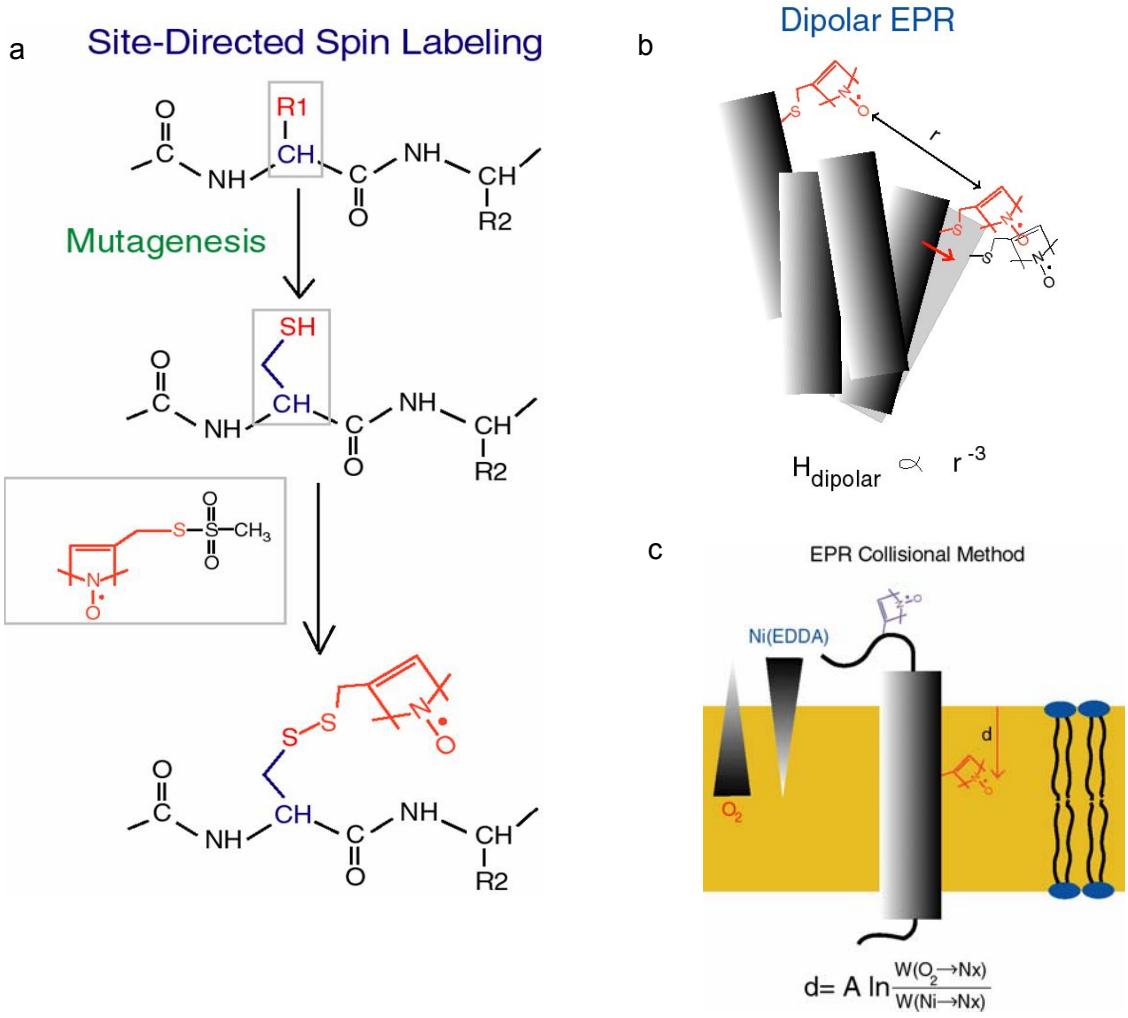

Figure 1-6. A Schematic description of site-directed spin labeling (SDSL) and electron paramagnetic resonance (EPR) spectroscopy.

(a). Spin labeling reaction.

(b). Dipolar interaction of spin labels.

(c). Spin label immersion depth measurement.

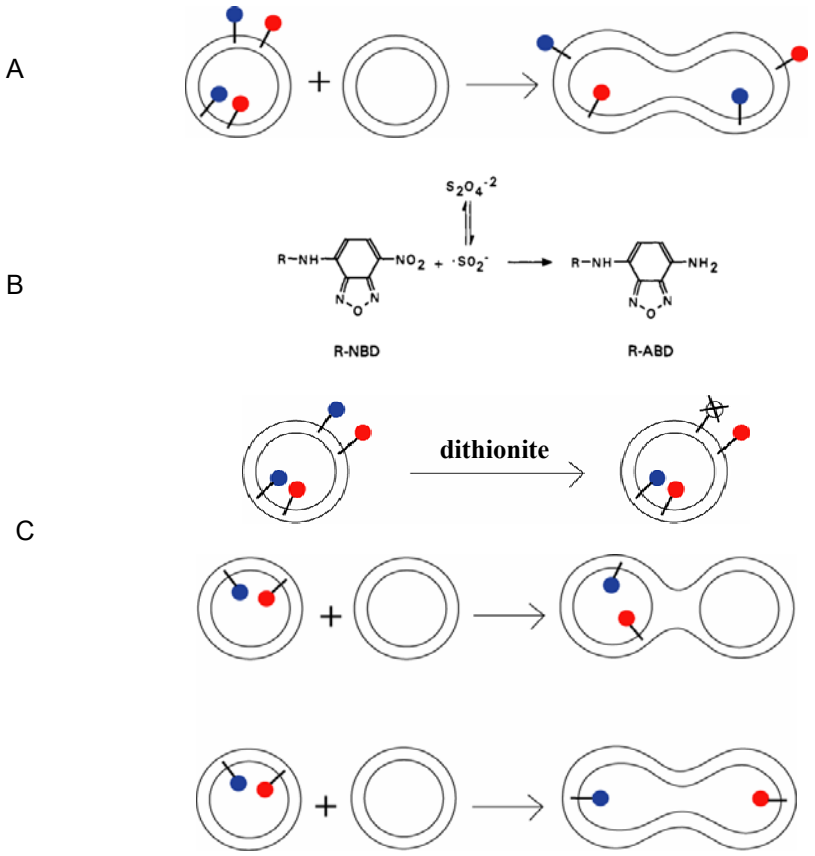

Figure 1-7. Lipid mixing assay based on fluorescence resonance energy transfer (FRET).

(a). The average spatial separation of the donor (NBD) and acceptor (Rhodamine) lipid probes increases upon fusion of labeled membranes with unlabeled membranes, resulting in decreased efficiency of proximity-dependent FRET, which is registered by increased donor fluorescence intensity and decreased acceptor fluorescence intensity.

(b). The NBD-labeled lipids can be reduced to ABD-labeled lipids with dithionite.

(c). By selectively reducing the NBD-labeled lipids in the outer leaflet, full fusion and hemi fusion can be distinguished experimentally.

1.7 Table

Table 1-1. List of human SNAREs and their properties.[7]

Name	Yeast homolog	Locations	AA	SNARE motif	TM domain	GenBank acc #	Synonyms	Type
Syntaxin1	Sso1p/Sso2p	PM	288	202-254	266-288	Q16623	HPC-1	Qa
Syntaxin2		PM	288	201-253	265-286	P32856	Epimorphin	Qa
Syntaxin3		PM	289	201-253	264-288	NM_004177		Qa
Syntaxin4		PM	297	210–262	274–296	Q12846		Qa
Syntaxin5	Sed5p	Go	301	219–271	280–301	U26648		Qa
Syntaxin6	Tlg1p	TGN, End	255	173–225	235–255	AJ002078		Qc
Syntaxin7	Pep12p	EE, LE	261	175–227	238–259	U77942		Qa
Syntaxin8	Syn8p	EE, LE	236	155–207	216–233	NP_004844		Qc
Syntaxin10		TGN	249	167–219	229–249	AF035531		Qc
Syntaxin11		TGN, LE	287	214–266	No	O75558		Qa
Syntaxin13		EE	276	188–240	251–273	NP_803173	Syntaxin12	Qa
Syntaxin16	Tlg2p	TGN	325	240–292	302–322	NP_001001433		Qa
Syntaxin17		ER	302	172–224	230–250	NP_060389		Qa
Syntaxin18	Ufe1p	ER	335	253–305	314–330	Q9P2W9		Qa
SNAP-23	Sec9p	PM	211	24–76, 156–208	No	NP_003816	Syndet	Qb, Qc
SNAP-25	Spo20p	PM	206	29–81, 150–202	No	NP_003072		Qb, Qc
SNAP-29		Go, End	258	60–112, 206–258	No	O95721	GS32	Qb, Qc
VAMP1		SV	118	34–86	97–117	P23763	Synaptobrevin1	R
VAMP2	Snc1p/Snc2p	SV	116	32–84	95–114	NP_055047	Synaptobrevin2	R
VAMP3		EE, RE	100	15–67	78–98	NP_004772	Cellubrevin	R
VAMP4		TGN, EE	141	53–105	119–137	NP_973723		R
VAMP5		PM	116	6–58	73–93	NP_006625		R
VAMP7	Nyv1p	LE, Ly, PM	220	126–178	189–214	NP_005629	Ti-VAMP	R
VAMP8		EE, LE	100	13–65	76–99	NP_003752	Endobrevin	R
Ykt6	Ykt6p	Go	198	139–191	Prenyl	AAB81131		R
Sec22a		ER, IC	282	135–187	190–208	AAD43013		?
Sec22b	Sec22p	IC, cis-Go	215	135–187	196–215	NP_004883	ERS-24	R
Sec22c		ER, IC	250	135–185	186–204	AAD02171		?
Bet1	Bet1p	IC, cis-Go	118	36–88	96–115	NP_005859		Qc
GS15	Sft1p	Go	111	25–77	87–106	AAF37877		Qc
GS27	Bos1p	IC, Go	212	130–182	192–212	O14653	Membrin, Gos-27	Qb
GS28	Gos1p	Go	250	170–222	231–250	O95249	GOS-28	Qb
Vti1a	Vti1p	trans-Go	217	132–184	193–214	BI830707, BF805294	Vti1-rp2	Qb
Vti1b		EE, LE	232	146–198	207–229	NP_006361	Vti1-rp1	Qb
Slt1	Slt1p/Use1p	ER	259	173–225	232–252	BC008455	Use1, p31	Qc
Sec20	Sec20p	ER	228	132–184	203–220	NP_001196	Bnip1	?

PM: plasma membrane; Go: Golgi apparatus; cis-Go: cis-Golgi compartments; trans-Go: trans-Golgi compartments; TGN: trans-Golgi network; End: endosomes; EE: early endosomes; LE: late endosomes; RE: recycling endosomes; Ly: Lysosomes; ER: endoplasmic reticulum; IC: ER-Golgi intermediate compartments; SV: synaptic vesicles; AA: number of amino acid residues; TM: transmembrane domain.

[7] Hong, W. (2005). SNAREs and traffic. Biochim Biophys Acta *1744*, 120-144.

CHAPTER 2: PROBING DOMAIN SWAPPING FOR THE NEURONAL SNARE COMPLEX WITH ELECTRON PARAMAGNETIC RESONANCE[1]

Dae-Hyuk Kweon[2], Yong Chen[2], Fan Zhang, Michelle Poirier,

Chang Sup Kim, and Yeon-Kyun Shin

2.1 Abstract

Highly conserved soluble *N*-ethylmaleimide sensitive factor attachment protein receptor (SNARE) proteins control membrane fusion at synapses. The target plasma membrane-associated SNARE proteins and the vesicle-associated SNARE protein assemble into a parallel four-helix bundle. Using a novel EPR approach, it is found that the SNARE four-helix bundles are interconnected via domain swapping that is achieved by substituting one of the two SNAP-25 helices with the identical helix from the second four-helical bundle. Domain swapping is likely to play a role in the multimerization of the SNARE complex that is required for successful membrane fusion. The new EPR application employed here should be useful to study other polymerizing proteins.

---

[1] This paper is published in *Biochemistry* 2002:41(17):5449-5452. Necessary modifications were made to fit the format of this thesis.

[2] Contributed equally to this paper.

2.2 Introduction

Neurotransmitter release at synapses requires fusion of synaptic vesicles with the presynaptic plasma membrane. In this process, the target plasma membrane proteins syntaxin-1A and SNAP-25 (synaptosome-associated protein of 25000 Da), and the VAMP2 (vesicle-associated membrane protein 2) interact with each other to form the ternary SNARE complex (Jahn and Sudhof, 1999; Lin and Scheller, 2000). The C-terminal domain of syntaxin, two separate helix domains from SNAP-25, and a soluble domain of VAMP2 are assembled into a core structure that is a 110 Å long parallel four-stranded coiled coil (Poirier et al., 1998b; Sutton et al., 1998). In full-length SNAP-25 two helix domains are, however, flanked by a 56 amino acid region. This putative loop appears to be sufficiently long to transverse the coiled coil, connecting the two SNAP-25 helices from tail to head. Interestingly, when the flanking loop region of SNAP-25 is present in the complex, several higher molecular mass bands are observed in the SDS-PAGE than that of the core complex (Fasshauer et al., 1998; Poirier et al., 1998a) (Figure 2-1a). The flanking loop region might play an essential role in causing the oligomerization of the SNARE complex. Multimerization has been observed for the native SNARE complex as well (Otto et al., 1997). Multimerization of the SNARE complex is required for membrane fusion as it is for viral membrane fusion systems (Blumenthal et al., 1996; Danieli et al., 1996).

One possible mechanism for the SNARE complex oligomerization is domain swapping (Bennett et al., 1995; Liu et al., 2001a): a domain in one molecule is replaced with the identical domain from the second molecule (Figure 2-1b). Such swapping scheme may propagate to make a polymeric protein chain (Figure 2-1b). The polymerization via domain

swapping has been proposed as the main mechanism for promoting the disease-causing fibril formation for proteins including human cystatin C (Janowski et al., 2001) and prion proteins (Knaus et al., 2001). Thus, what is learned from the SNARE oligomerzation might help to understand better the mechanisms of protein polymerization.

2.3 Experimental Procedures

2.3.1 Plasmid Construction and Mutagenesis

Recombinant glutathione *S*-transferase (GST) fusion proteins were expressed in *Escherichia coli* from the pGEX-KG vector (Guan and Dixon, 1991), a derivative of the pGEX-2T vector (Amersham Pharmacia Biotech, Uppsala, Sweden). Plasmids encoding syntaxin-1A (amino acids 191-266), VAMP2 (amino acids 1-94), and SNAP-25 (amino acids 1-206) were prepared as previously described (Calakos et al., 1994; Poirier et al., 1998a). The four native cysteines in the loop region of SNAP-25 were changed to alanines. All cysteine mutants were generated by a QuickChange site-directed mutagenesis kit (Stratagene, La Jolla, CA) with some modifications and confirmed by DNA sequencing (Iowa State University DNA Sequencing Facility).

2.3.2 Protein Expression, Purification, and Spin Labeling

GST fusion proteins were expressed in *E. coli* BL21(DE3) Codon Plus RIL (Stratagene, La Jolla, CA) and purified using glutathione-agarose chromatography. The cells were grown at 37 °C in LB supplied with 2 g/l glucose, 100 μg/ml ampicillin, and 50 μg/ml

chloramphenicol until the OD_{600} reached 0.6-0.8. Protein expression was induced by addition of IPTG to final concentration 0.3 mM, and the cells were grown for 6 hours at 30 °C for SNAP-25, at 22 °C for VAMP2, and at 16 °C for syntaxin-1A. The cell pellets were collected by centrifugation. After being washed with an excess volume of PBST-Met buffer, a 10-fold molar excess of MTSSL spin label was added, and the sample was incubated at room temperature for 4 hours and incubated further at 4 °C overnight. After unreacted free spin labels were washed out, the spin-labeled protein was cleaved off from GST bound to the resin with thrombin. To prepare the ternary SNARE complex, equimolar amounts of syntaxin-1A, VAMP2, and SNAP-25 were mixed and incubated at 4 °C overnight. The ternary complex was purified with a Bio-Rad UNO Q1 perfusion column, equipped in the Bio-Rad Duoflow system, in 15 mM Tris-HCl (pH 8.4) buffer using a NaCl gradient from 15 mM to 0.5 M. Protein concentrations were estimated by Bio-Rad protein assay using BSA as a standard.

2.3.3 EPR Data Collection and Analysis

EPR spectra were obtained using a Bruker ESP 300 spectrometer (Bruker, Germany) equipped with a low-noise microwave amplifier (Miteq, Hauppauge, NY) and a loop-gap resonator (Medical Advances, Milwaukee, WI). The modulation amplitude was set at no greater than one-fourth of the line width. Spectra were collected at either room temperature or 130 K in the first-derivative mode. For the composite EPR spectrum the Fourier deconvolution method was used to decompose the noninteracting spectral component and the *J*-coupling spectral component (Rabenstein and Shin, 1995).

2.4 Results and Discussion

2.4.1 EPR Strategy to Detect Domain Swapping

The domain swapping hypothesis for the neuronal SNARE complex can be tested using site-directed spin-labeling EPR (Hubbell et al., 2000). When two nitroxide spin labels are placed sufficiently close to one another (less than 7 Å), the spin exchange or the *J*-coupling interaction would be turned on and becomes the dominant interaction. This spin exchange is observable only when the two nitroxides are physically in contact, and it decays exponentially as a function of the distance. Often, the *J*-coupling has been observed for two spin labels attached to two tertiary-contacting internal positions (Poirier et al., 1998b).

The short-range *J*-coupling interaction is theoretically different from the long-range dipolar interaction, although the two contributions are hardly separable. The dipolar interaction has the inverse cube dependence on the distance, and it stretches up to 25 Å (Hubbell et al., 2000). The dipolar interaction causes a simple line broadening and is frequently used to estimate the interspin distance (Liu et al., 2001b; Ottemann et al., 1999).

Typically at low temperatures, the spin exchange causes the smearing of the hyperfine features of the EPR spectrum, resulting in a bell-shaped absorption line (Figure 2-2b) that is distinctly different and easily separable from the noninteracting EPR spectra.

Here, the experimental strategy is to utilize a selected pair of positions that are physically in contact and could be *J*-coupled when spin labeled (Figure 2-2a). However, if domain swapping occurs, two spin labels separately enter into two adjacent molecules, losing the *J*-coupling interactions when the sample is mixed with the wild type. Conversely, if we

individually prepare two singly labeled polypeptide chains at the corresponding positions, the domain swapping would bring two spin labels from separate polypeptide chains into one molecule so that the *J*-coupling is turned on.

For the SNARE proteins positions 39 and 160 in SNAP-25 qualify well as the test pair (Figure 2-2a). For this pair, the *J*-coupling interaction has been previously observed in the ternary SNARE complex (Poirier et al., 1998b) as well as in the binary SNARE complex (Xiao et al., 2001) of sytaxin-1A and SNAP-25. In those cases, the N-terminal and the C-terminal fragments of SNAP-25 were separately prepared and assembled into the core four-helix bundle, and the putative loop region was not present.

For the EPR investigation the SNAP-25 construct representing amino acids 1-206, the C-terminal domain of syntaxin-1A of amino acids 191-266, and VAMP2 (amino acids 1-94) were expressed in bacteria with a glutatione *S*-trasferase (GST) affinity tag. Single cysteine mutants S39C and L160C and the double cysteine mutant S39C/L160C of SNAP-25 were made, and the mutants were derivatized with methanethiosulfonate spin label (MTSSL).

2.4.2 Spin Labels from Separate SNAP-25 Polypeptides Assemble into One SNARE Complex

First of all, it is important to establish that spin labels attached to position 39 and position 160 of SNAP-25 interact with one another only when they are within the same core four-helix bundle.

The SNARE complex containing the singly labeled SNAP-25 S39C mutant does not show any indication of spectral broadening due to either the *J*-coupling or the dipolar interaction (Figure 2-2c) when compared with several known noninteracting spectra (data not

shown). The same is true for the SNARE complex containing the singly labeled SNAP-25 L160C mutant (Figure 2-2c). Further, when we mixed the former SNARE complex and the latter, we observed an EPR spectrum that is identical to the sum of two spectra taken individually for two singly labeled complexes. This indicates that the individual four-helix bundles are sufficiently separated, despite the possibility of the interconnection due to domain swapping.

However, when we used the 1:1 mixture of singly labeled SNAP-25 S39C and singly labeled SNAP-25 L160C to form the SNARE complex with VAMP2 and syntaxin-1A, we observed some significant spectral broadening in the EPR spectrum (Figure 2-3a). It is most likely that the intermolecular domain swapping played a role. The N-terminal helix carrying the nitroxide at position 39 in one SNAP-25 polypeptide chain and the C-terminal helix carrying the nitroxide at position 160 in another SNAP-25 polypeptide chain might have assembled into the same four-helix bundle (inset of Figure 2-3a).

The EPR spectrum of the mixed SNARE complex is a composite one consisting of two components, one noninteracting and the other bell-shaped and *J*-coupled. The Fourier deconvolution method has been developed to effectively resolve such two spectral components (Rabenstein and Shin, 1995). Using this method, we found that the broad bell-shaped component (red line in Figure 2-3b) is nearly identical to the EPR spectra from the S39C/L160C doubly labeled core complex (Figure 2-2b). This suggests that the two nitroxides are *J*-coupled and physically in contact in a single four-helix bundle, although they are from two separate SNAP-25 polypeptide chains. These EPR data strongly support the intermolecular domain swapping for the SNARE complex.

2.4.3 The Spin Dimer in a Single SNAP-25 Chain Splits into Two Separate Four-Helical Bundles

The domain swapping hypothesis for the SNARE complex can be tested further using the S39C/L160C doubly labeled mutants of SNAP-25. As expected, the SNARE complex containing SNAP-25 S39C/L160C shows a strongly *J*-coupled EPR spectrum, except for some slight contamination of the singly labeled species due to the less than quantitative (~90%) spin labeling (red line in Figure 2-4a). However, when we made the SNARE complex with the 1:2 mixture of SNAP-25 S39C/L160C and unlabeled SNAP-25, a dramatic decrease of spin-spin interactions was observed (blue line in Figure 2-4a), likely due to the domain swapping. If the SNARE four-helix bundles are linked from one another by sharing helix domains of a SNAP-25 peptide chain (inset of Figure 2-4a), the spin dimer from a doubly labeled SNAP-25 S39C/L160C would dissociate. The unlabeled SNAP-25 would then fill the remaining helix positions in a "give and take" manner. This would result in the decrease of the population of the *J*-coupled spin dimer and the increase of the spin monomer.

We note that adding the preformed unlabeled complex to the preformed complex containing labeled SNAP-25 S39C/L160C did not change the EPR spectrum in the period of 24 hours, suggesting that the component exchange hardly occurs once the complex is formed.

Using the Fourier deconvolution analysis, we found that this EPR spectrum is a composite one, composed of a noninteracting spectral species and the *J*-coupled spectral species (red line in Figure 2-4b). This is consistent with the diminished *J*-coupled spin pair caused by the domain swapping with the unlabeled SNAP-25.

2.4.4 Multimerization May Be Important for SNARE-Induced Membrane Fusion

For viral membrane fusion proteins such as influenza hemagglutinin (HA) the clustering of HA at the fusion site is essential for the successful fusion (Blumenthal et al., 1996; Danieli et al., 1996). Likewise, we expect that a similar molecular clustering is perhaps required for the SNARE-induced membrane fusion. For the native SNARE proteins multiple SDS-resistant high molecular mass bands were observed in the SDS-PAGE analysis (Otto et al., 1997). This can occur through several mechanisms such as the interaction between transmembrane domains. However, we speculate that the domain swapping can also play a role in the multimerization of the SNARE complex on the membrane surface. The domain swapping perhaps induces ring structures of several four-helix bundles to be interconnected. Conceivably, the ring structure on the membrane surface could direct the effort of individual molecules toward membrane fusion collectively onto the fusion site. It is now necessary to establish the exact functional roles of the interhelical loop of SNAP-25. The membrane fusion assays based on PC-12 cells (Chen et al., 1999) and the in vitro assay developed by Weber and co-workers (Weber et al., 1998) should be adequate for this task.

2.4.5 New EPR Method for Studying the Protein Polymerization

Three-dimensional (3D) domain swapping has emerged as a mechanism for protein polymerization. This has been observed for other oligomeric proteins in the formation of highly ordered aggregates such as the fibrils characteristic of amyloid plaques. Domain swapping has also been proposed to play a role in mutimerization of the G-protein-coupled receptors (GPCR) (Gouldson et al., 2000). Despite the emerging biological significance of

domain swapping, studying this phenomenon in polymerized forms or aggregates has been technically challenging.

In this work the EPR strategy employing the *J*-coupled nitroxide pair has proven highly effective in verifying the domain swapping in the neuronal SNARE complex. The *J*-coupling is a short-range interaction, only observable for physically contacting nitroxide pairs. Experiments can be judiciously designed to turn on or to turn off this specific interaction in accordance with the pattern of domain swapping. This EPR approach should be generally applicable to other protein systems, including proteins directly involved in neurodegenerative diseases. Although the short-range *J*-coupling has been utilized in the present study, the same approach employing the dipolar broadening should also be effective for other cases.

2.5 References

Bennett, M.J., Schlunegger, M.P., and Eisenberg, D. (1995). 3D domain swapping: a mechanism for oligomer assembly. Protein Sci *4*, 2455-2468.

Blumenthal, R., Sarkar, D.P., Durell, S., Howard, D.E., and Morris, S.J. (1996). Dilation of the influenza hemagglutinin fusion pore revealed by the kinetics of individual cell-cell fusion events. J Cell Biol *135*, 63-71.

Calakos, N., Bennett, M.K., Peterson, K.E., and Scheller, R.H. (1994). Protein-protein interactions contributing to the specificity of intracellular vesicular trafficking. Science *263*, 1146-1149.

Chen, Y.A., Scales, S.J., Patel, S.M., Doung, Y.C., and Scheller, R.H. (1999). SNARE complex formation is triggered by Ca2+ and drives membrane fusion. Cell *97*, 165-174.

Danieli, T., Pelletier, S.L., Henis, Y.I., and White, J.M. (1996). Membrane fusion mediated by the influenza virus hemagglutinin requires the concerted action of at least three hemagglutinin trimers. J Cell Biol *133*, 559-569.

Fasshauer, D., Eliason, W.K., Brunger, A.T., and Jahn, R. (1998). Identification of a minimal core of the synaptic SNARE complex sufficient for reversible assembly and disassembly. Biochemistry *37*, 10354-10362.

Gouldson, P.R., Higgs, C., Smith, R.E., Dean, M.K., Gkoutos, G.V., and Reynolds, C.A. (2000). Dimerization and domain swapping in G-protein-coupled receptors: a computational study. Neuropsychopharmacology *23*, S60-77.

Guan, K.L., and Dixon, J.E. (1991). Eukaryotic proteins expressed in Escherichia coli: an improved thrombin cleavage and purification procedure of fusion proteins with glutathione S-transferase. Anal Biochem *192*, 262-267.

Hubbell, W.L., Cafiso, D.S., and Altenbach, C. (2000). Identifying conformational changes with site-directed spin labeling. Nat Struct Biol *7*, 735-739.

Jahn, R., and Sudhof, T.C. (1999). Membrane fusion and exocytosis. Annu Rev Biochem *68*, 863-911.

Janowski, R., Kozak, M., Jankowska, E., Grzonka, Z., Grubb, A., Abrahamson, M., and Jaskolski, M. (2001). Human cystatin C, an amyloidogenic protein, dimerizes through three-dimensional domain swapping. Nat Struct Biol *8*, 316-320.

Knaus, K.J., Morillas, M., Swietnicki, W., Malone, M., Surewicz, W.K., and Yee, V.C. (2001). Crystal structure of the human prion protein reveals a mechanism for oligomerization. Nat Struct Biol *8*, 770-774.

Lin, R.C., and Scheller, R.H. (2000). Mechanisms of synaptic vesicle exocytosis. Annu Rev Cell Dev Biol *16*, 19-49.

Liu, Y., Gotte, G., Libonati, M., and Eisenberg, D. (2001a). A domain-swapped RNase A dimer with implications for amyloid formation. Nat Struct Biol *8*, 211-214.

Liu, Y.S., Sompornpisut, P., and Perozo, E. (2001b). Structure of the KcsA channel intracellular gate in the open state. Nat Struct Biol *8*, 883-887.

Ottemann, K.M., Xiao, W., Shin, Y.K., and Koshland, D.E., Jr. (1999). A piston model for transmembrane signaling of the aspartate receptor. Science *285*, 1751-1754.

Otto, H., Hanson, P.I., and Jahn, R. (1997). Assembly and disassembly of a ternary complex of synaptobrevin, syntaxin, and SNAP-25 in the membrane of synaptic vesicles. Proc Natl Acad Sci U S A *94*, 6197-6201.

Poirier, M.A., Hao, J.C., Malkus, P.N., Chan, C., Moore, M.F., King, D.S., and Bennett, M.K. (1998a). Protease resistance of syntaxin.SNAP-25.VAMP complexes. Implications for assembly and structure. J Biol Chem *273*, 11370-11377.

Poirier, M.A., Xiao, W., Macosko, J.C., Chan, C., Shin, Y.K., and Bennett, M.K. (1998b). The synaptic SNARE complex is a parallel four-stranded helical bundle. Nat Struct Biol *5*, 765-769.

Rabenstein, M.D., and Shin, Y.K. (1995). Determination of the distance between two spin labels attached to a macromolecule. Proc Natl Acad Sci U S A *92*, 8239-8243.

Sutton, R.B., Fasshauer, D., Jahn, R., and Brunger, A.T. (1998). Crystal structure of a SNARE complex involved in synaptic exocytosis at 2.4 A resolution. Nature *395*, 347-353.

Weber, T., Zemelman, B.V., McNew, J.A., Westermann, B., Gmachl, M., Parlati, F., Sollner, T.H., and Rothman, J.E. (1998). SNAREpins: minimal machinery for membrane fusion. Cell *92*, 759-772.

Xiao, W., Poirier, M.A., Bennett, M.K., and Shin, Y.K. (2001). The neuronal t-SNARE complex is a parallel four-helix bundle. Nat Struct Biol *8*, 308-311.

2.6 Figures and Captions

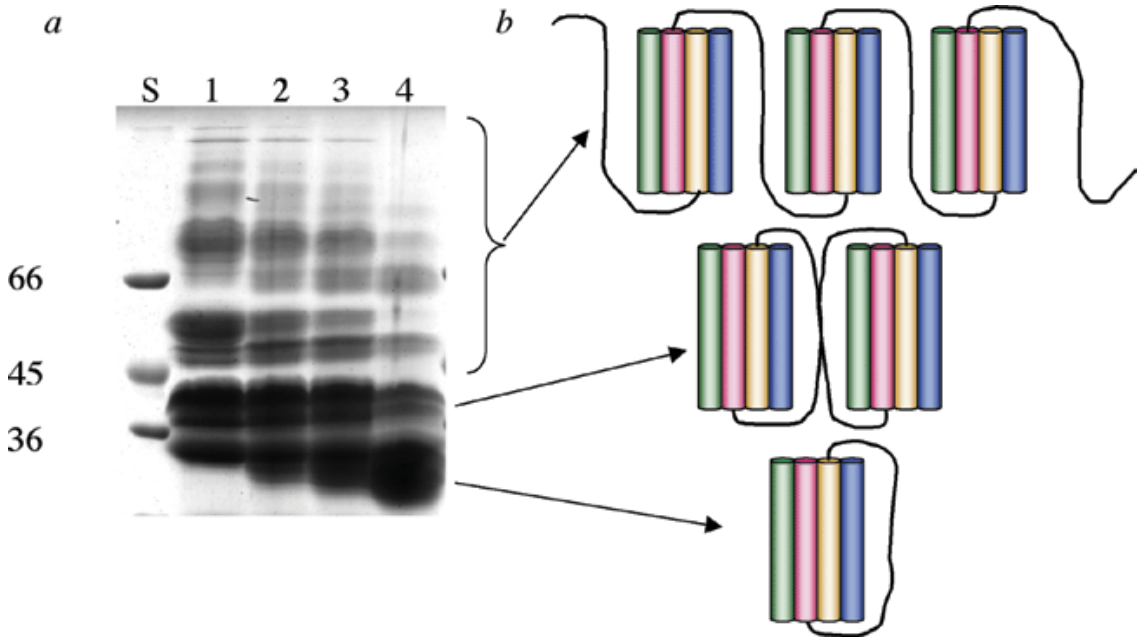

Figure 2-1. SDS-PAGE analysis of the SNARE complexes.

(a). Ternary SNARE complexes are resistant to SDS. Lane S is the size marker. The lane 1 shows the appearance of the high molecular weight bands for the SNARE complex made of VAMP2 (amino acids 1-94), syntaxin-1A (amino acids 191-266), and SNAP-25 (amino acids 1-206), consistent with the western blot analysis in a previous report (Poirier et al., 1998b). Lanes 2-4 show SDS-PAGE analysis of the trypsin-digested SNARE complex for 3, 10, and 30 min, respectively. The trypsin-treated core SNARE complex migrates near 35 kDa, similar to the previous report (Poirier et al., 1998b).

(b). Hypothetical models of the SNARE complex. Bottom: nondomain swapped SNARE complex. Middle: domain swapped dimer. Top: polymerized SNARE complex. The components of the four-helix bundle are color coded (green, syntaxin-1A; blue, VAMP2; red, N-terminal helix of SNAP-25 [SNAP-25(N)]; yellow, C-terminal helix of SNAP-25 [SNAP-25(C)]).

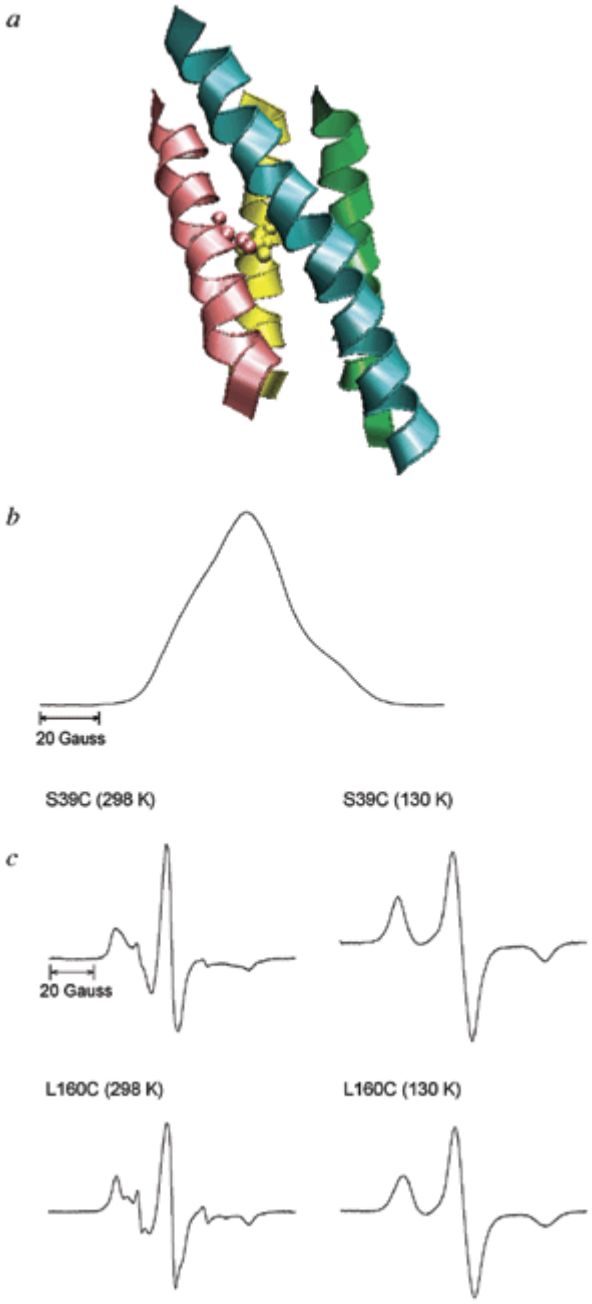

Figure 2-2. EPR spectra for Spin-labeled SNAP-25 mutants.

(a). The selected test pair in the SNARE core complex. Position 39 on SNAP-25(N) (red) and position 160 on SNAP-25(C) (yellow) are spatially close from one another in the crystal structure (Sutton et al., 1998).

(b). Low-temperature absorbance EPR spectrum of the SNARE core complex made of SNAP-25(N) S39C, SNAP-25(C) L160C, syntaxin-1A, and VAMP2 (Poirier et al., 1998a).

(c). Room temperature and low-temperature derivative mode EPR spectra for SNARE complexes containing singly labeled SNAP-25.

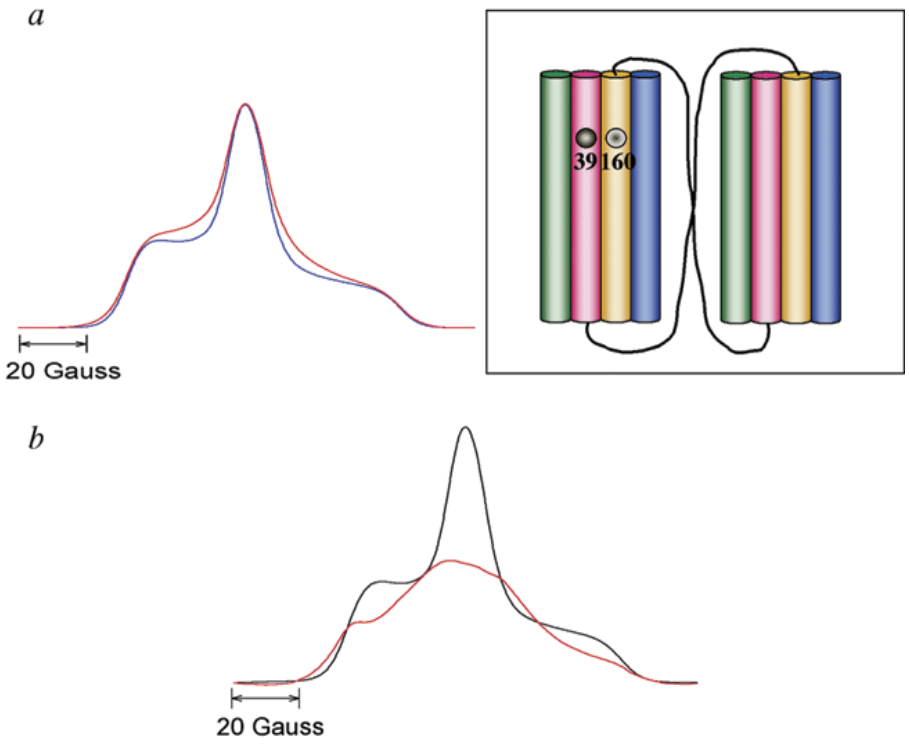

Figure 2-3. Single-labeled SNAP-25 assemble into one SNARE complex.

(a). The absorbance spectrum of the SNARE complex made of the 1:1 mixture of SNAP-25 S39C and L160C, syntaxin-1A, and VAMP2 collected at 130 K (red line) is compared with the sum of the absorbance spectrum from the SNARE complex containing SNAP-25 S39C and that from the SNARE complex containing SNAP-25 L160C (blue line). (Inset) Schematic model of the domain swapped SNARE complex dimer. Two four-helix bundles are intertwined by sharing two SNAP-25 polypeptide chains while maintaining the all-parallel coiled-coil structure. The N-terminal helix with the spin label at position 39 from one SNAP-25 and the C-terminal helix with the spin label at position 160 from another come to the same four-helical bundle and turn on the spin exchange *J*-coupling.

(b). The absorbance spectrum of the SNARE complex containing the 1:1 mixture of SNAP-25 S39C and L160C was decomposed into the noninteracting component (black line) (66%) and the *J*-coupled component (red line) (33%) using the Fourier deconvolution method and spectral subtraction.

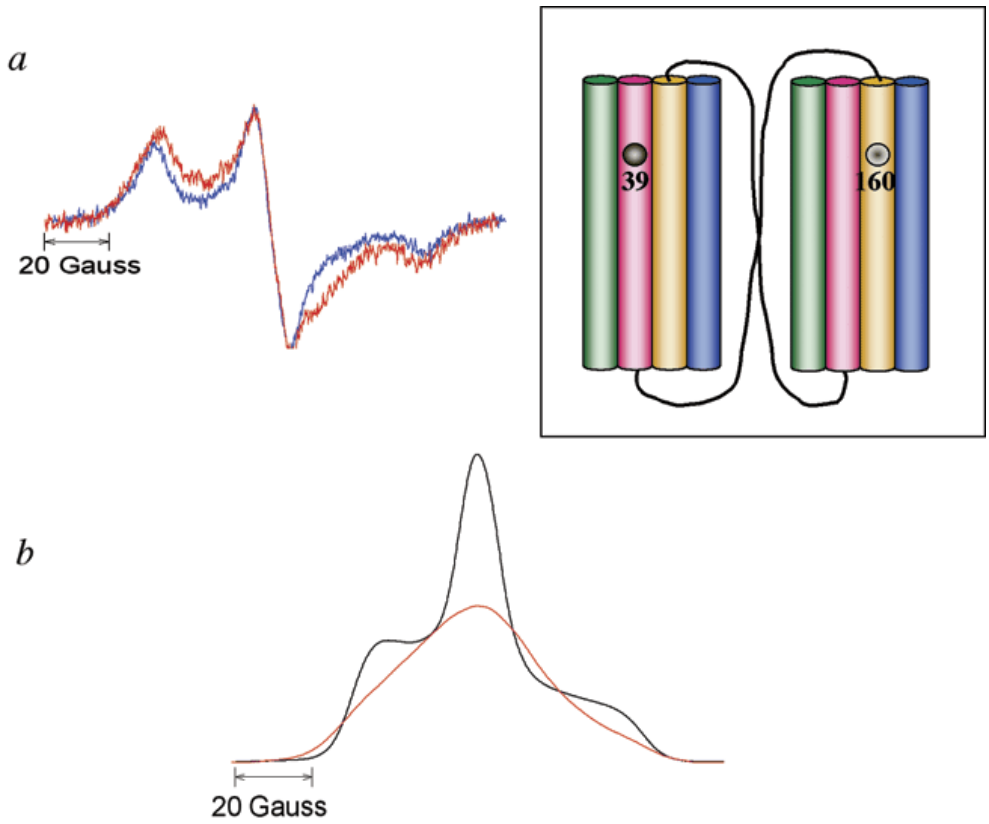

Figure 2-4. Double-labeled SNAP-25 splits into two separate SNARE complexes.

(a). The derivative mode EPR spectrum from the SNARE complex containing a 1:2 mixture of SNAP-25 S39C/L160C and unlabeled SNAP-25 (blue line), collected at 130 K, is compared with that from the complex containing only SNAP-25 S39C/L160C (red line). (Inset) A domain swapped dimer containing SNAP-25 S39C/L160C. Two spin labels attached to a single SNAP-25 peptide chain divide into two separate four-helix bundles.

(b). The absorbance EPR spectrum from the SNARE complex containing a 1:2 mixture of SNAP-25 S39C/L160C and unlabeled SNAP-25 was decomposed into two components (50% noninteracting and 50% *J*-coupled) using the Fourier deconvolution method and spectral subtraction. The *J*-coupled component is essentially the same as that in Figure 2-2b.

CHAPTER 3: CONSTITUTIVE VERSUS REGULATED SNARE ASSEMBLY: A STRUCTURAL BASIS[1]

Yong Chen[2], Yibin Xu[2], Fan Zhang and Yeon-Kyun Shin

3.1 Abstract

SNARE complex formation is essential for intracellular membrane fusion. Vesicle-associated (v-) SNARE intertwines with target membrane (t-) SNARE to form a coiled coil that bridges two membranes and facilitates fusion. For the SNARE family involved in neuronal communications, complex formation is tightly regulated by the v-SNARE-membrane interactions. However, it was found using EPR that complex formation is spontaneous for a different SNARE family that is involved in protein trafficking in yeast. Further, reconstituted yeast SNAREs promoted membrane fusion, different from the inhibited fusion for reconstituted neuronal SNAREs. The EPR structural analysis showed that none of the coiled-coil residues of yeast v-SNARE is buried in the hydrophobic layer of the membrane, making the entire coiled-coil motif accessible, again different from the deep insertion of the membrane-proximal region of neuronal v-SNARE into the bilayer. Importantly, yeast membrane fusion is constitutively active, while synaptic membrane fusion is regulated, consistent with the present results for two SNARE families. Thus, the v-SNARE−membrane interaction may be a major molecular determinant for regulated versus constitutive membrane fusion in cells.

---

[1] This paper is published in *EMBO J* 2004, 23, 681-689. Necessary modifications were made to fit the format of this thesis.

[2] Contributed equally to this paper.

3.2 Introduction

Fusion of cargo vesicles to the target membrane is the prevailing mechanism for the delivery of fresh lipids and proteins to organelles, and for the secretion of neurotransmitters and hormones. The machinery that brings about intracellular membrane fusion is thought to be built around the SNARE proteins that are widely conserved from yeast to humans (Brunger, 2001; Jahn and Sudhof, 1999; Lin and Scheller, 2000; Rizo and Sudhof, 2002; Rothman, 1994; Sollner et al., 1993). A crucial step is the formation of the core SNARE complex between the vesicle-associated (v-) SNARE and the target plasma membrane (t-) SNARE. Conserved coiled-coil motifs from individual SNAREs associate and twist to form a stable helical bundle (Antonin et al., 2002; Hanson et al., 1997; Katz et al., 1998; Kweon et al., 2003a; Lin and Scheller, 1997; Poirier et al., 1998; Sutton et al., 1998).

The SNARE family involved in neurotransmitter release at synapses and that participating in yeast protein trafficking are two best characterized systems (Gerst, 2003; Jahn et al., 2003). In the neuron, an integral membrane protein synaptobrevin is v-SNARE, and syntaxin-1A and SNAP-25 are two t-SNARE proteins residing in the plasma membrane. In yeast, Snc is v-SNARE, while Sso and Sec9 are yeast counterparts of syntaxin and SNAP-25, respectively (Aalto et al., 1993; Brennwald et al., 1994; Ferro-Novick and Jahn, 1994; Protopopov et al., 1993). There are remarkable sequence similarities between these two SNARE families, implying conserved functions (Weimbs et al., 1997).

Perhaps the most profound difference between two fusion systems is the way in which membrane fusion is regulated (Gerst, 2003; Jahn et al., 2003). Yeast fusion machinery is constitutively active to support the steady-state flow of lipids and proteins to cell compartments, although regulatory factors such as Sec1, the N-terminal domain of Sso1p,

and protein kinase A have been identified (Jahn and Sudhof, 1999; Marash and Gerst, 2001; Nicholson et al., 1998). In contrast, membrane fusion in the neuron is tightly regulated and primarily triggered by the Ca^{2+} signal (Chen et al., 1999). Several regulatory proteins such as Ca^{2+}-sensing synaptotagmin (Chapman, 2002; Sudhof, 2002), Munc-13 (Augustin et al., 1999; Rosenmund et al., 2002), and complexin (Chen et al., 2002; Pabst et al., 2002) have been found in neuronal cells. At present, the exact roles of individual regulators are not well understood beyond the general belief that SNARE assembly is influenced by the regulators.

Previously, Rothman and co-workers demonstrated that SNAREs are the minimal fusion machinery (Weber et al., 1998). Their results suggest that SNARE complex formation directly promotes membrane fusion. However, it has been recently shown that neuronal v- and t-SNAREs reconstituted into the separate membranes do not spontaneously engage one another to form the complex (Hu et al., 2002; Kweon et al., 2003b). The assistance of other proteins such as calcium sensor appears to be necessary for SNARE assembly and membrane fusion (Hu et al., 2002). The structure of membrane-bound synaptobrevin determined with EPR provided important insights into the mechanism of this regulation of SNARE complex formation (Kweon et al., 2003b). For yeast SNAREs, however, such regulation might not be operative because membrane fusion is constitutively active.

In this work, we demonstrate that yeast v- and t-SNAREs reconstituted on the separate membranes spontaneously associate to form the complex, different from the inhibition observed for neuronal SNAREs (Hu et al., 2002; Kweon et al., 2003b). The EPR results correlated well with the results of fusion that significant membrane fusion was observed for reconstituted yeast SNAREs in the fusion assay, while no fusion was detected for reconstituted neuronal SNAREs under biologically relevant conditions. Further, using

EPR, we examined the structure and the membrane topology of reconstituted yeast v-SNARE Snc2p. It was found that none of the amino acids in the coiled-coil motif is deeply inserted into the acyl chain region of the bilayer, making the coiled-coil motif fully available for complex formation.

3.3 Results

3.3.1 EPR Assay of Core SNARE Complex Formation

The coiled-coil motif of yeast v-SNARE Snc2p is largely unstructured and freely moving in solution. However, when complexed with t-SNAREs (Couve and Gerst, 1994; Rossi et al., 1997), the polypeptide becomes α-helical (Nicholson et al., 1998), which significantly reduces the degree of freedom for the peptide backbone as well as for the amino-acid side chains. Site-directed spin labeling (SDSL) and EPR spectroscopy are very effective in detecting such secondary structural changes (Hubbell et al., 2000; Hubbell et al., 1998).

In SDSL, native amino acids are site-specifically replaced one by one with cysteines, to which the nitroxide side chain is attached. The EPR line shape is sensitive to the motional rates of the nitroxide. The helix formation usually involves a large EPR line-shape change from a narrow spectrum reflecting the fast motion of the nitroxide to a broad spectrum reflecting the slow motion (Hubbell et al., 1996; McHaourab et al., 1996). Further, with SDSL, conformational changes can be monitored at various locations of the polypeptide chain.

First, as a control, we examined the core complex formation between soluble SNAREs using SDSL and EPR spectroscopy. Soluble parts of individual SNAREs containing coiled-coil motifs Sso1pH3 (amino acids 185−265 of Sso1p), Sec9c (amino acids 401−651 of Sec9), and Snc2pS (amino acids 1−93 of Snc2p) were subcloned and expressed in *Escherichia coli*. The purity of all recombinant proteins was examined by the SDS−PAGE analysis after purification (Figure 3-1A). For EPR measurements, five spin-labeled mutants of Snc2pS covering the coiled-coil motif (R32C, I46C, G53C, E60C, and G76C) were prepared and labeled with methanethiosulfonate spin label (MTSSL). EPR spectra of spin-labeled Snc2pS were all narrow, reflecting the fast motion of the nitroxide, characteristic of a freely moving random coil (Figure 3-2B). However, as expected, the addition of t-SNAREs Sec9c and Sso1pH3 changed the EPR spectra to all broad, reflecting the slow motion of the nitroxides, which indicates the transition from an unstructured state to the helical structure due to spontaneous core complex formation (Figure 3-2C).

Next, recombinant SNAREs containing transmembrane domains (TMD) Sso1pHT (amino acids 185−290 of Sso1p) and Snc2pF (amino acids 1−115 of Snc2p) were examined with EPR. Five cysteine mutants of Snc2pF at the same positions (R32C, I46C, G53C, E60C, and G76C) were prepared for spin labeling (Figure 3-2A). Again, the purity of SNARE proteins was examined with SDS−PAGE (Figure 3-1A). Spin-labeled mutants were then reconstituted into 1-palmitoyl-2-oleoylphosphatidylcholine (POPC) vesicles containing 15 mol% negatively charged dioleoylphosphatidylserine (DOPS), a lipid composition commonly used to mimic the native cellular membrane (McNew et al., 2000; Parlati et al., 1999; Weber et al., 1998). We reconstituted t-SNAREs into separate vesicles of the same lipid composition for the mixing experiment. After reconstitution, the integrity of vesicles

was verified with negative-staining electron microscopy (Figure 3-1B). Except for G76C, EPR spectra are narrow and reflect the fast motion of the nitroxide, indicating that the coiled-coil motif region is largely unstructured and freely moving (Figure 3-3A). The spectrum for membrane-proximal G76C is relatively broad, most likely due to the membrane-peptide interaction because the polypeptide chain is anchored to the membrane via TMD (see below). However, when mixed with soluble t-SNAREs or vesicles carrying t-SNAREs, we observed the broad component (arrows in Figure 3-3C and 3-3D) for all mutants, clearly indicating that SNARE complex formation has occurred, consistent with the previous reported results (McNew et al., 2000). EPR spectra were collected at 20 °C within 30 min after mixing t- and v-SNAREs. There were no significant further spectral changes after 30 min.

For reconstituted SNAREs, complex formation is less than quantitative. The narrow spectral components (asterisks in Figure 3-3) represent unstructured Snc2pF that does not participate in complex formation. The standard spectral decomposition analysis (see the legend of Figure 3-3) revealed that the percentages of complex formation for Snc2pF range from 33 to 91%, depending on the spin-labeled positions, indicating some but not serious perturbations due to spin labeling.

Such spontaneous SNARE assembly for the yeast system is quite different from what has been observed for neuronal SNAREs for which SNARE complex formation is inhibited due to the v-SNARE−membrane interactions (Kweon et al., 2003b). EPR is sufficiently sensitive to detect small spectral changes due to complex formation, as little as a few percents. No spectral changes were detected for reconstituted neuronal SNAREs within experimental uncertainty (Kweon et al., 2003b) (see the Supplementary data), indicating negligible SNARE complex formation.

3.3.2 Membrane-bound Structure of Snc2pF

To explore the structural basis for spontaneous complex formation for reconstituted yeast SNAREs, we investigated the membrane-bound structure of Snc2pF using SDSL EPR. For neuronal SNARE assembly, it was found that the COOH-terminal end of the v-SNARE coiled-coil motif plays a key role in inhibiting neuronal SNARE assembly. This region inserts deeply into the membrane with high affinity, reducing its accessibility to t-SNAREs, which perhaps restricts SNARE assembly kinetically and thermodynamically (Kweon et al., 2003b).

We prepared 20 consecutive spin-labeled mutants of Snc2pF (G76C-L95C) for SDSL EPR. After reconstitution into the membrane, the EPR spectra of spin-labeled mutants were collected at room temperature (Figure 3-4). From G76C through R81C, EPR spectra are composed of two components. The narrow component represents the freely moving polypeptide chain in the solution phase. The broad component represents the species interacting with the membrane surface. However, from K82C through L95, EPR spectra display mainly broad lineshapes, typical for the nitroxides interacting fully with the viscous bilayer (Rabenstein and Shin, 1995). We do not observe any sign of the spin-spin coupling in the EPR spectra, suggesting that synaptobrevin is mostly monomeric.

The EPR saturation method to measure accessibilities (Altenbach et al., 1994) was used to characterize the secondary structure and membrane topology of yeast v-SNARE Snc2pF at the water-membrane interface (Kim et al., 2002; Kweon et al., 2002). We measured the accessibility of the nitroxide to a water-soluble paramagnetic reagent, nickel-ethylenediaminediacetic acid (NiEDDA) (W_{NiEDDA}), to estimate the solvent exposure of the

spin-labeled site. We also determined the accessibility to a nonpolar paramagnetic reagent, molecular oxygen (W_{O2}), to probe the immersion into the membrane interior.

For reconstituted Snc2pF, an overall decrease in W_{NiEDDA} was observed along the sequence, while an overall increase was detected for W_{O2} (Figure 3-5A). Importantly, we notice substantial peaks and valleys in the region of 84−91, suggesting the presence of a secondary structure. It was previously found that the ratio of W_{O2} to W_{NiEDDA} is proportional to the immersion depth of spin label. The immersion depths were calculated from the standard curve (Altenbach et al., 1994; Macosko et al., 1997).

The immersion depths show a periodic oscillation in the region of residues 84−91. We fit the data with a sine function with an additional variable that incorporates the tilt of the helix with respect to the membrane. The immersion depth results fit well with an α-helical geometry in this region (Figure 3-5B). In addition, the fitting suggested that this short two-turn helical segment has a tilted orientation, at an angle of 40° with respect to the membrane normal (Kweon et al., 2003b; Macosko et al., 1997).

We note that EPR reported an immersion depth of ~11 Å for position 90, for which the native residue is lysine. However, it is likely that the location of the lysine side chain is shallower. The positive charge on K90 could snorkel out to seek the negative changes on phosphate, in contrast to what is expected for a relatively nonpolar nitroxide side chain.

3.3.3 Comparison of Membrane Topologies of Yeast Snc2pF and Neuronal Synaptobrevin

It appears that yeast Snc2pF and neuronal synaptobrevin share similar overall membrane topology: The long unstructured region is connected to the short helical segment

that enters the membrane with an oblique angle. Presumably, the short helical segment is joined to the membrane-spanning α-helical TMD via a few disordered residues (Figure 3-6) (Kweon et al., 2003b).

However, the difference between two structures does exist with the location of the short helical segment along the primary sequence. For synaptobrevin, the helical segment is part of the coiled-coil motif, and it is oriented in such a way that the membrane-seeking tryptophan (Trp) residues are located near the C-terminal end of the segment. As a result, two Trp residues are inserted deep into the acyl chain region of the bilayer (Kweon et al., 2003a; Yau et al., 1998). In contrast, for Snc2pF, two Trp residues are located near the beginning of the short helical segment. Moreover, the orientation of the helix makes two Trp residues point upward and makes deep penetration into the membrane difficult (Figure 3-6B). Consequently, the affinity of the short helical segment to the membrane for Snc2p is likely to be much lower than that for neuronal synaptobrevin (Thorgeirsson et al., 1996; Wimley and White, 1996).

Further, the crystal structure of the neuronal core SNARE complex suggests that the coiled coil terminates at residue 92 for synaptobrevin (Sutton et al., 1998). On the basis of the sequence alignment, the corresponding terminal residue for Snc2pF should be position 89 (Figure 3-6C). If this is true, none of the amino acids in the coiled-coil motif appears to be inserted into the acyl chain region of the bilayer for Snc2pF (Figure 3-5A), suggesting some but weak affinity of the interfacial region to the membrane.

One might argue that the substitution of the nitroxide side chain might have contributed somewhat to the discrepancy between neuronal and yeast v-SNAREs. We compared the fluorescence quenching of Trp residues by lipid quenchers in which

fluorescence-quenching bromines are attached to the acyl chain (Figure 3-7) (Abrams and London, 1992; Chattopadhyay and London, 1987). It is shown that added lipid quenchers (6,7)- and (11,12)-PC influence the Trp fluorescence of Snc2pF much less than it does for synaptobrevin, which suggests that Trp residues of synaptobrevin are deeper in the membrane than those of Snc2p, consistent with the EPR results.

3.3.4 Proteoliposome Fusion Assays Support the Structure-based Regulatory Mechanism

SNARE assembly might drive membrane fusion. Since reconstituted yeast SNAREs form the complex spontaneously, in contrast to the inhibition of neuronal SNARE assembly, we expect spontaneous membrane fusion with yeast SNAREs. To test this, we reconstituted Sso1pHT into POPC vesicles containing 15 mol% DOPS. We also reconstituted Snc2pF into the separate vesicles of the same lipid composition, but with fluorescent lipids for the measurement of lipid mixing. In both cases, the lipid-to-protein ratio was approximately 300:1.

First, as a control, we mixed Sso1pHT-reconstituted vesicles and Snc2pF-reconstituted vesicles without Sec9c. Over a period of 100 min, we did not observe any fluorescence change (black line in Figure 3-8). However, when we preincubated Sso1pHT-reconstituted vesicles with Sec9c for 30 min and subsequently mixed this solution with Snc2pF-reconstituted vesicles, we observed the slow but steady increase of fluorescence signal (red line in Figure 3-8), indicating lipid mixing. The fluorescence change detected in the period of 6,000 seconds corresponds to one 'round of fusion' on the basis of the calculation given by Rothman and coworkers (McNew et al., 2000).

In sharp contrast, when neuronal SNAREs were tested under identical conditions, we did not observe any fluorescence change (blue line in Figure 3-8), indicating that no lipid mixing had occurred during the period of nearly 2 hours. The results are in accordance with the previous EPR data that suggest the inhibition of neuronal SNARE assembly under such conditions. However, our current results are quite different from those from the Rothman fusion assay in which slow but apparent lipid mixing was observed (Weber et al., 1998). The Rothman fusion assay required an unnatural lipid-to-protein ratio of ~20:1 for vesicular SNARE synaptobrevin, which is exceedingly higher than the ratio of 150-1000:1 in natural synaptic vesicles (Kweon et al., 2003b; Weber et al., 1998). Thus, the results from the lipid-mixing fusion assays are fully consistent with the present EPR data, and support the proposed mechanism for the regulation of SNARE assembly and membrane fusion by the membrane.

The time scale of membrane fusion appears to be much slower than the time scale of SNARE assembly assayed by EPR. We, however, note that the protein concentration used in the fusion assay is at least 10 times less than that used for the EPR assay, which is qualitatively in line with the difference between the two time scales, warranting further investigation.

3.4 Discussion

Yeast v-SNARE Snc2p shares 50% sequence identity with the neuronal counterpart synaptobrevin (Figure 3-6C). Further, the EPR results suggest that the structure and the membrane topology of Snc2p are generally similar to those of synaptobrevin. Yet, there are significant differences between the two in the detailed arrangement of amino acids in the

topological structure. For neuronal synaptobrevin, the COOH-terminal region of the coiled-coil motif is deeply inserted into the membrane, restricting the accessibility of the region for SNARE assembly. Particularly, two Trp residues, which are anchored in the acyl chain region of the bilayer, help stabilize the short helical segment in the membrane. This membrane-embedded segment controls the fate of the entire coiled-coil motif for complex formation (Kweon et al., 2003b). In contrast, the interfacial residues of Snc2p are bound shallow in the polar surface of membrane and none of the coiled-coil residues is anchored into the acyl chain region of the bilayer. This is likely to make the whole coiled-coil motif accessible to t-SNAREs for complex formation.

There are several factors that might have contributed to the topological differences between the two systems. First, the putative TMD of synaptobrevin is three residues shorter than that of Snc2p (Figure 3-6C). Therefore, the interfacial region of synaptobrevin could be pulled more towards the membrane than it is for Snc2p. Second, for Snc2p, position 88 is negatively charged aspartic acid, whereas the corresponding residue in synaptobrevin is asparagine. In an attempt to understand the effect of the aspartic acid to asparagine mutation, we made the D88N mutant of Snc2p. However, this mutation alone did not alter the ability of Snc2p to interact with t-SNAREs spontaneously. Therefore, it appears that multiple factors contribute cooperatively to the better stability of synaptobrevin in the membrane than Snc2p.

In conclusion, using EPR assay, we have demonstrated that yeast SNARE assembly is spontaneous (Figure 3-3), leading to spontaneous membrane fusion (red line in Figure 3-8). In contrast, neuronal SNARE assembly is tightly regulated (Kweon et al., 2003b), resulting in the inhibition of membrane fusion (blue line in Figure 3-8). Interestingly though, the EPR

results suggested that yeast Snc2p shares the same global membrane topology with neuronal synaptobrevin. However, unlike the case with synaptobrevin, the coiled-coil motif of Snc2p floats in or above the polar region of the bilayer, so that it may readily engage with t-SNAREs to form the SNARE complex. The yeast-trafficking fusion machinery is constitutively active and need not be regulated, in sharp contrast to the tightly regulated neuronal exocytosis. Further, the key neuronal regulatory proteins such as synaptotagmin are not found in yeast systems. Therefore, although speculative, the EPR data might suggest that the v-SNARE−membrane interaction plays a central role in determining whether particular membrane fusion machinery should be regulated or constitutive.

3.5 Materials and Methods

3.5.1 Plasmid Constructs and Site-directed Mutagenesis

Genes for yeast SNAREs were obtained from Dr. James McNew at Rice University. DNA sequences encoding Sso1pH3 (amino acids 185−265), Sso1pHT (amino acids 185−290), Snc2pS (amino acids 1−93), and Snc2pF (amino acids 1−115) are inserted into the pGEX-KG vector between *Eco*RI and *Hind*III sites as N-terminal glutathione *S*-transferase (GST) fusion proteins. Sec9c (amino acids 401−651) is inserted into pET-24b(+) between *Nde*I and *Xho*I sites as a C-terminal His_6-tagged protein. In order to introduce a unique cysteine residue for the specific nitroxide attachment, native cysteine 266 of Sso1pHT and native cysteine 94 of Snc2pF were mutated to alanines. QuickChange site-directed mutagenesis (Stratagene) was used to generate all mutants and DNA sequences were confirmed by the Iowa State University DNA Sequencing Facility.

3.5.2 Protein Expression, Purification, and Spin Labeling

Recombinant GST fusion proteins were expressed in *E. coli* Rosetta (DE3) pLysS (Novagene). The cells were grown at 37 °C in LB medium with glucose (2 g/l), ampicillin (100 μg/ml), and chloramphenicol (25 μg/ml) until the A_{600} reached 0.6−0.8. Isopropyl-β-D-thiogalactopyranoside (IPTG) was added to a final concentration of 1 mM. The cells were grown further for four more hours at 22 °C. The cell pellets were collected by centrifugation at 6,000 r.p.m. for 10 minutes.

GST fusion proteins were purified by affinity chromatography using glutathione-agarose beads (Sigma). The frozen cell pellet was resuspended in resuspension buffer (phosphate-buffered saline, pH 7.4, with 0.5% Triton X-100 (v/v), PBST) with 2 mM 4-(2-aminoethyl)benzenesulfonyl fluoride (AEBSF) and 5 mM dithiothreitol (DTT). The cells were broken by sonication on an ice bath. For Snc2pF and Sso1pHT, 1% of *n*-lauroyl sarcosine was added to the solution before sonication. The cell lysate was centrifuged at 15,000 × ***g*** for 20 min at 4 °C. The supernatant was mixed with glutathione-agarose beads in the resuspension buffer and nutated at 4 °C for 40 min. The protein-bound beads were washed with an excess volume of washing buffer (phosphate-buffered saline, PBS, pH 7.4). For Sso1pHT and Snc2pF, 0.2% (v/v) Triton X-100 was added, while no detergent was added for Sso1pH3 and Snc2pS when washing. The beads were then washed with thrombin cleavage buffer (50 mM Tris−HCl, 150 mM NaCl, 2.5 mM $CaCl_2$, pH 8.0), either with 0.2% Triton X-100 for Sso1pHT and Snc2pF, or without detergent for Sso1pH3 and Snc2pS. Finally, the proteins were cleaved from the resin by thrombin (Sigma) at room temperature

for 40 min. AEBSF was added to the protein after cleaving from the resin (2 mM final concentration). The protein was stored at -80 °C with 10% glycerol.

Cysteine mutants of Snc2pF were spin-labeled before thrombin cleavage. After the cell lysate was incubated with beads and washed with PBS buffer with 0.2% Triton X-100, DTT was added to a final concentration of 5 mM at 4 °C for 40 min. The beads were then washed eight times with an excess volume of PBS buffer with 0.2% Triton X-100 to remove DTT. An approximately 20-fold excess of (1-oxyl-2,2,5,5-tetramethylpyrrolinyl-3-methyl) methanethiosulfonate spin label (MTSSL) was added to the protein, and the reaction mixture was left overnight at 4 °C. Free MTSSL was removed by washing with excess PBS buffer with 0.2% Triton X-100. The proteins were cleaved by thrombin in cleavage buffer with 0.2% Triton X-100.

The His_6-tagged protein Sec9c was expressed in *E. coli* Rosetta (DE3) pLysS. The cells were grown at 37 °C in LB medium with glucose (2 g/l), kanamycin (30 μg/ml), and chloramphenicol (25 μg/ml) until the A_{600} reached 0.6−0.8. After the addition of IPTG (1 mM), the cells were grown further for four more hours at 30 °C. The cell pellets were collected by centrifugation at 6,000 r.p.m. for 10 min.

For purification, the frozen cell pellet was resuspended in lysis buffer (PBS buffer with 20 mM imidazole, 0.5% Triton X-100, 2 mM AEBSF, pH 8.0). After sonication on ice, the cell lysate was centrifuged at 15,000 × ***g*** for 15 min at 4 °C. The supernatant was mixed with nickel-nitrilotriacetic acid-agarose beads (Qiagen) in lysis buffer. The mixture was nutated for binding at 4 °C for 40 min. After binding, the beads were washed with washing buffer (PBS buffer with 50 mM imidazole, pH 8.0). Then the protein was eluted by elution

buffer (PBS buffer with 250 mM imidazole, pH 8.0). The protein can be kept at -80 °C with 10% glycerol. All purified proteins were examined with 15% SDS−PAGE.

3.5.3 Membrane Reconstitution and Electron Microscopy

Large unilamellar vesicles (~100 nm in diameter) of POPC containing 15 mol% of DOPS were prepared in cleavage buffer containing no detergent using an extruder. The total lipid concentration was 100 mM. Proteins were mixed with vesicles at an ~1:300 protein-to-lipid molar ratio. The detergent was removed by treating the sample with Bio-beads SM2 (Bio-Rad). Bio-beads were first washed extensively with deionized water. After washing, water was decanted from Bio-beads as much as possible using a pipette after centrifugation. Bio-beads were then directly added to the sample in the ratio of 200 mg per 1 ml of the mixed solution. After 45 min of nutation, Bio-beads were removed from the sample by taking out the solution using a pipette after centrifugation at 5,000 × ***g***. The same procedure was repeated three times. We found that this new Bio-beads method improved the yield of protein incorporation into vesicles.

The reconstituted vesicles were concentrated using 100 kDa molecular weight centrifugal filter (Millipore) before taking the EPR spectra. Protein-reconstituted vesicles were characterized with negative-staining electron microscopy. The sample was stained with 1% phosphotungstic acid (pH 6.7) after the protein sample was spread on the 200-mesh formvar and carbon-coated grids. The micrograph (Figure 3-1B) was taken on a JEOL 1200 EX electron microscope. Most vesicles were ~100 nm in diameter.

All EPR measurements were performed with samples prepared with the Bio-beads method. The EPR binding assay experiments were repeated using samples prepared with the dialysis method for proper comparison with the result from neuronal synaptobrevin. The results from the two methods were identical within experimental uncertainty. Conversely, neuronal SNAREs were reconstituted into vesicles using the Bio-beads method. We observed the complete inhibition of SNARE assembly, identical to our previous results obtained with the samples prepared with the dialysis method (the data are provided as Supplementary data).

3.5.4 EPR Data Collection and Accessibility Measurements

EPR spectra were obtained using a Bruker ESP 300 spectrometer equipped with a loop-gap resonator. The accessibility measurements were performed following the procedure described elsewhere (Kweon et al., 2002, 2003b).

3.5.5 Fluorescence-quenching Experiment

The wild-type sequence of Snc2pF was reconstituted into POPC vesicles containing 15 mol% DOPS, using the dialysis method that was used for the reconstitution of synaptobrevin in our previous work. The concentration of Snc2pF was 5 μM and total lipid concentration was ~2.5 mM. The detailed procedure of the fluorescence experiment is described elsewhere (Kweon et al., 2003b). The data were collected at 20 °C.

3.5.6 Fusion Assays

For lipid-mixing assay, two different vesicle solutions that represent the initial conditions were separately prepared. Chloroform solutions of POPC and DOPS were mixed in a test tube (85:15 mol/mol). Also, 2 mol% each of *N*-(lissamine Rhodamine B sulfonyl)-phosphatidylethanolamine (N-Rh-PE) and *N*-(7-nitro-2,1,3-benzoxadiazol-4-yl)phosphatidyl-ethanolamine (N-NBD-PE) were included to a portion of the mixture. After drying the solution with a blow of nitrogen, the test tubes are put in vacuum for several hours for further drying. Snc2pF (or synaptobrevin) was reconstituted into the fraction containing fluorescence labels, while Sso1pHT (or syntaxin) was reconstituted into the unlabeled fraction. The detergent in the samples was removed by the Bio-beads method. The samples were then dialyzed overnight, following the procedure described elsewhere (Kweon et al., 2003b), to remove any trace amount of detergent that might interfere with the fluorescence measurements. After dialysis, the solution was centrifuged at 10,000 × ***g*** to get rid of protein and lipid aggregates. The lipid-to-protein ratio was aimed at approximately 300:1. Prior to the fusion assay, Sso1pHT-reconstituted vesicles were mixed with Sec9c in a molar ratio of 1:1, and the mixture was incubated at 37 °C for 30 min to help the formation of the binary t-SNARE complex. To monitor the lipid mixing, Snc2pF-reconstituted vesicles were mixed with the t-SNARE-reconstituted vesicles in a ratio of 1:9. The final solution contains approximately 1 mM lipids. Fluorescence was measured at excitation and emission wavelengths of 465 and 530 nm, respectively. Fluorescence changes were recorded with a Varian Cary Eclipse model fluorescence spectrophotometer using a quartz cell of 400 μl with the 2 mm path length. We used the same conditions in an attempt to monitor the lipid mixing induced by neuronal SNAREs. We used recombinant Syntaxin-1A without the Habc domain

(SynHT, amino acids 199−288), SNAP-25 (amino acids 1−206), and full-length synaptobrevin (amino acids 1−116) for the fusion assay. Expression, purification, and reconstitution of these neuronal SNAREs are described elsewhere (Kweon et al., 2003b).

3.6 Acknowledgments

This work was supported by grants from the United States National Institute of Health.

3.7 References

Aalto, M.K., Ronne, H., and Keranen, S. (1993). Yeast syntaxins Sso1p and Sso2p belong to a family of related membrane proteins that function in vesicular transport. EMBO J *12*, 4095-4104.

Abrams, F.S., and London, E. (1992). Calibration of the parallax fluorescence quenching method for determination of membrane penetration depth: refinement and comparison of quenching by spin-labeled and brominated lipids. Biochemistry *31*, 5312-5322.

Altenbach, C., Greenhalgh, D.A., Khorana, H.G., and Hubbell, W.L. (1994). A collision gradient method to determine the immersion depth of nitroxides in lipid bilayers: application to spin-labeled mutants of bacteriorhodopsin. Proc Natl Acad Sci U S A *91*, 1667-1671.

Antonin, W., Fasshauer, D., Becker, S., Jahn, R., and Schneider, T.R. (2002). Crystal structure of the endosomal SNARE complex reveals common structural principles of all SNAREs. Nat Struct Biol *9*, 107-111.

Augustin, I., Rosenmund, C., Sudhof, T.C., and Brose, N. (1999). Munc13-1 is essential for fusion competence of glutamatergic synaptic vesicles. Nature *400*, 457-461.

Brennwald, P., Kearns, B., Champion, K., Keranen, S., Bankaitis, V., and Novick, P. (1994). Sec9 is a SNAP-25-like component of a yeast SNARE complex that may be the effector of Sec4 function in exocytosis. Cell *79*, 245-258.

Brunger, A.T. (2001). Structural insights into the molecular mechanism of calcium-dependent vesicle-membrane fusion. Curr Opin Struct Biol *11*, 163-173.

Chapman, E.R. (2002). Synaptotagmin: a Ca(2+) sensor that triggers exocytosis? Nat Rev Mol Cell Biol *3*, 498-508.

Chattopadhyay, A., and London, E. (1987). Parallax method for direct measurement of membrane penetration depth utilizing fluorescence quenching by spin-labeled phospholipids. Biochemistry *26*, 39-45.

Chen, X., Tomchick, D.R., Kovrigin, E., Arac, D., Machius, M., Sudhof, T.C., and Rizo, J. (2002). Three-dimensional structure of the complexin/SNARE complex. Neuron *33*, 397-409.

Chen, Y.A., Scales, S.J., Patel, S.M., Doung, Y.C., and Scheller, R.H. (1999). SNARE complex formation is triggered by Ca2+ and drives membrane fusion. Cell *97*, 165-174.

Couve, A., and Gerst, J.E. (1994). Yeast Snc proteins complex with Sec9. Functional interactions between putative SNARE proteins. J Biol Chem *269*, 23391-23394.

Ferro-Novick, S., and Jahn, R. (1994). Vesicle fusion from yeast to man. Nature *370*, 191-193.

Gerst, J.E. (2003). SNARE regulators: matchmakers and matchbreakers. Biochim Biophys Acta *1641*, 99-110.

Hanson, P.I., Roth, R., Morisaki, H., Jahn, R., and Heuser, J.E. (1997). Structure and conformational changes in NSF and its membrane receptor complexes visualized by quick-freeze/deep-etch electron microscopy. Cell *90*, 523-535.

Hu, K., Carroll, J., Fedorovich, S., Rickman, C., Sukhodub, A., and Davletov, B. (2002). Vesicular restriction of synaptobrevin suggests a role for calcium in membrane fusion. Nature *415*, 646-650.

Hubbell, W.L., Cafiso, D.S., and Altenbach, C. (2000). Identifying conformational changes with site-directed spin labeling. Nat Struct Biol *7*, 735-739.

Hubbell, W.L., Gross, A., Langen, R., and Lietzow, M.A. (1998). Recent advances in site-directed spin labeling of proteins. Curr Opin Struct Biol *8*, 649-656.

Hubbell, W.L., McHaourab, H.S., Altenbach, C., and Lietzow, M.A. (1996). Watching proteins move using site-directed spin labeling. Structure *4*, 779-783.

Jahn, R., Lang, T., and Sudhof, T.C. (2003). Membrane fusion. Cell *112*, 519-533.

Jahn, R., and Sudhof, T.C. (1999). Membrane fusion and exocytosis. Annu Rev Biochem *68*, 863-911.

Katz, L., Hanson, P.I., Heuser, J.E., and Brennwald, P. (1998). Genetic and morphological analyses reveal a critical interaction between the C-termini of two SNARE proteins and a parallel four helical arrangement for the exocytic SNARE complex. EMBO J *17*, 6200-6209.

Kim, C.S., Kweon, D.H., and Shin, Y.K. (2002). Membrane topologies of neuronal SNARE folding intermediates. Biochemistry *41*, 10928-10933.

Kweon, D.H., Kim, C.S., and Shin, Y.K. (2002). The membrane-dipped neuronal SNARE complex: a site-directed spin labeling electron paramagnetic resonance study. Biochemistry *41*, 9264-9268.

Kweon, D.H., Kim, C.S., and Shin, Y.K. (2003a). Insertion of the membrane-proximal region of the neuronal SNARE coiled coil into the membrane. J Biol Chem *278*, 12367-12373.

Kweon, D.H., Kim, C.S., and Shin, Y.K. (2003b). Regulation of neuronal SNARE assembly by the membrane. Nat Struct Biol *10*, 440-447.

Lin, R.C., and Scheller, R.H. (1997). Structural organization of the synaptic exocytosis core complex. Neuron *19*, 1087-1094.

Lin, R.C., and Scheller, R.H. (2000). Mechanisms of synaptic vesicle exocytosis. Annu Rev Cell Dev Biol *16*, 19-49.

Macosko, J.C., Kim, C.H., and Shin, Y.K. (1997). The membrane topology of the fusion peptide region of influenza hemagglutinin determined by spin-labeling EPR. J Mol Biol *267*, 1139-1148.

Marash, M., and Gerst, J.E. (2001). t-SNARE dephosphorylation promotes SNARE assembly and exocytosis in yeast. Embo J *20*, 411-421.

McHaourab, H.S., Lietzow, M.A., Hideg, K., and Hubbell, W.L. (1996). Motion of spin-labeled side chains in T4 lysozyme. Correlation with protein structure and dynamics. Biochemistry *35*, 7692-7704.

McNew, J.A., Parlati, F., Fukuda, R., Johnston, R.J., Paz, K., Paumet, F., Sollner, T.H., and Rothman, J.E. (2000). Compartmental specificity of cellular membrane fusion encoded in SNARE proteins. Nature *407*, 153-159.

Nicholson, K.L., Munson, M., Miller, R.B., Filip, T.J., Fairman, R., and Hughson, F.M. (1998). Regulation of SNARE complex assembly by an N-terminal domain of the t-SNARE Sso1p. Nat Struct Biol *5*, 793-802.

Pabst, S., Margittai, M., Vainius, D., Langen, R., Jahn, R., and Fasshauer, D. (2002). Rapid and selective binding to the synaptic SNARE complex suggests a modulatory role of complexins in neuroexocytosis. J Biol Chem *277*, 7838-7848.

Parlati, F., Weber, T., McNew, J.A., Westermann, B., Sollner, T.H., and Rothman, J.E. (1999). Rapid and efficient fusion of phospholipid vesicles by the alpha-helical core of a SNARE complex in the absence of an N-terminal regulatory domain. Proc Natl Acad Sci U S A *96*, 12565-12570.

Poirier, M.A., Xiao, W., Macosko, J.C., Chan, C., Shin, Y.K., and Bennett, M.K. (1998). The synaptic SNARE complex is a parallel four-stranded helical bundle. Nat Struct Biol *5*, 765-769.

Protopopov, V., Govindan, B., Novick, P., and Gerst, J.E. (1993). Homologs of the synaptobrevin/VAMP family of synaptic vesicle proteins function on the late secretory pathway in S. cerevisiae. Cell *74*, 855-861.

Rabenstein, M., and Shin, Y.K. (1995). A peptide from the heptad repeat of human immunodeficiency virus gp41 shows both membrane binding and coiled-coil formation. Biochemistry *34*, 13390-13397.

Rizo, J., and Sudhof, T.C. (2002). SNAREs and Munc18 in synaptic vesicle fusion. Nat Rev Neurosci *3*, 641-653.

Rosenmund, C., Sigler, A., Augustin, I., Reim, K., Brose, N., and Rhee, J.S. (2002). Differential control of vesicle priming and short-term plasticity by Munc13 isoforms. Neuron *33*, 411-424.

Rossi, G., Salminen, A., Rice, L.M., Brunger, A.T., and Brennwald, P. (1997). Analysis of a yeast SNARE complex reveals remarkable similarity to the neuronal SNARE complex and a novel function for the C terminus of the SNAP-25 homolog, Sec9. J Biol Chem *272*, 16610-16617.

Rothman, J.E. (1994). Mechanisms of intracellular protein transport. Nature *372*, 55-63.

Sollner, T., Bennett, M.K., Whiteheart, S.W., Scheller, R.H., and Rothman, J.E. (1993). A protein assembly-disassembly pathway in vitro that may correspond to sequential steps of synaptic vesicle docking, activation, and fusion. Cell *75*, 409-418.

Sudhof, T.C. (2002). Synaptotagmins: why so many? J Biol Chem *277*, 7629-7632.

Sutton, R.B., Fasshauer, D., Jahn, R., and Brunger, A.T. (1998). Crystal structure of a SNARE complex involved in synaptic exocytosis at 2.4 A resolution. Nature *395*, 347-353.

Thorgeirsson, T.E., Russell, C.J., King, D.S., and Shin, Y.K. (1996). Direct determination of the membrane affinities of individual amino acids. Biochemistry *35*, 1803-1809.

Weber, T., Zemelman, B.V., McNew, J.A., Westermann, B., Gmachl, M., Parlati, F., Sollner, T.H., and Rothman, J.E. (1998). SNAREpins: minimal machinery for membrane fusion. Cell *92*, 759-772.

Weimbs, T., Low, S.H., Chapin, S.J., Mostov, K.E., Bucher, P., and Hofmann, K. (1997). A conserved domain is present in different families of vesicular fusion proteins: a new superfamily. Proc Natl Acad Sci U S A *94*, 3046-3051.

Wimley, W.C., and White, S.H. (1996). Experimentally determined hydrophobicity scale for proteins at membrane interfaces. Nat Struct Biol *3*, 842-848.

Yau, W.M., Wimley, W.C., Gawrisch, K., and White, S.H. (1998). The preference of tryptophan for membrane interfaces. Biochemistry *37*, 14713-14718.

3.8 Figures and Captions

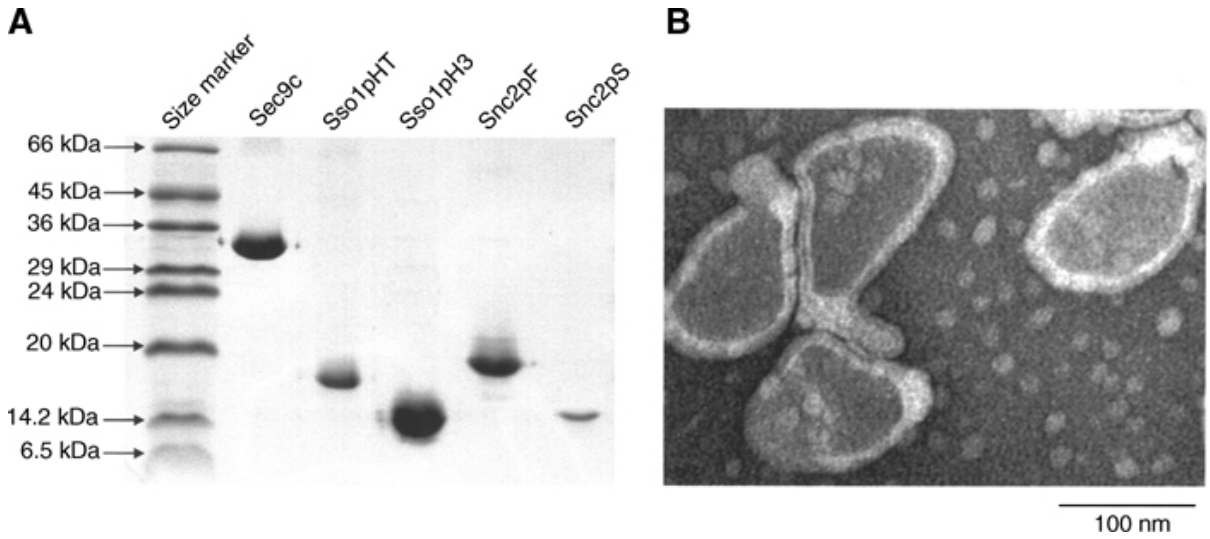

Figure 3-1. Characterization of SNARE proteins and lipid vesicles.

(A). SDS−PAGE analysis of recombinant SNARE proteins used in this study.

(B). Electron micrograph of negatively stained Snc2pF-reconstituted vesicles.

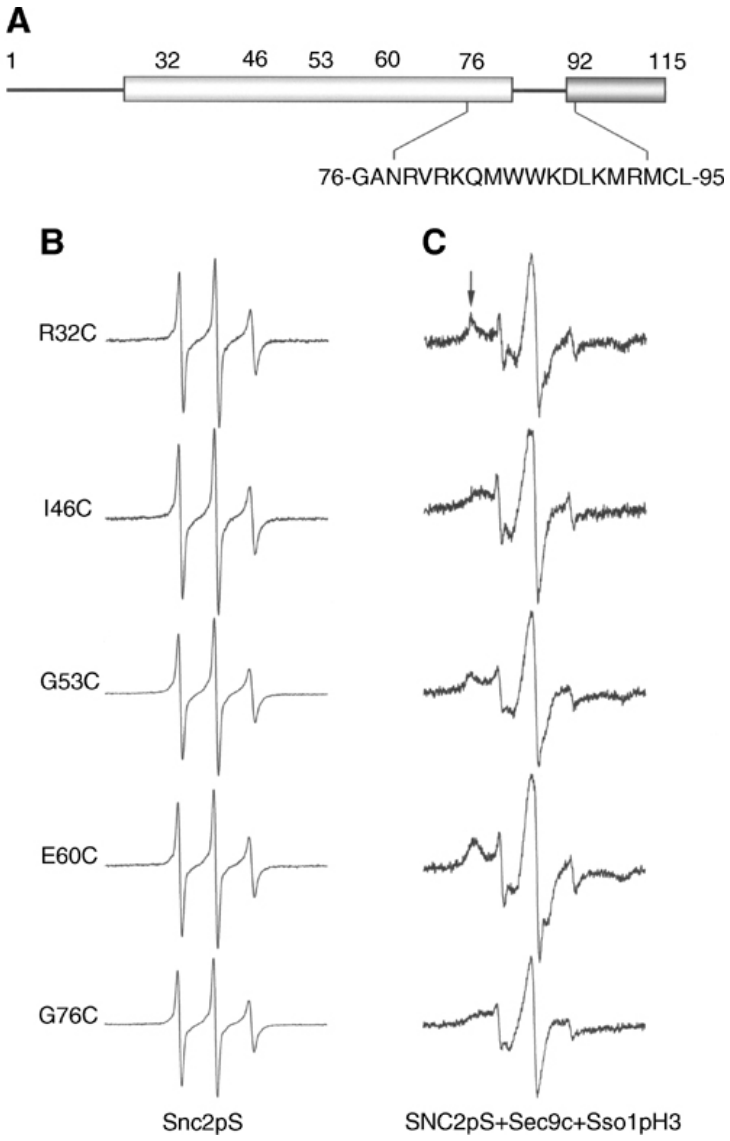

Figure 3-2. SDSL EPR detects SNARE complex formation at various positions.

(A). Spin-labeled positions are indicated on the primary structural diagram. Amino-acid sequence from positions 76−95 is shown.

(B). Room temperature EPR spectra for spin-labeled Snc2pS at various positions.

(C). Spectra for Snc2pS after mixing with the four-fold molar excess of Sec9c and Sso1pH3. The arrows indicate the immobile spectral component resulting from the formation of SNARE complexes.

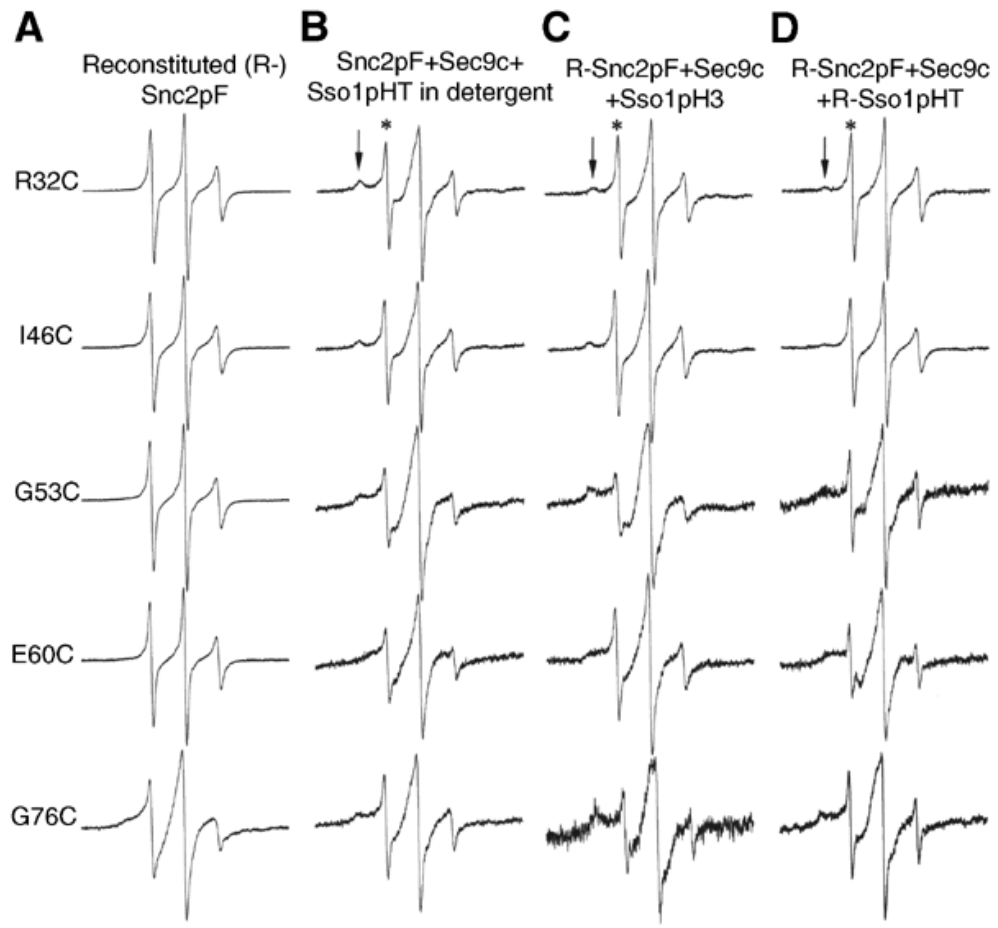

Figure 3-3. EPR assay of SNARE complex formation.

(A). EPR spectra for reconstituted (R-) Snc2pF mutants.

(B). EPR spectra for detergent solubilized Snc2pF mutants after mixing with Sso1pHT and Sec9c. EPR spectra are composed of two components: the sharp one (*) representing uncomplexed Snc2pF and the broad one (arrows) representing the SNARE complex. For each spin-labeled mutant, the composite spectrum is basically the sum of the spectrum in (A) and the spectrum similar to those in Figure 3-2C, in an appropriate ratio. The standard spectral decomposition analysis (Thorgeirsson et al., 1996) provides the fraction of Snc2pF in the complex ($f_{complex}$) and that in an unstructured form

(f_{free}). For each mutant, the percentage of complex formation was calculated from the equation $[f_{complex}/(f_{complex}+f_{free})\times 100]$: R32C, 68%; I46C, 60%; G53C, 84%; E60C, 82%; and G76C, 40%.

(C). EPR spectra for R-Snc2pF mixed with Sso1pH3 and Sec9c (soluble t-SNAREs) in the absence of the detergent. The percentages of complex formation for individual mutants are: R32C, 60%; I46C, 62%; G53C, 91%; E60C, 76%; and G76C, 50%.

(D). EPR spectra taken after mixing R-Snc2pF with R-Sso1pHT and Sec9c. The percentages of complex formation for individual mutants are: R32C, 38%; I46C, 33%; G53C, 82%; E60C, 85%; and G76C, 49%. In all cases, the four-fold molar excess of t-SNAREs was mixed with reconstituted v-SNARE mutants.

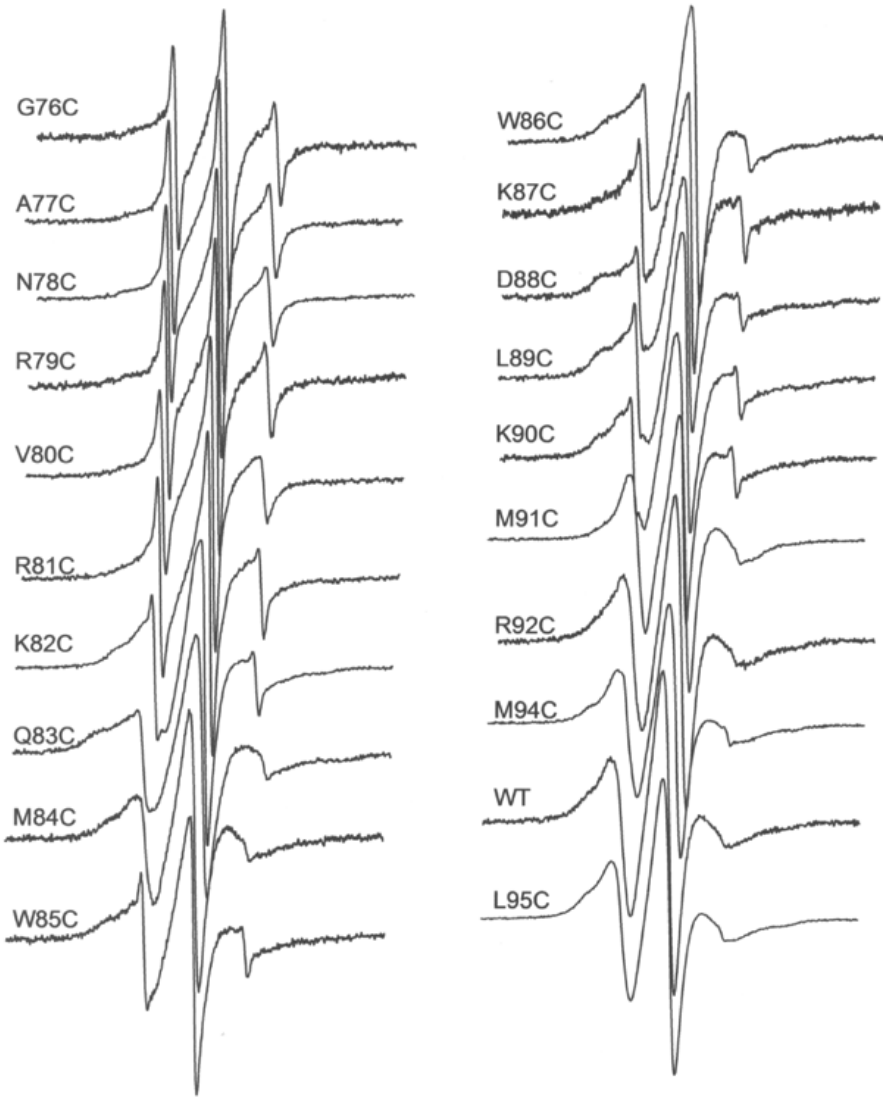

Figure 3-4. Room temperature EPR spectra for the interfacial region of reconstituted (R-) Snc2pF.

We note that the EPR spectrum for G76C here is slightly different from that in Figure 3-3A: the sharp component is a little less in the latter. The spectral decomposition analysis of the spectrum of G76C in Figure 3-4 indicated that there was an approximately 5% contamination of freely diffusing free spin species in the sample, which should not alter the accessibility parameter values. The first derivative mode presentation of EPR spectra makes such small contamination conspicuous.

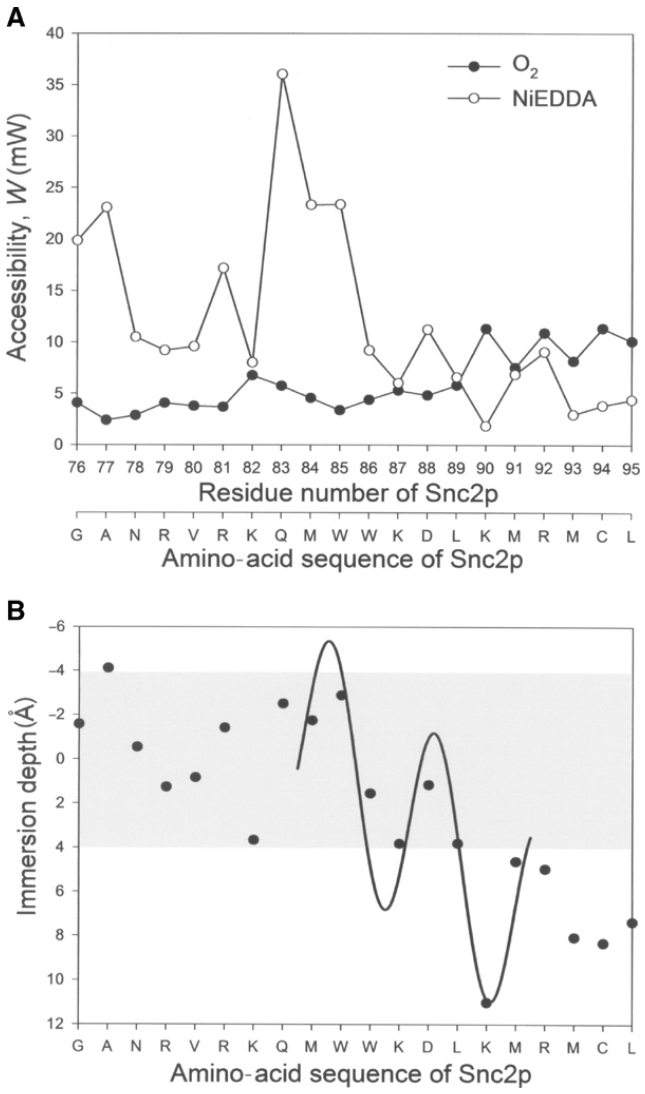

Figure 3-5. EPR accessibility measurements.

(A). Accessibility parameters W_{O2} (closed circles) and W_{NiEDDA} (open circles) are plotted against the amino-acid sequence.

(B). Membrane immersion depths versus the amino-acid sequence of Snc2pF. The head group region of the lipid vesicles is shown shaded. The solid line represents the fit on the basis of a tilted α-helical model (see text). Typical accessibility parameter values for the fully exposed residues are approximately 30 and 4 mW for NiEDDA and O_2, respectively, and typical W_{NiEDDA} and W_{O2} values for the fully membrane-inserted residues are around 2 and 12 mW, respectively.

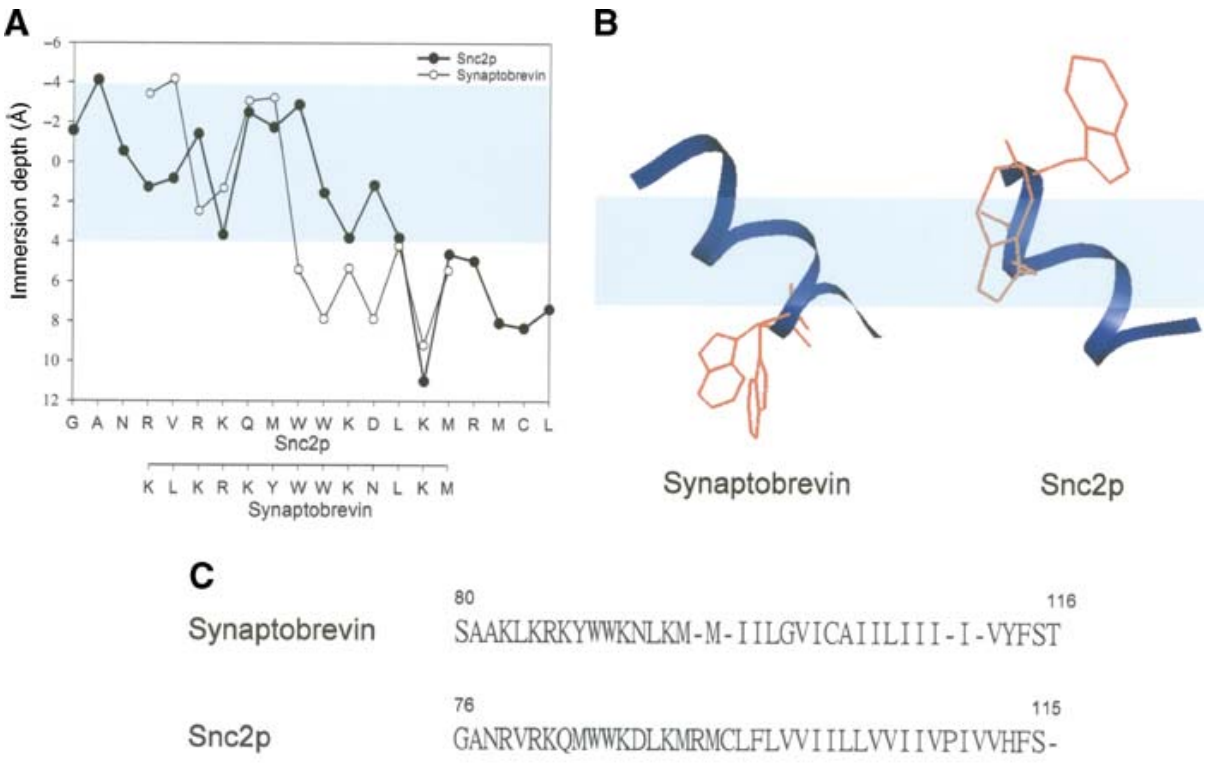

Figure 3-6. Comparison of membrane topologies of the interfacial regions between neuronal and yeast v-SNAREs.

(A). Membrane immersion depths of Snc2pF (closed circles) and those of synaptobrevin (open circles). The shaded region is the head group of the lipid bilayer.

(B). Topological models for Snc2p and synaptobrevin. Amino-acid side chains for two interfacial tryptophans are shown highlighted.

(C). Sequence alignment of the membrane-proximal regions of synaptobrevin and Snc2p.

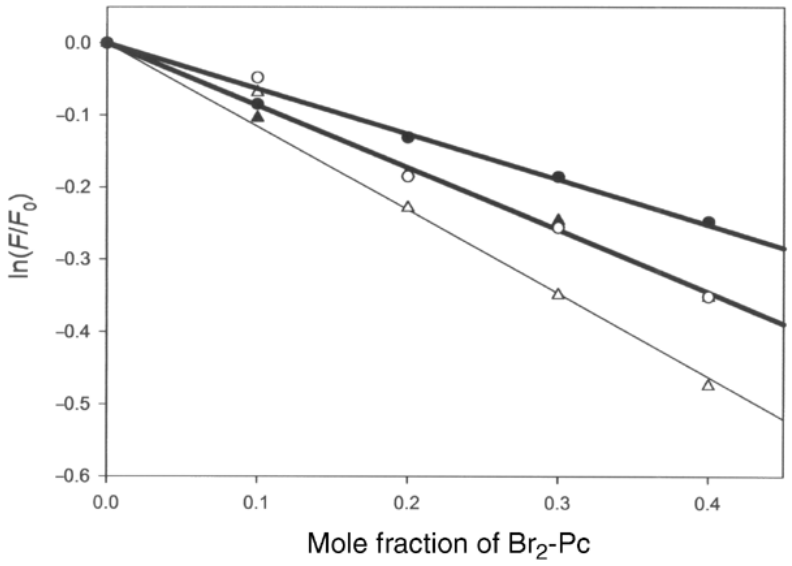

Figure 3-7. Comparison of fluorescence quenching by lipid quenchers for the two Trp residues between Snc2pF and synaptobrevin.

The logarithm of the ratio $\ln(F/F_0)$, where F_0 is the fluorescence intensity in the absence and F is that in the presence of the lipid quencher, is plotted against the mole fraction of 6,7-Br_2-PC for synaptobrevin (open triangles) and Snc2pF (closed triangles), and the mole fraction of 11,12-Br_2-PC for synaptobrevin (open circles) and Snc2pF (closed circles).

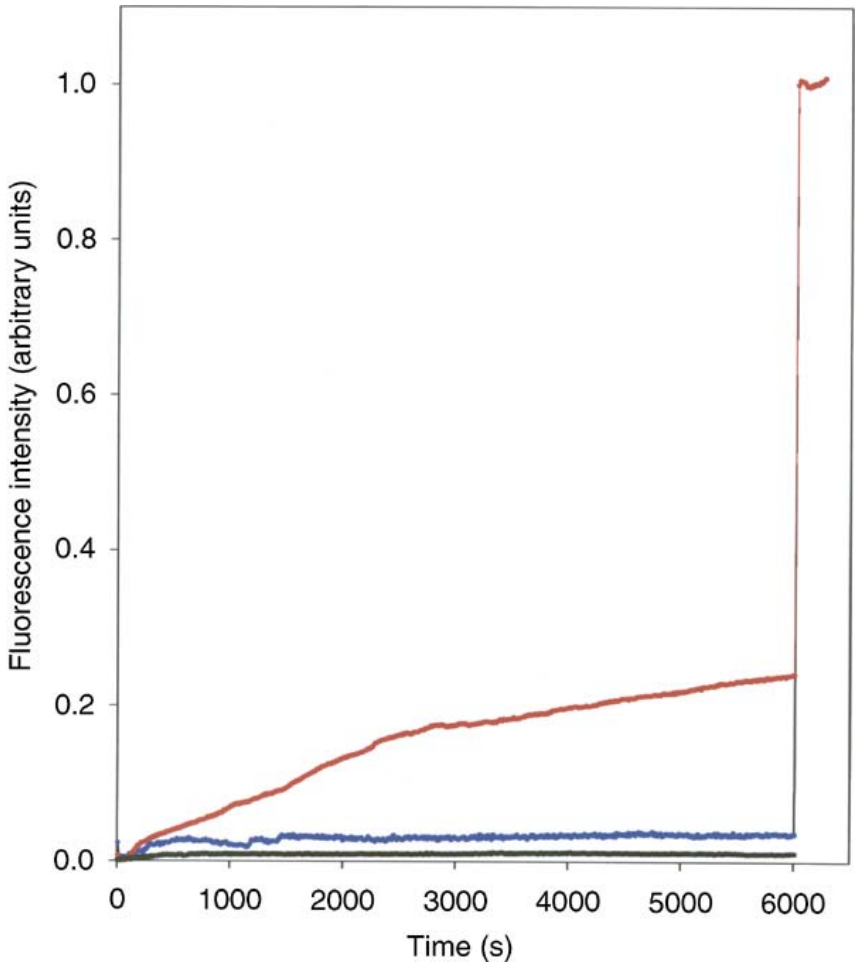

Figure 3-8. Lipid-mixing fusion assays monitored by fluorescence.

The donor/acceptor pairs N-Rh-PE/N-NBD-PE were incorporated into the vesicles containing v-SNARE. Fusion between v-SNARE-reconstituted vesicles and t-SNARE-reconstituted vesicles leads to the dilution of dyes and, consequently, an increase in the average distance between the donor and the acceptor, which results in an increase in donor fluorescence. The red line is the time trace of the fluorescence change after mixing reconstituted yeast v- and t-SNAREs. The black line is the control run after mixing only reconstituted Sso1pHT and reconstituted Snc2pF without adding Sec9c. The blue line is the time trace for neuronal SNAREs, indicating virtually no lipid mixing. The fusion reaction was terminated by introducing 1% (v/v) Triton X-100, which results in the sudden jump in the fluorescence intensity.

3.9 Supplementary Data

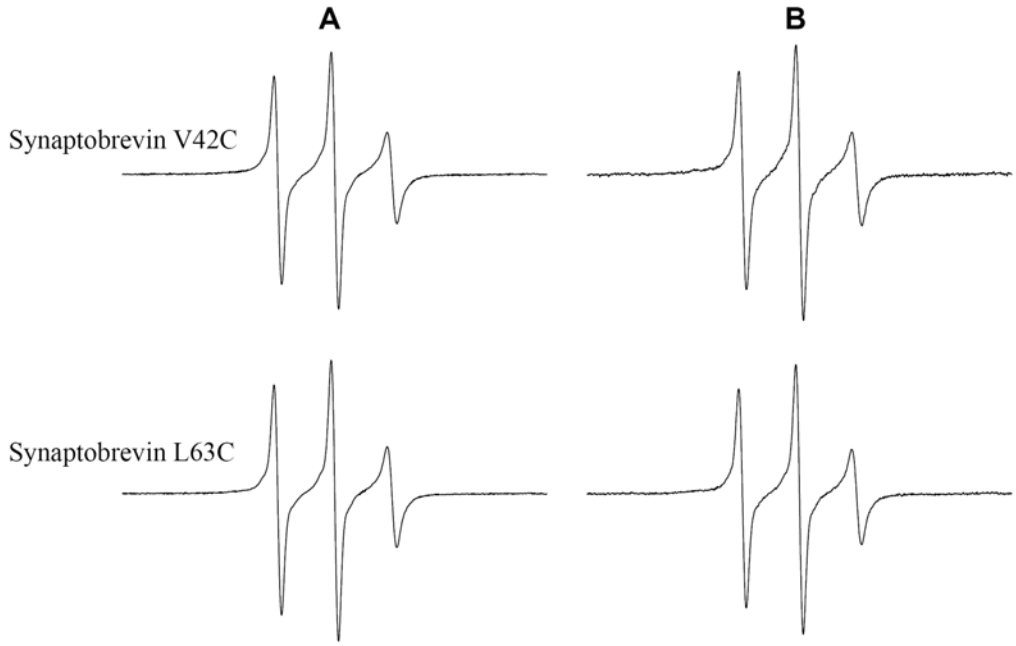

Figure 3-9. EPR assay of neuronal SNARE complex formation.

Recombinant Syntaxin-1A without the Habc domain (SynHT, amino acids 199-288), SNAP-25 (amino acid 1-206), and full-length synaptobrevin (amino acids 1-116) were used in this study. Spin labeled synaptobrevin mutants were reconstituted into POPC vesicles containing 15 mole% DOPS. SynHT was reconstituted into a separate vesicle fraction of the same lipid composition. In both cases, the lipid-to-protein ratio was 300:1. Reconstituted synaptobrevin was mixed with the four-fold excess of a 1:1 mixture of reconstituted SynHT and SNAP-25.

(A). EPR spectra before mixing with t-SNAREs.

(B). EPR spectra after mixing with t-SNAREs.

For each mutant, the EPR spectra before and after the mixing were virtually identical, indicating that no apparent SNARE assembly has occurred. The spectrum did not change over the period of one day. The final concentration of synaptobrevin was approximately 20 μM.

CHAPTER 4: YKT6 IS A CORE CONSTITUENT OF MEMBRANE FUSION MACHINERIES AT THE *ARABIDOPSIS TRANS*-GOLGI NETWORK[1]

Yong Chen, Yeon-Kyun Shin[2] and Diane C. Bassham[2]

4.1 Abstract

SNARE complex formation is essential for membrane fusion in exocytotic and vacuolar trafficking pathways. Vesicle-associated (v-) SNARE associates with a target membrane (t-) SNARE to form a SNARE complex bridging two membranes, which may facilitate membrane fusion. The Arabidopsis genome encodes a large number of predicted SNARE proteins that might function primarily as fusogens for vesicle transport in endomembrane systems. The SNAREs SYP41, SYP61 and VTI12 reside in the *trans*-Golgi network and have been proposed to function together in vesicle fusion with this organelle. Here, we use a liposome fusion assay to demonstrate that VTI12 and either SYP41 or SYP61, but not both, are required for membrane fusion. This indicates that SYP41 and SYP61 are likely to function in independent vesicle fusion reactions in Arabidopsis. In addition, we have identified two new functionally interchangeable components, YKT61 and YKT62, that show sequence similarity to the multifunctional yeast SNARE YKT6. Both YKT61 and YKT62 interact with SYP41 and are essential for membrane fusion mediated by either

[1] This paper is published in *JMB* 2005, 350(1), 92-101. Necessary modifications were made to fit the format of this thesis.

[2] Corresponding authors

SYP41 or SYP61. These results therefore define the core constituents required for membrane fusion at the Arabidopsis *trans*-Golgi network.

4.2 Introduction

Proteins that reside in endomembrane organelles, or that are secreted from the cell, reach their site of function by transport through the endomembrane system. This system consists of a series of membrane-enclosed compartments that are connected by a flow of transport vesicles moving protein and lipid cargo from one organelle to the next along the pathway. The fidelity of vesicle trafficking, and therefore of protein localization, is critical to cellular function, and is controlled by the packaging of the appropriate cargo into a budding transport vesicle, and by fusion of that vesicle with the correct target organelle (Sanderfoot and Raikhel, 1999).

The fusion of a transport vesicle with its target membrane, or the homotypic fusion of two identical membrane compartments, requires pairing of cognate soluble *N*-ethylmaleimide-sensitive factor attachment protein receptor (SNARE) partners anchored separately to two membranes (McNew et al., 2000; Sollner et al., 1993). For fusion to occur, the membrane-proximal SNARE motif of the vesicle (v-) SNARE must interact with those of the target membrane (t-) SNARE in parallel to form a four-stranded helical bundle (Poirier et al., 1998; Sutton et al., 1998), which brings the two membranes into close proximity. The SNARE complex shares striking structural similarity with viral fusion proteins, including influenza hemagglutinin and HIV gp41 (Skehel and Wiley, 1998). Thus, SNARE assembly is thought to provide the energy for membrane fusion, as is believed to be the case for the

viral fusion proteins (Eckert and Kim, 2001). There is evidence that specific SNARE pairing is sufficient to drive membrane fusion in a cell-free reconstituted system (Chen et al., 2004; McNew et al., 2000; Weber et al., 1998).

The Arabidopsis genome encodes 54 predicted SNARE proteins based on sequence similarity to yeast and mammalian SNAREs (Bock et al., 2001; Sanderfoot et al., 2000; Uemura et al., 2004). A SNARE complex consists typically of four proteins/helices generating a four-stranded coiled-coil, with three helices donated by the t-SNARE and one by the v-SNARE. A function of plant SNAREs in vesicle fusion has been postulated on the basis of a number of indirect criteria. For example, an Arabidopsis mutant lacking the cytokinesis-specific t-SNARE KNOLLE accumulates unfused vesicles at the plane of cell division (Lauber et al., 1997; Lukowitz et al., 1996), and a dominant-negative SNARE mutant inhibits secretion in tobacco (Geelen et al., 2002). However, while there is evidence that plant SNAREs play a role in vesicle trafficking, it is not known whether SNARE assembly is sufficient to drive membrane fusion.

We have shown previously that the neuronal syntaxin-like t-SNARE SYP41 resides in the *trans*-Golgi network (TGN) in Arabidopsis, and interacts with two other SNAREs, VTI12 and SYP61 (Bassham et al., 2000; Sanderfoot et al., 2001a). While these three SNAREs (presumably with another, unidentified SNARE partner) have been proposed to form a SNARE complex and to function in vesicle fusion at the TGN, it is not known whether they are all present in the same complex, and whether they catalyze vesicle fusion. In addition, a T-DNA knockout mutant in the *SYP41* gene is gametophytic lethal (Sanderfoot et al., 2001b) and a double knockout in *VTI12* and the partially redundant gene *VTI11* is embryo lethal (Surpin et al., 2003). However, a knockout in *SYP61* has the relatively mild

phenotype of sensitivity to abiotic stresses (Zhu et al., 2002), even though SYP61 appears to be encoded by a single gene. This wide variation in the severity of mutant phenotypes suggests that SYP41, SYP61 and VTI12 do not simply function together as a protein complex in a single reaction.

Here, to address the role of these TGN-localized SNAREs in membrane fusion directly, we utilize purified recombinant SNAREs in an *in vitro* liposome fusion assay. Our results show that liposomes containing either SYP41 or SYP61 are competent for fusion with VTI12-containing liposomes, indicating that these two proteins can function independently of each other. We have also identified YKT61 and YKT62 as functionally interchangeable components of the SNARE complexes, required for both SYP41- and SYP61-mediated vesicle fusion.

4.3 Results

4.3.1 Expression of Recombinant SNAREs in Escherichia Coli

It was considered likely that, in addition to SYP41, SYP61 and VTI12, a fourth SNARE would be necessary for TGN vesicle fusion. YKT6 is a multifunctional SNARE that was identified as being required for ER-to-Golgi and intra-Golgi transport in yeast (Lupashin et al., 1997; McNew et al., 1997). It is also required for several transport pathways to the yeast vacuole (Dilcher et al., 2001), whereas in mammals it plays a role in transport from endosomes to the TGN (Tai et al., 2004). Arabidopsis homologs of YKT6 were therefore considered good candidates for components of the TGN SNARE complex. Arabidopsis has two genes, YKT61 and YKT62, that could encode YKT6-like proteins (Sanderfoot et al.,

2000). YKT61 is expressed ubiquitously throughout the plant, whereas expression of YKT62 has not been detected, although a putative TATA box is present in its promoter (Uemura et al., 2004). YKT62 may therefore be expressed under specific environmental conditions, or restricted to certain developmental stages.

Full-length cDNAs encoding SYP41, SYP61, VTI12, YKT61 and YKT62 were generated by RT-PCR using RNA isolated from Arabidopsis seedlings. The identity of the cDNAs was confirmed by sequencing, indicating that YKT62 is expressed under these conditions. The cDNAs were further cloned and expressed in *E. coli* as fusions with an N-terminal His_6 tag and purified using Ni-NTA resin. Purified proteins were separated by SDS-PAGE and stained with Coomassie brilliant blue (Figure 4-1a). In each case, a band of the expected molecular mass for the His-fusion was obtained. The purity of each protein was estimated as at least 90%.

4.3.2 YKT61 and YKT62 Interact with TGN SNAREs in vitro

The ability of the recombinant proteins to interact was assessed using an *in vitro* binding assay. SYP41 (~10 μg) was incubated with an equal amount of each of the other SNAREs, both singly and in combination. Interactions were detected by co-immuno-precipitation using immobilized SYP41 antibodies (Bassham et al., 2000), followed by SDS-PAGE and silver-staining (Figure 4-1b). VTI12, YKT61 and YKT62 each co-precipitated individually with SYP41, indicating that each of these proteins can interact with SYP41 directly. In addition, when SYP41 was incubated with SYP61+VTI12+YKT61 (or YKT62), both VTI12 and YKT61 (or YKT62) were seen to co-precipitate. The efficiency of SYP41

immunoprecipitation was greater than 90%, and up to 50% of the VTI12, YKT61 and YKT62 co-precipitated (Figure 4-1b). No immunoprecipitation of any of the SNAREs was observed when the experiment was performed in the absence of SYP41 (data not shown).

From the silver-stained gel (Figure 4-1b), it was not clear whether any SYP61 co-precipitated with SYP41. A degradation product of SYP41, apparently generated during the incubation with the antibody column, migrated at the same position in the gel as SYP61. This prevented us from determining whether a small amount of SYP61 might be present, possibly due to a weak or transient interaction. To clarify this, the above binding assay was repeated, except that 5 μg of each protein was used instead of 10 μg. The immunoprecipitate was separated by SDS-PAGE and transferred to a nitrocellulose membrane, and SYP61 was detected using affinity-purified antibodies (Sanderfoot et al., 2001a). It is evident from the immunoblot that SYP61 also co-precipitates with SYP41, both individually and in combination with VTI12 and YKT61 or YKT62 (Figure 4-1c), although at a much lower efficiency than the other SNAREs. These data demonstrate that interactions between the recombinant proteins recapitulate those seen *in vivo*, and implicate YKT61 and YKT62 as previously unknown members of the TGN SNARE complex. However, they suggest also that SYP61 is not present in stoichiometric amounts in the complex, and therefore that these proteins may not simply constitute a four-helix SNARE complex *in vivo*.

4.3.3 Fusion of Proteoliposomes by Recombinant Arabidopsis SNAREs

To determine whether the Arabidopsis TGN SNAREs are able to drive membrane fusion, a proteoliposome fusion assay was employed (Chen et al., 2004; Struck et al., 1981).

First, recombinant SYP41 and SYP61 were incorporated together into phospholipid vesicles containing 60 mol% 1,2-dioleoyl-*sn*-glycero-3-phosphocholine (DOPC), 20 mol% 1-palmitoyl-2-oleoyl-*sn*-glycero-3-(phospho-rac-(1-glycerol)) (POPG), and 20 mol% 1-palmitoyl-2-oleoyl-*sn*-glycero-3-phos-phoethanolamine (POPE) using a Bio-beads/dialysis method (Chen et al., 2004). VTI12 was incorporated into separate vesicles of the same lipid composition, except for an additional 1.5 mol% each of *N*-(7-nitro-2,1,3,benzoxadiazol-4-yl) (NBD) and rhodamine-labeled fluorescent lipids (NBD-PE and rhodamine-PE) replacing an equal amount of DOPC. After the reconstitution, the vesicles were examined with negative-staining electron microscopy (Figure 4-2a), and the efficiency of reconstitution was determined with SDS-PAGE and staining with Coomassie brilliant blue (Figure 4-2b). The diameter of vesicles was approximately 100 nm, and the reconstitution efficiency was more than 40%.

Fusion of a SYP41/SYP61-reconstituted liposome (acceptor vesicle) with a fluorescence-tagged VTI12-reconstituted liposome (donor vesicle) would result in dilution of the fluorescent lipids, leading to a decrease in fluorescence quenching between NBD and rhodamine, and consequently an increase in NBD fluorescence. YKT61 and YKT62 lack transmembrane domains, and are likely to associate with membranes *in vivo via* a lipid modification. However, recombinant YKT61 and YKT62 do not have lipid modifications, and these proteins were added directly to the liposome fusion reaction in the soluble form.

When SYP41/SYP61-containing vesicles were mixed with VTI12-containing fluorescent vesicles, no change in fluorescence was observed, similar to the case with the incubation of protein-free liposomes, indicating that no liposome fusion occurred. However, addition of either YKT61 or YKT62 to the mixture resulted in a rapid increase in

fluorescence within five minutes, indicating that liposome fusion had occurred. YKT61 and YKT62 did not cause liposome fusion when one or both liposomes were protein-free, demonstrating that both the vesicle-bound SNAREs and YKT61 or YKT62 are required for membrane fusion (Figure 4-3).

4.3.4 SYP41 and SYP61 Can Function in Independent Membrane Fusion Events

While SYP41 and SYP61 physically interact *in vivo* (Sanderfoot et al., 2001a) and *in vitro* (Figure 4-1c), *syp41* and *syp61* knockout mutants have very different phenotypes, indicating that they have at least partially independent functions. We therefore tested whether SYP41 or SYP61 can function in vesicle fusion as the sole t-SNARE. Recombinant SYP41 was incorporated into acceptor liposomes in the absence of SYP61, and fusion with VTI12-containing donor liposomes assayed in the presence of either YKT61 or YKT62 (Figure 4-4a). Surprisingly, efficient fusion was observed under these conditions, indicating that SYP41 alone is sufficient to act as the t-SNARE in this fusion reaction. Similarly, SYP61 functioned in fusion in the absence of SYP41 (Figure 4-4b). In each case, no difference was observed between YKT61 and YKT62 in the rate of fusion, and these proteins appear to be inter-changeable in the reaction. These results indicate that a SYP41/SYP61 complex is not necessary for liposome fusion, and raise the possibility that these proteins function in independent vesicle fusion reactions *in vivo*.

To confirm that the observed liposome fusion reflects a requirement for the SNARE proteins, we took advantage of the availability of antibodies against SYP41 (Bassham et al., 2000). Affinity-purified SYP41 antibodies were incubated with the SYP41-reconstituted

acceptor liposomes prior to mixing with VTI12-reconstituted donor liposomes and soluble YKT61 (Figure 4-5a) or YKT62 (data not shown). Liposome fusion was inhibited completely by the antibodies when compared with the control reaction in the absence of the SYP41 antibody, or in the presence of pre-immune serum, demonstrating a specific requirement for SYP41 in membrane fusion.

As a further confirmation of the specificity of fusion, a soluble form of VTI12 was synthesized lacking the transmembrane domain. This soluble protein efficiently inhibited the fusion reaction containing reconstituted SYP41 and VTI12 and soluble YKT61 (Figure 4-5b), presumably by competing with reconstituted VTI12 for interaction with the other components.

4.3.5 Inner Leaflet Lipid Mixing Assay

While an increase in lipid fluorescence of liposomes is indicative of the mixing of lipids, this could theoretically occur by hemifusion between the outer leaflets of the liposomes, with no mixing of vesicle contents, rather than by complete fusion of both leaflets. To confirm that the Arabidopsis SNAREs are able to drive complete liposome fusion, an inner leaflet mixing assay employing dithionite was performed (McIntyre and Sleight, 1991). Under controlled conditions, sodium dithionite reduces NBD attached to the lipid head group in the outer leaflet to a non-fluorescent derivative, *N*-(7-amino-2,1,3-benzoxadiazole) (ABD), while leaving NBD in the inner leaflet largely unaffected (Figure 4-6a). When the dithionite-treated liposomes are used in fusion assays, any increase in fluorescence seen must be due to dequenching of fluorescent lipids in the inner leaflets, indicating complete fusion of both

halves of the lipid bilayer. Fusion assays were performed using SYP41- or SYP61-reconstituted liposomes and VTI12-reconstituted dithionite-treated fluorescent liposomes, in the presence of YKT61 (Figure 4-6b and 4-6c) or YKT62 (data not shown). The rate and extent of lipid mixing was identical for both dithionite-treated and untreated liposomes, indicating that complete fusion of the liposomes occurred in each case.

4.4 Discussion

The Arabidopsis genome encodes a large number of proteins that are predicted to be homologous to SNARE proteins from other organisms that have been characterized as parts of the membrane fusion machinery. Here, we demonstrate that a set of TGN-localized SNAREs from Arabidopsis are able to drive rapid and efficient membrane fusion in a cell-free fusion assay. Membrane fusion requires either SYP41 or SYP61 in one liposome, VTI12 in the other liposome, and an additional component, either YKT61 or YKT62. Our results therefore define the components required for the fusion of vesicles at the Arabidopsis TGN.

It has been shown both *in vivo* (Sanderfoot et al., 2001a) and *in vitro* (this work) that SYP41 and SYP61 can interact physically, suggesting that they function together as a t-SNARE. Unexpectedly, we found that it is not necessary for both SYP41 and SYP61 to be present for membrane fusion to occur. Liposomes reconstituted with either SYP41 or SYP61 are competent for fusion with VTI12-containing liposomes in the presence of YKT61/62. The hallmark of a SNARE complex is the parallel four-helix bundle that forms the core structure that bridges two membranes, facilitating fusion (Poirier et al., 1998; Sutton et al.,

1998). Sequence analysis indicates that each Arabidopsis TGN SNARE contains only one SNARE motif. Therefore, it is possible, although speculative, that the core structure of the Arabidopsis TGN SNARE complex might be a three-helix bundle instead of the usual four-helix bundle. It is possible also that one of the components contributes two copies to make a four-helix bundle (Xiao et al., 2001). Resolution of these possibilities awaits a more detailed structural analysis of the complex.

One question that remains unanswered is whether a SNARE complex containing both SYP41 and SYP61 actually forms and is functional for membrane fusion. The co-immunoprecipitation of these two proteins from Arabidopsis detergent extracts (Sanderfoot et al., 2001a) suggests that this complex is present *in vivo*. However, the dramatically different phenotypes of knockout mutants in SYP41 (pollen-lethal) (Sanderfoot et al., 2001b) and SYP61 (salt- and osmotic stress-sensitive) (Zhu et al., 2002) may indicate that at least some functions of these two proteins are independent of each other. It is possible that three different SNARE complexes function in distinct membrane fusion events *in vivo*, one containing SYP41, one containing SYP61, and one containing both proteins. If so, point mutations in these SNAREs that prevent formation of only one of the three potential complexes could provide valuable information as to the trafficking pathways requiring each of the complexes.

In addition to the known TGN SNAREs, we have identified new components required for vesicle fusion, YKT61 and YKT62. Ykt6 is a multifunctional SNARE in yeast and mammals (Dilcher et al., 2001; Tai et al., 2004), and has been proposed to participate in recycling from endosomes to the TGN (Tai et al., 2004). Arabidopsis has two Ykt6 homologs, YKT61 and YKT62 (Sanderfoot et al., 2000) that we have shown to be

interchangeable in SYP41/SYP61/VTI12-mediated liposome fusion. This may reflect functional redundancy or, alternatively, reaction specificity may be conferred by other regulatory proteins that, while not necessary in our *in vitro* system, are likely to be critical for appropriate control of membrane fusion *in vivo*.

Interestingly, it has been reported that expression of YKT62 was undetectable in various Arabidopsis tissues, whereas YKT61 was expressed ubiquitously(Uemura et al., 2004). We were able to isolate a YKT62 cDNA from young Arabidopsis seedlings, indicating that expression of this gene may be regulated by age or developmental stage of the plant. Several products were obtained by reverse transcription-polymerase chain reaction (RT-PCR) using YKT62-specific primers, and sequencing demonstrated that these consisted of multiple splice variants, resulting in small, in-frame deletions when compared with the mRNA predicted from the Arabidopsis genome sequence. A cDNA corresponding to the predicted sequence was used for all of our experiments; it will be interesting to determine whether the other splice variants are functional and whether any differences in function can be ascribed to these variants.

In conclusion, we have defined TGN-localized SNARE partners that can fuse proteoliposomes *in vitro* and are likely to function as the core of the fusion machinery in two distinct membrane fusion reactions *in vivo*. Additional SNAREs reside at the TGN in Arabidopsis, including the two SYP41-like proteins, SYP42 and SYP43 (Bassham et al., 2000). These proteins, while closely related in sequence, are known to have distinct functions, and it will be interesting to determine the function and specificity of these SNAREs in membrane fusion. Our *in vitro* experiments, when combined with *in vivo* studies

of cargo trafficking, will provide insight into the mechanisms and pathways of vesicle transport in the plant endomembrane system.

4.5 Materials and Methods

4.5.1 Plasmid Construction

The DNA fragments encoding full-length SYP41, SYP61, VTI12, YKT61 and YKT62 were obtained by PCR amplification from the *Arabidopsis thaliana* cDNAs using specific primers carrying an NdeI site and an XhoI site. These PCR products were digested and cloned into the pET-28b(+) expression vector (Novagen) between *Nde*I and *Xho*I sites. A DNA fragment encoding the soluble form of VTI12 (VTI12s, including amino acid residues 1–199), which was obtained by deletion of the transmembrane domain of wild-type VTI12, was subcloned into pET-28b(+) using the same *Nde*I and *Xho*I sites. All the constructs were verified by DNA sequencing from the Iowa State University DNA Sequencing and Synthesis Facility.

4.5.2 Protein Expression and Purification

Recombinant proteins of SYP41, SYP61, VTI12, VTI12s, YKT61 and YKT62 were expressed in *E. coli* strain Rosetta (DE3) pLysS (Novagen) as N-terminal His_6-tagged proteins. A sample (12 ml) of bacteria was inoculated overnight and transferred into 600 ml of Luria–Burtani media (LB broth) supplied with glucose (2 mg/ml), kanamycin (30 μg/ml), and chloramphenicol (25 μg/ml). The cells were grown at 37 °C until the absorbance at 600

nm (A_{600}) reached 0.6–0.8. Isopropyl-β-D-thiogalactopyranoside (IPTG) was added to 0.5 mM final concentration, and the cells were grown for four to six hours at 16 °C to induce the overexpression of recombinant proteins. The bacteria were then collected by low-speed centrifugation for ten minutes at 4 °C. The cell pellets were stored at −80 °C.

For purification, the cell pellets were resuspended in 10 ml of lysis buffer (50 mM NaH_2PO_4 (pH 8.0), 300 mM NaCl, 10 mM imidazole, 0.2% (v/v) Triton X-100, 10 mM β-mercaptoethanol, 2 mM 4-(2-aminoethyl)-benzenesulfonyl fluoride). For the soluble protein VTI12s, no detergent was added to the buffers used below. After breaking the cells by sonication on an ice-bath, *n*-lauroyl sarcosine was added to a final concentration of 1% (w/v) followed by rocking at 4 °C for 30 minutes. The cell lystate was then centrifuged at 15,000 × ***g*** for 20 minutes at 4 °C. The supernatant was collected and applied to a 2 ml bed volume of nickel-nitrilotriacetic acid (Ni-NTA) agarose beads (Qiagen), which were equilibrated with lysis buffer. The mixture was rocked for binding at 4 °C for 40 minutes. Then the beads were washed extensively with washing buffer I (50 mM NaH_2PO_4 (pH 8.0), 300 mM NaCl, 20 mM imidazole, 0.2% Triton X-100) and washing buffer II (50 mM Tris–HCl (pH 8.0), 300 mM NaCl, 50 mM imidazole, 0.2% Triton X-100). Finally, the recombinant proteins were eluted out from the beads by elution buffer (50 mM Tris–HCl (pH 8.0), 300 mM NaCl, 250 mM imidazole, 0.2% Triton X-100) except SYP41, which was eluted from the beads by 0.1% (w/v) SDS instead of 0.2% Triton X-100 in the elution buffer. The purified proteins can be stored at −80 °C in the presence of 10% (v/v) glycerol.

The purities of the recombinant SYP41, SYP61, VTI12, VTI12s, YKT61 and YKT62 were checked by SDS/10% PAGE and staining with Coomassie brilliant blue R-250.

4.5.3 Immunoprecipitation

Affinity-purified SYP41 antibodies were covalently cross-linked to protein A-Sepharose resin as described (Bassham et al., 2000). Ten micrograms each of the appropriate recombinant proteins was mixed in a total volume of 200 µl of phosphate-buffered saline containing 1 mM EDTA and 1% (v/v) Triton X-100 and incubated on ice for one hour. A 40 µl bed volume of SYP41 antibody resin in the above buffer was added, followed by incubation at 4 °C for one hour with rocking. The resin was washed five times in the same buffer, and bound protein eluted from the antibodies using 100 mM citric acid (pH 2.2) for ten minutes at room temperature. Samples were analyzed by SDS-PAGE and staining with silver or by immunoblotting using affinity-purified antibodies against SYP61.

4.5.4 Preparation of Lipid Vesicles

DOPC, POPG and POPE were chosen to mimic the phospholipids in plants. Two kinds of lipid vesicles were prepared for fusion assays: one with a pair of fluorescent dyes and the other without dyes. For the vesicles in the absence of fluorescent dyes, DOPC, POPG and POPE were dissolved and mixed in chloroform in a molar ratio of 60:20:20. A lipid film was deposited onto the wall of a glass test-tube by evaporating the chloroform under a stream of nitrogen gas, and the film was dried thoroughly to remove the residual organic solvent by placing the test-tube on a vacuum pump overnight. After that, the lipid film was hydrated by fusion assay buffer (25 mM HEPES (pH 7.4), 100 mM KCl), the total lipid concentration was set to 100 mM. Large unilamellar vesicles (LUVs) with a diameter of about 100 nm were prepared by an extruder (Avanti Polar Lipids). For the vesicles

containing fluorescent dyes, DOPC, POPG, POPE, NBD-PE (*N*-(7-nitro-2,1,3-benzoxadiazol-4-yl)phosphatidyl-ethanolamine) and rhodamine-PE (*N*-(lissamine rhodamine B sulfonyl)phosphatidyl-ethanolamine) were mixed at 57:20:20:1.5:1.5 molar ratios. LUVs were made following the same procedure as the vesicles without dyes, except the final lipid concentration was set to 10 mM.

4.5.5 Membrane Reconstitution

In order to reconstitute proteins into membrane, lipid vesicles were mixed with proteins at a 1:200 protein-to-lipid molar ratio. The detergent in the samples was removed by the Bio-beads/dialysis method. Bio-beads SM-2 were washed extensively with deionized water, and equilibrated with fusion assay buffer. Then the Bio-beads were added directly into the protein/lipid mixture in the amount of 200 mg of beads to 1 ml of solution. The mixture was rocked at 4 °C for 40 minutes, and the supernatant was taken out after centrifugation at 12,000 × ***g*** for five minutes at 4 °C. The same procedure was repeated three times. Then the protein reconstituted vesicles were dialyzed overnight against the fusion assay buffer containing 1 g/l of Bio-beads SM-2 to remove the trace amount of detergent. After dialysis, the sample was centrifuged at 12,000 × ***g*** to remove the protein and lipid aggregates. The detergent in YKT61 and YKT62 was removed by the same process, despite no lipid vesicle being added. The reconstitution efficiency was determined using SDS-PAGE, visualized by staining with Coomassie brilliant blue. The amount of protein in vesicles was estimated by comparing the band in the gel with that of the same protein of known concentration. In all cases, the efficiency was estimated to be in the range of 40–60%

(Figure 4-2b). The final protein-to-lipid molar ratios after reconstitution in all samples were approximately in the range of 1:400–1:500.

4.5.6 Electron Microscopy

SNARE-reconstituted vesicles were characterized with negative-staining electron microscopy at Iowa State University Bessey Microscopy Facility. The vesicles were diluted to 2–5 mM total lipids concentration, spread on 200-mesh formvar and carbon-coated grids, and stained with 1% (w/v) phosphotungstic acid (pH 6.7). The electron micrograph (Figure 4-2a) was taken on a JEOL 1200EX scanning/transmission electron microscope. Most vesicles showed approximately 100 nm in diameter.

4.5.7 Total Lipid Mixing Assay

In order to perform lipid mixing assays, VTI12 was reconstituted into donor vesicles containing fluorescent dyes (NBD-PE and rhodamine-PE), and either SYP41, or SYP61, or both were reconstituted into acceptor vesicles without fluorescent dyes. The donor and acceptor vesicles were mixed in a molar ratio of 1:9, and an equimolar amount of YKT61 or YKT62 to SYP41 or SYP61 was added directly to the mixture. The total lipid concentration was about 0.5 mM and the total sample volume was set to 100 µl. Fusion of donor vesicles with acceptors decreases quenching between rhodamine and NBD, and therefore increases the NBD fluorescence.

NBD fluorescence was followed with an excitation wavelength at 460 nm and emission at 530 nm. The fluorescence change was monitored at intervals of ten seconds

using a Cary Eclipse fluorescence spectrophotometer (Varian) with a 10 mm path length quartz cell (Starna) at 25 °C for 20 minutes. The maximum fluorescence intensity (MFI) was obtained by adding 1 µl of 25% (w/v) *n*-dodecylmaltoside into the reaction mixture to a final concentration of 0.25% (Parlati et al., 1999).

4.5.8 Inner Leaflet Lipid Mixing Assay

An inner layer lipid mixing assay was performed to confirm the fusion of both lipid bilayer halves mediated by SNARE proteins. The fluorescent dye NBD could be reduced to the non-fluorescent form ABD by dithionite; therefore, NBD fluorescence from the outer leaflet of the lipid vesicles could be eliminated selectively (McIntyre and Sleight, 1991).

The protein-reconstituted donor vesicles with fluorescent-labeled lipids located exclusively in the inner layer were prepared before the lipid mixing assay. Sodium dithionite (200 mM in 50 mM Tris-HCl, pH 10.0) was added directly into the protein-reconstituted donor vesicles. By controlling the amount of dithionite as well as reaction time, the reduction could be limited to the outer leaflet. Under experimental conditions, NBD fluorescence (emission at 534 nm) change was relatively small due to the quenching by rhodamine (emission at 590 nm); therefore, rhodamine fluorescence was chosen to monitor the reaction. Rhodamine fluorescence was monitored at 25 °C either by fluorescent scanning from 500 nm to 700 nm with the excitation at 460 nm, or by measuring the fluorescence changes at 590 nm with the excitation at 460 nm. Immediately after the fluorescence intensity at 590 nm reached approximately 50% of the intensity before treatment with dithionite, the reaction was stopped and the extra amount of sodium dithionite was removed

by centrifugation with a Sephacryl spin column (MicroSpin S-400 HR, Amersham), which was equilibrated with fusion assay buffer, at 3,000 r.p.m. for one minute. These vesicles with NBD-PE located only in the inner leaflets were subject to the lipid mixing assay described above.

4.5.9 Inhibition of Lipid Mixing

SYP41 antibody was purified by affinity chromatography. Before performing the total lipid mixing assay for the combination of reconstituted-SYP41 (acceptor), soluble YKT61, and reconstituted VTI12 (donor), either the SYP41 antibody or the pre-immune serum were incubated with reconstituted-SYP41 vesicles for 30 minutes at room temperature. The same procedure was followed as that described above for the lipid mixing assay.

For the inhibition by the soluble form of VTI12, reconstituted-SYP41 vesicles, YKT61 and VTI12s were mixed and incubated for 30 minutes at room temperature before adding reconstituted-VTI12 vesicles, and then the lipid mixing assay was performed as described above.

4.6 Acknowledgments

We thank Yan Xiong for sequencing the YKT62 splice variants. This work was supported by funds from the Iowa State University Plant Sciences Institute (to D.C.B.) and National Institute of Health (to Y.K.S.).

4.7 References

Bassham, D.C., Sanderfoot, A.A., Kovaleva, V., Zheng, H., and Raikhel, N.V. (2000). AtVPS45 complex formation at the trans-Golgi network. Mol Biol Cell *11*, 2251-2265.

Bock, J.B., Matern, H.T., Peden, A.A., and Scheller, R.H. (2001). A genomic perspective on membrane compartment organization. Nature *409*, 839-841.

Chen, Y., Xu, Y., Zhang, F., and Shin, Y.K. (2004). Constitutive versus regulated SNARE assembly: a structural basis. EMBO J *23*, 681-689.

Dilcher, M., Kohler, B., and von Mollard, G.F. (2001). Genetic interactions with the yeast Q-SNARE VTI1 reveal novel functions for the R-SNARE YKT6. J Biol Chem *276*, 34537-34544.

Eckert, D.M., and Kim, P.S. (2001). Mechanisms of viral membrane fusion and its inhibition. Annu Rev Biochem *70*, 777-810.

Geelen, D., Leyman, B., Batoko, H., Di Sansebastiano, G.P., Moore, I., and Blatt, M.R. (2002). The abscisic acid-related SNARE homolog NtSyr1 contributes to secretion and growth: evidence from competition with its cytosolic domain. Plant Cell *14*, 387-406.

Lauber, M.H., Waizenegger, I., Steinmann, T., Schwarz, H., Mayer, U., Hwang, I., Lukowitz, W., and Jurgens, G. (1997). The Arabidopsis KNOLLE protein is a cytokinesis-specific syntaxin. J Cell Biol *139*, 1485-1493.

Lukowitz, W., Mayer, U., and Jurgens, G. (1996). Cytokinesis in the Arabidopsis embryo involves the syntaxin-related KNOLLE gene product. Cell *84*, 61-71.

Lupashin, V.V., Pokrovskaya, I.D., McNew, J.A., and Waters, M.G. (1997). Characterization of a novel yeast SNARE protein implicated in Golgi retrograde traffic. Mol Biol Cell *8*, 2659-2676.

McIntyre, J.C., and Sleight, R.G. (1991). Fluorescence assay for phospholipid membrane asymmetry. Biochemistry *30*, 11819-11827.

McNew, J.A., Parlati, F., Fukuda, R., Johnston, R.J., Paz, K., Paumet, F., Sollner, T.H., and Rothman, J.E. (2000). Compartmental specificity of cellular membrane fusion encoded in SNARE proteins. Nature *407*, 153-159.

McNew, J.A., Sogaard, M., Lampen, N.M., Machida, S., Ye, R.R., Lacomis, L., Tempst, P., Rothman, J.E., and Sollner, T.H. (1997). Ykt6p, a prenylated SNARE essential for endoplasmic reticulum-Golgi transport. J Biol Chem *272*, 17776-17783.

Parlati, F., Weber, T., McNew, J.A., Westermann, B., Sollner, T.H., and Rothman, J.E. (1999). Rapid and efficient fusion of phospholipid vesicles by the alpha-helical core of a SNARE complex in the absence of an N-terminal regulatory domain. Proc Natl Acad Sci U S A *96*, 12565-12570.

Poirier, M.A., Xiao, W., Macosko, J.C., Chan, C., Shin, Y.K., and Bennett, M.K. (1998). The synaptic SNARE complex is a parallel four-stranded helical bundle. Nat Struct Biol *5*, 765-769.

Sanderfoot, A.A., Assaad, F.F., and Raikhel, N.V. (2000). The Arabidopsis genome. An abundance of soluble N-ethylmaleimide-sensitive factor adaptor protein receptors. Plant Physiol *124*, 1558-1569.

Sanderfoot, A.A., Kovaleva, V., Bassham, D.C., and Raikhel, N.V. (2001a). Interactions between syntaxins identify at least five SNARE complexes within the Golgi/prevacuolar system of the Arabidopsis cell. Mol Biol Cell *12*, 3733-3743.

Sanderfoot, A.A., Pilgrim, M., Adam, L., and Raikhel, N.V. (2001b). Disruption of individual members of Arabidopsis syntaxin gene families indicates each has essential functions. Plant Cell *13*, 659-666.

Sanderfoot, A.A., and Raikhel, N.V. (1999). The specificity of vesicle trafficking: coat proteins and SNAREs. Plant Cell *11*, 629-642.

Skehel, J.J., and Wiley, D.C. (1998). Coiled coils in both intracellular vesicle and viral membrane fusion. Cell *95*, 871-874.

Sollner, T., Whiteheart, S.W., Brunner, M., Erdjument-Bromage, H., Geromanos, S., Tempst, P., and Rothman, J.E. (1993). SNAP receptors implicated in vesicle targeting and fusion. Nature *362*, 318-324.

Struck, D.K., Hoekstra, D., and Pagano, R.E. (1981). Use of resonance energy transfer to monitor membrane fusion. Biochemistry *20*, 4093-4099.

Surpin, M., Zheng, H., Morita, M.T., Saito, C., Avila, E., Blakeslee, J.J., Bandyopadhyay, A., Kovaleva, V., Carter, D., Murphy, A.*, et al.* (2003). The VTI family of SNARE proteins is necessary for plant viability and mediates different protein transport pathways. Plant Cell *15*, 2885-2899.

Sutton, R.B., Fasshauer, D., Jahn, R., and Brunger, A.T. (1998). Crystal structure of a SNARE complex involved in synaptic exocytosis at 2.4 A resolution. Nature *395*, 347-353.

Tai, G., Lu, L., Wang, T.L., Tang, B.L., Goud, B., Johannes, L., and Hong, W. (2004). Participation of the syntaxin 5/Ykt6/GS28/GS15 SNARE complex in transport from the early/recycling endosome to the trans-Golgi network. Mol Biol Cell *15*, 4011-4022.

Uemura, T., Ueda, T., Ohniwa, R.L., Nakano, A., Takeyasu, K., and Sato, M.H. (2004). Systematic analysis of SNARE molecules in Arabidopsis: dissection of the post-Golgi network in plant cells. Cell Struct Funct *29*, 49-65.

Weber, T., Zemelman, B.V., McNew, J.A., Westermann, B., Gmachl, M., Parlati, F., Sollner, T.H., and Rothman, J.E. (1998). SNAREpins: minimal machinery for membrane fusion. Cell *92*, 759-772.

Xiao, W., Poirier, M.A., Bennett, M.K., and Shin, Y.K. (2001). The neuronal t-SNARE complex is a parallel four-helix bundle. Nat Struct Biol *8*, 308-311.

Zhu, J., Gong, Z., Zhang, C., Song, C.P., Damsz, B., Inan, G., Koiwa, H., Zhu, J.K., Hasegawa, P.M., and Bressan, R.A. (2002). OSM1/SYP61: a syntaxin protein in Arabidopsis controls abscisic acid-mediated and non-abscisic acid-mediated responses to abiotic stress. Plant Cell *14*, 3009-3028.

4.8 Figures and Captions

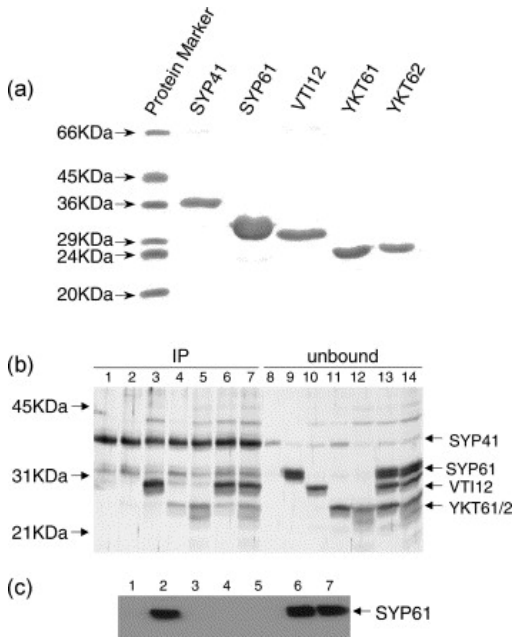

Figure 4-1. YKT61 and YKT62 interact with TGN SNAREs *in vitro*.

(a). Purified proteins were separated by SDS/10%PAGE and stained with Coomassie brilliant blue R-250. The calculated molecular masses for the His_6-tagged SYP41, SYP61, VTI12, YKT61 and YKT62 are 38.3 kDa, 29.9 kDa, 27.2 kDa, 24.7 kDa and 25.1 kDa, respectively.

(b, c). *In vitro* binding assays. Recombinant SNARE proteins were mixed and incubated on ice for one hour to allow binding, followed by immunoprecipitation using immobilized SYP41 antibodies. Precipitating proteins (lanes 1-7) were analyzed by SDS-PAGE and silver staining (b) or immunoblotting using SYP61 antibodies (c). Supernatants after immunoprecipitation are shown in lanes 8–14. Assays contained the following proteins: SYP41 alone (lanes 1 and 8), SYP41+SYP61 (lanes 2 and 9), SYP41+VTI12 (lanes 3 and 10), SYP41+YKT61 (lanes 4 and 11), SYP41+YKT62 (lanes 5 and 12), SYP41+SYP61+VTI12+YKT61 (lanes 6 and 13), SYP41+SYP61+VTI12+YKT62 (lanes 7 and 14).

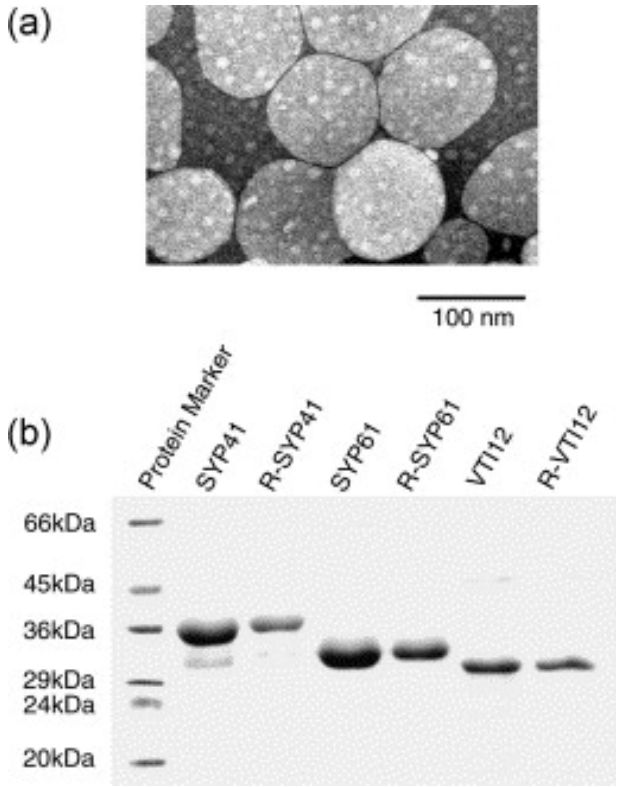

Figure 4-2. Charaterization of reconstituted vesicles.

(a). Negative-staining electron micrograph of protein-reconstituted vesicles.

(b). The efficiency of reconstitution of proteins into liposomes was estimated by SDS-PAGE and staining with Coomassie brilliant blue R-250. The protein bands without the prefix R- were the starting materials in detergent before reconstitution and those with the prefix R- were after the reconstitution. The reconstitution efficiency was calculated from the ratio of the integrated densities of the two bands before and after reconstitution. The reconstitution efficiencies were 40% for SYP41, 55% for SYP61, and 60% for VTI12.

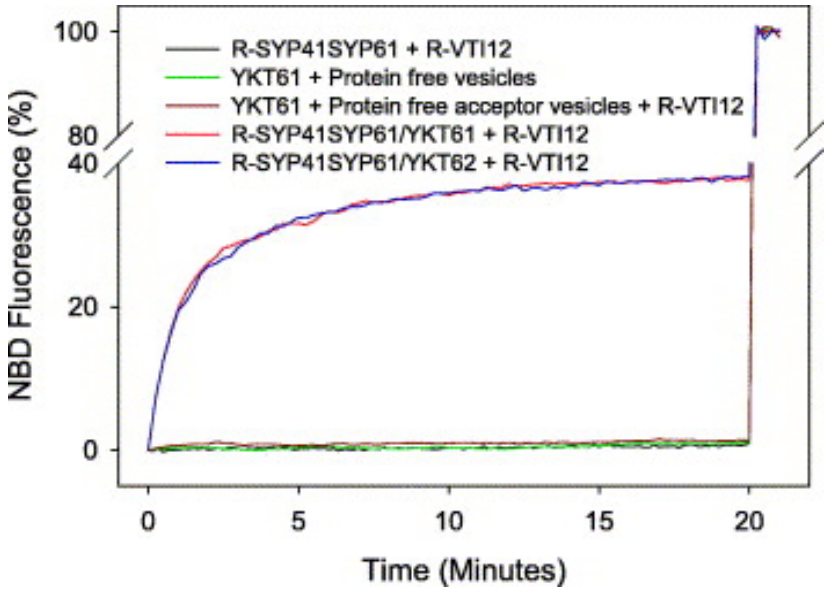

Figure 4-3. SNARE proteins mediate membrane fusion.

Purified SYP41 and SYP61 proteins were co-reconstituted into acceptor vesicles (R-SYP41SYP61), and VTI12 was reconstituted into donor vesicles (R-VTI12). NBD fluorescence was monitored with the excitation wavelength at 460 nm and the emission at 530 nm. The fluorescence intensities were plotted versus time, and normalized against the maximal fluorescence intensity (MFI), which was obtained by adding n-dodecylmaltoside to 0.25% (w/v) (sudden jumps at 20 minutes). Mixing the donor vesicles with acceptor vesicles did not induce fluorescence change (black). However, adding either YKT61 (red) or YKT62 (blue) into the mixture caused a significant increase of the fluorescence signal, indicating that the lipid mixing between donor and acceptor vesicles occurred. When protein-free donor and acceptor vesicles were mixed with YKT61 (green), or when protein-free acceptor vesicles and R-VTI12 vesicles were mixed with YKT61 (dark red), no fluorescence change was observed.

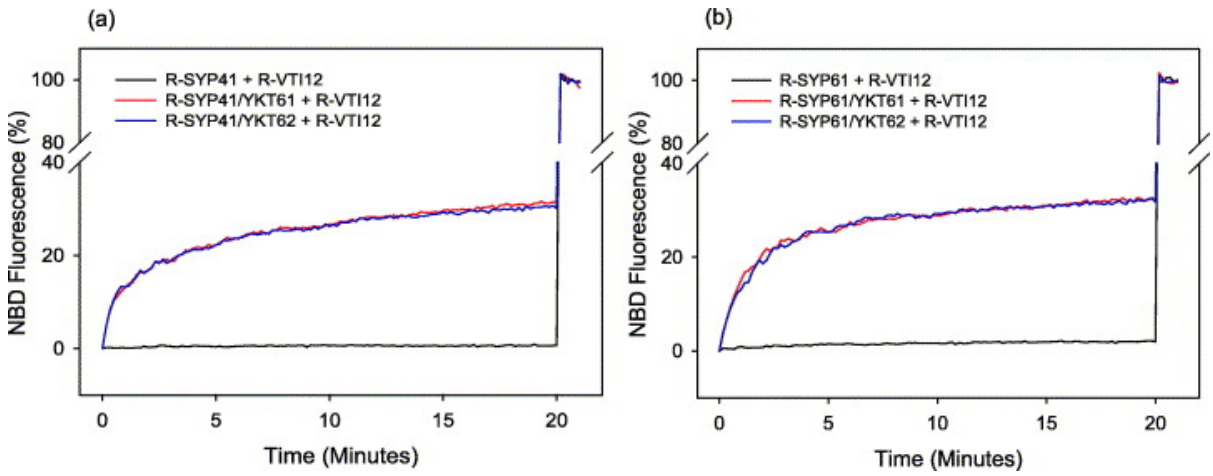

Figure 4-4. SYP41 and SYP61 can function independently.

(a). SYP41 was reconstituted into the acceptor vesicles (R-SYP41), and VTI12 was reconstituted into the donor vesicles (R-VTI12) with fluorescent lipids. When R-SYP41, R-VTI12, and either YKT61 (red trace) or YKT62 (blue trace) were mixed, apparent lipid mixing was observed.

(b). Mixing of the SYP61-reconstituted vesicles (R-SYP61), VTI12-reconstituted vesicles (R-VTI12), and either YKT61 (red trace) or YKT62 (blue trace) induced the increase in fluorescence signal, indicative of lipid mixing.

In both (a) and (b), the black lines are the controls in the absence of YKT61 or YKT62.

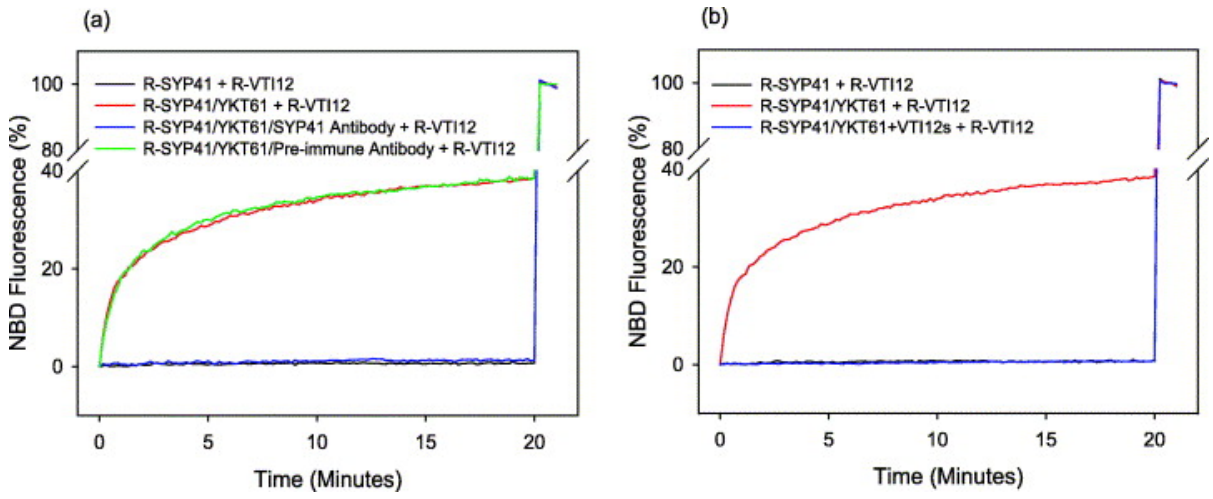

Figure 4-5. SNARE-mediated membrane fusion can be inhibited by SYP41 antibody or a soluble VTI12 fragment.

(a). Inhibition by SYP41 antibody. SYP41-reconstituted vesicles (R-SYP41) were incubated with either SYP41 antibody or pre-immune serum at 25 °C for 30 minutes before adding VTI12-reconstituted donor vesicles (R-VTI12) and YKT61. The fluorescence intensity did not change over time (blue trace) for the SYP41 antibody-treated sample, showing the inhibition of membrane fusion by the antibodies. There was no significant effect on lipid mixing for the pre-immune serum-treated sample (green trace).

(b). Inhibition by soluble VTI12. SYP41-reconstituted vesicles (R-SYP41) were mixed with YKT61 and a soluble VTI12 fragment (VTI12s) for 30 minutes, followed by addition of VTI12-reconstituted donor vesicles (R-VTI12). The fluorescence intensity did not change over time (blue trace), indicating that VTI12s completely inhibited the fusion reaction.

In both (a) and (b), the black trace is the control in the absence of YKT61, and the red trace shows the membrane fusion without adding inhibitors.

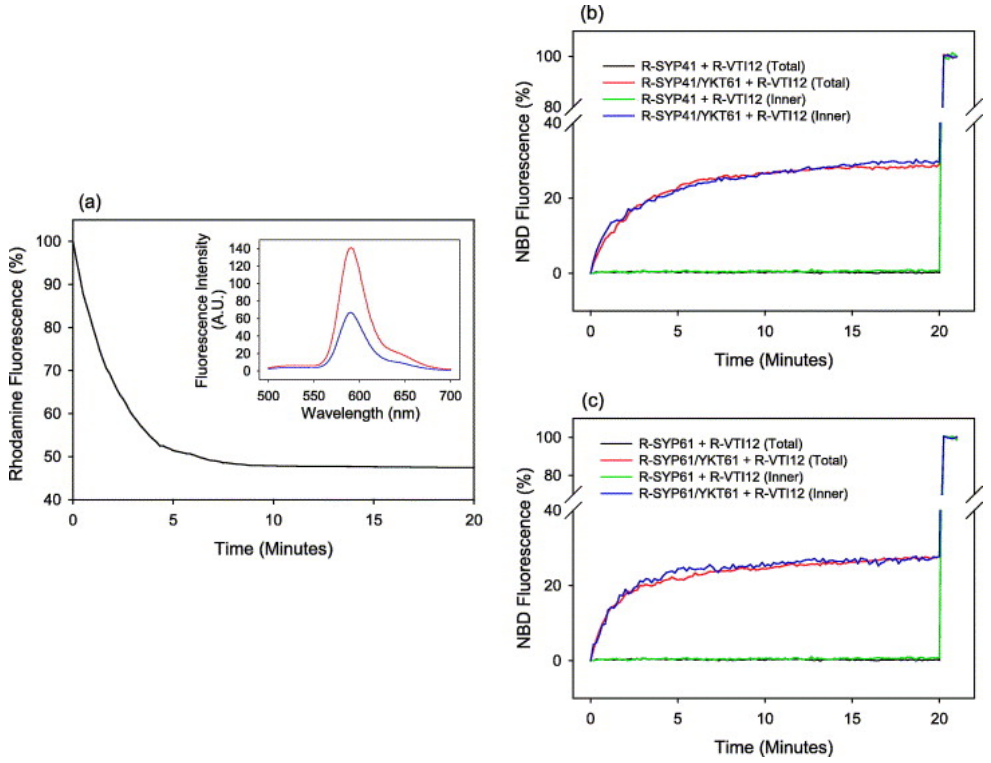

Figure 4-6. SNARE proteins mediate lipid mixing on both halves of the lipid bilayer.

(a). Reduction of NBD-PE by dithionite. The reduction of NBD-PE in donor vesicles by dithionite was measured as a loss of fluorescence resonance energy transfer between NBD and rhodamine (excitation at 460 nm and detection at 590 nm). The trace was normalized with respect to the fluorescent intensity before treatment with dithionite and plotted versus time. The inset shows the fluorescence spectra before (red) and after the dithionite treatment (blue) in arbitrary units.

(b, c). Total and inner leaflet lipid mixing assays. (b) Total lipid mixing (when R-SYP41, R-VTI12, and YKT61 were mixed, red trace) was compared with the inner leaflet mixing (when R-SYP41, dithionite-treated R-VTI12, and YKT61 were mixed, blue trace). The time traces of the fluorescence change were normalized with respect to corresponding MFIs, which were 15.2 and 7.1 on an arbitrary scale for the total and the inner leaflet lipid mixing assays, respectively. The black and green traces are the controls without YKT61 for total and inner leaflet mixing assays, respectively. (c) As for (b), except R-SYP61 was used instead of SYP41.

CHAPTER 5: CONCLUSIONS AND FUTURE WORKS

5.1 Conclusions

SNARE proteins are central players for intracellular fusion reactions. They are involved in all steps of the secretory and endocytic pathways in eukaryotes. The v-SNARE engages with the t-SNARE to form a coiled coil that bridges two membranes (Antonin et al., 2002; Hanson et al., 1997; Katz et al., 1998; Lin and Scheller, 1997; Poirier et al., 1998; Sutton et al., 1998), facilitating the fusion (McNew et al., 2000; Weber et al., 1998).

In synaptic membrane fusion, synaptobrevin-2 forms a SNARE complex with syntaxin-1A and SNAP-25. The core of the SNARE complex is so tight that it is resistant to SDS. SDS-PAGE analysis shows that SNARE complexes are able to form multimers (Otto et al., 1997). With EPR spectroscopy, we are able to show that one possible mechanism for SNARE complex oligomerization is by domain swapping of SNAP-25. It is thought that several SNARE complexes form a ring-like structure at the onset of membrane fusion (Hua and Scheller, 2001; Rickman et al., 2005; Tokumaru et al., 2001). The domain swapping mechanism may help the formation of this ring-like structure and facilitate the fusion.

In yeast, membrane fusion involved in Golgi-to-plasma membrane trafficking is constitutive, in contrast to synaptic membrane fusion which is tightly regulated. Previous EPR results suggested that the membrane proximal region of synaptobrevin, the neuronal

counterpart of v-SNARE Snc2p, is sequestered in the membrane and may regulate formation of the SNARE core complex (Kweon et al., 2003). To investigate the structural basis for the differences between neuronal and yeast SNAREs, we determined the structure and the membrane topology of Snc2p using SDSL EPR. We prepared 20 consecutive spin-labeled mutants (G76C-L95C), covering a part of the coiled coil motif and the linker region between the coiled coil and the transmembrane domain. The immersion depths of residues 84-91, measured with EPR, fit well with α-helical geometry at an angle of 40° with respect to the membrane normal. Although the overall structure of Snc2p is very similar to that of synaptobrevin, the immersion depths of two tryptophan residues in Snc2p are shallower than the corresponding tryptophan residues in synaptobrevin, making entire parts of the SNARE motif exposed and available for SNARE assembly. The results suggest that the membrane topology adopted by v-SNARE might be a factor that determines whether a specific membrane fusion is constitutive or regulated.

In plants (Arabidopsis), it has been previously shown that the neuronal syntaxin-like t-SNARE SYP41 resides in the *trans*-Golgi network (TGN) and interacts with two other SNAREs, VTI12 and SYP61 (Bassham et al., 2000; Sanderfoot et al., 2001). To test whether these SNARE protein interactions are enough to trigger a fusion, we utilized the *in vitro* fluorescent lipid mixing assay. The results suggest that YKT61 (or YKT62) can interact with these SNAREs to form a SNARE complex that promotes membrane fusion; and SYP41 and SYP61 might act independently with VTI12 and YKT61 (or YKT62).

5.2 Future works

5.2.1 SNAREs Involved in Mast Cell Degranulation

A typical character of mast cells is the preformed secretory granules in the cytoplasm. They store histamine and serotonin in the granules, as well as a variety of proteases that become active only on their release. After activation through the high affinity IgE receptor (FcεRI), the granules undergo massive exocytosis and release their contents, causing many of the symptoms associated with acute and chronic allergic diseases (Blank and Rivera, 2004; Wedemeyer et al., 2000). The degranulation process is mediated by SNARE proteins, including synaptobrevin-2, syntaxin-4A and SNAP-23 (Guo et al., 1998; Paumet et al., 2000; Puri and Roche, 2006). Syntaxin-4A and SNAP-23 have been subcloned and expressed in *E. coli*. The preliminary data suggested that synaptobrevin-2, syntaxin-4A and SNAP-23 are able to induce membrane fusion *in vitro*. Further structure study and function analysis will be performed using spin-labeling EPR and a fluorescent liposome fusion assay.

5.2.2 Effects of Complexin, Synaptotagmin and Ca^{2+}

The synaptic membrane fusion is tightly regulated and is triggered by Ca^{2+}. The study of SNARE proteins and membrane fusion is moving towards the examination of such regulation factors, for example, as complexin and synaptotagmin. Complexins are ~20 kD proteins associated with the SNARE complexes mediating exocytosis at neuronal synapses

(Ishizuka et al., 1995; McMahon et al., 1995; Takahashi et al., 1995). The human genome encodes four complexins that are broadly expressed in neuronal and neuroendocrine cells. Complexin I and II are soluble proteins; complexin III and IV are membrane-anchored by C-terminal prenylation (Reim et al., 2005). Complexins can bind to the four-helix bundle SNARE complex in a 1:1 fashion, indicating the regulatory function (Chen et al., 2002). There are 13 synaptogagmins encoded in human genome (Sudhof, 2002). Synaptotagmin contains an N-terminal transmembrane domain, a variable linker, and most importantly, two C-terminal Ca^{2+} binding domains, C2A and C2B. Among them, synaptotagmin 1 and 2 were thought to function as the Ca^{2+} sensor in neurotransmitter release (Fernandez-Chacon et al., 2001; Koh and Bellen, 2003; Tucker et al., 2004). Recent studies have shown that complexin and synaptotagmin 1 regulate liposome fusion with Ca^{2+} by interacting with SNARE proteins (Giraudo et al., 2006; Lu et al., 2006; Schaub et al., 2006; Tang et al., 2006). Previous studies suggested that synaptotagmin 1 is expressed in mast cells and regulates mast cell function (Baram et al., 1999; Baram et al., 1998; Kimura et al., 2001). The role of complexins and synaptoagmins will be tested using recombinant SNAREs participating in mast cell degranulation.

5.2.3 Single Molecular Fusion Assay

The current fluorescent lipid mixing assay is a very powerful technique to analyze SNARE-mediated membrane fusion. It leads to identification of the core fusion machinery

(Weber et al., 1998), discovery of the hemifusion intermediate (Lu et al., 2005; Xu et al., 2005), and characterization of the regulators for SNARE proteins (Bhalla et al., 2006; Lu et al., 2006; Tucker et al., 2004). However, this ensemble analysis has its limitations especially on the characterization of fusion intermediates, which are transient and not synchronized. A new generation of fusion assay based on the total internal reflection fluorescence (TIRF) microscopy has been developed and makes it possible to track a single fusion event along the time (Bowen et al., 2004; Fix et al., 2004; Liu et al., 2005; Melikyan et al., 2005; Yoon, 2006). With this new technique, we expect to elucidate the fusion intermediates and mechanism among different SNARE proteins and their regulators.

5.3 References

Antonin, W., Fasshauer, D., Becker, S., Jahn, R., and Schneider, T.R. (2002). Crystal structure of the endosomal SNARE complex reveals common structural principles of all SNAREs. Nat Struct Biol *9*, 107-111.

Baram, D., Adachi, R., Medalia, O., Tuvim, M., Dickey, B.F., Mekori, Y.A., and Sagi-Eisenberg, R. (1999). Synaptotagmin II negatively regulates Ca2+-triggered exocytosis of lysosomes in mast cells. J Exp Med *189*, 1649-1658.

Baram, D., Linial, M., Mekori, Y.A., and Sagi-Eisenberg, R. (1998). Ca2+-dependent exocytosis in mast cells is stimulated by the Ca2+ sensor, synaptotagmin I. J Immunol

161, 5120-5123.

Bassham, D.C., Sanderfoot, A.A., Kovaleva, V., Zheng, H., and Raikhel, N.V. (2000). AtVPS45 complex formation at the trans-Golgi network. Mol Biol Cell *11*, 2251-2265.

Bhalla, A., Chicka, M.C., Tucker, W.C., and Chapman, E.R. (2006). Ca(2+)-synaptotagmin directly regulates t-SNARE function during reconstituted membrane fusion. Nature structural & molecular biology *13*, 323-330.

Blank, U., and Rivera, J. (2004). The ins and outs of IgE-dependent mast-cell exocytosis. Trends in immunology *25*, 266-273.

Bowen, M.E., Weninger, K., Brunger, A.T., and Chu, S. (2004). Single molecule observation of liposome-bilayer fusion thermally induced by soluble N-ethyl maleimide sensitive-factor attachment protein receptors (SNAREs). Biophysical journal *87*, 3569-3584.

Chen, X., Tomchick, D.R., Kovrigin, E., Arac, D., Machius, M., Sudhof, T.C., and Rizo, J. (2002). Three-dimensional structure of the complexin/SNARE complex. Neuron *33*, 397-409.

Fernandez-Chacon, R., Konigstorfer, A., Gerber, S.H., Garcia, J., Matos, M.F., Stevens, C.F., Brose, N., Rizo, J., Rosenmund, C., and Sudhof, T.C. (2001). Synaptotagmin I functions as a calcium regulator of release probability. Nature *410*, 41-49.

Fix, M., Melia, T.J., Jaiswal, J.K., Rappoport, J.Z., You, D., Sollner, T.H., Rothman, J.E., and

Simon, S.M. (2004). Imaging single membrane fusion events mediated by SNARE proteins. Proceedings of the National Academy of Sciences of the United States of America *101*, 7311-7316.

Giraudo, C.G., Eng, W.S., Melia, T.J., and Rothman, J.E. (2006). A clamping mechanism involved in SNARE-dependent exocytosis. Science *313*, 676-680.

Guo, Z., Turner, C., and Castle, D. (1998). Relocation of the t-SNARE SNAP-23 from lamellipodia-like cell surface projections regulates compound exocytosis in mast cells. Cell *94*, 537-548.

Hanson, P.I., Roth, R., Morisaki, H., Jahn, R., and Heuser, J.E. (1997). Structure and conformational changes in NSF and its membrane receptor complexes visualized by quick-freeze/deep-etch electron microscopy. Cell *90*, 523-535.

Hua, Y., and Scheller, R.H. (2001). Three SNARE complexes cooperate to mediate membrane fusion. Proc Natl Acad Sci U S A *98*, 8065-8070.

Ishizuka, T., Saisu, H., Odani, S., and Abe, T. (1995). Synaphin: a protein associated with the docking/fusion complex in presynaptic terminals. Biochemical and biophysical research communications *213*, 1107-1114.

Katz, L., Hanson, P.I., Heuser, J.E., and Brennwald, P. (1998). Genetic and morphological analyses reveal a critical interaction between the C-termini of two SNARE proteins and a parallel four helical arrangement for the exocytic SNARE complex. The EMBO journal *17*, 6200-6209.

Kimura, N., Shiraishi, S., Mizunashi, K., Ohtsu, H., and Kimura, I. (2001). Synaptotagmin I expression in mast cells of normal human tissues, systemic mast cell disease, and a human mast cell leukemia cell line. J Histochem Cytochem *49*, 341-346.

Koh, T.W., and Bellen, H.J. (2003). Synaptotagmin I, a Ca2+ sensor for neurotransmitter release. Trends in neurosciences *26*, 413-422.

Kweon, D.H., Kim, C.S., and Shin, Y.K. (2003). Regulation of neuronal SNARE assembly by the membrane. Nature structural biology *10*, 440-447.

Lin, R.C., and Scheller, R.H. (1997). Structural organization of the synaptic exocytosis core complex. Neuron *19*, 1087-1094.

Liu, T., Tucker, W.C., Bhalla, A., Chapman, E.R., and Weisshaar, J.C. (2005). SNARE-driven, 25-millisecond vesicle fusion in vitro. Biophysical journal *89*, 2458-2472.

Lu, X., Xu, Y., Zhang, F., and Shin, Y.K. (2006). Synaptotagmin I and Ca(2+) promote half fusion more than full fusion in SNARE-mediated bilayer fusion. FEBS letters *580*, 2238-2246.

Lu, X., Zhang, F., McNew, J.A., and Shin, Y.K. (2005). Membrane fusion induced by neuronal SNAREs transits through hemifusion. J Biol Chem *280*, 30538-30541.

McMahon, H.T., Missler, M., Li, C., and Sudhof, T.C. (1995). Complexins: cytosolic proteins that regulate SNAP receptor function. Cell *83*, 111-119.

McNew, J.A., Parlati, F., Fukuda, R., Johnston, R.J., Paz, K., Paumet, F., Sollner, T.H., and Rothman, J.E. (2000). Compartmental specificity of cellular membrane fusion

encoded in SNARE proteins. Nature *407*, 153-159.

Melikyan, G.B., Barnard, R.J., Abrahamyan, L.G., Mothes, W., and Young, J.A. (2005). Imaging individual retroviral fusion events: from hemifusion to pore formation and growth. Proc Natl Acad Sci U S A *102*, 8728-8733.

Otto, H., Hanson, P.I., and Jahn, R. (1997). Assembly and disassembly of a ternary complex of synaptobrevin, syntaxin, and SNAP-25 in the membrane of synaptic vesicles. Proc Natl Acad Sci U S A *94*, 6197-6201.

Paumet, F., Le Mao, J., Martin, S., Galli, T., David, B., Blank, U., and Roa, M. (2000). Soluble NSF attachment protein receptors (SNAREs) in RBL-2H3 mast cells: functional role of syntaxin 4 in exocytosis and identification of a vesicle-associated membrane protein 8-containing secretory compartment. J Immunol *164*, 5850-5857.

Poirier, M.A., Xiao, W., Macosko, J.C., Chan, C., Shin, Y.K., and Bennett, M.K. (1998). The synaptic SNARE complex is a parallel four-stranded helical bundle. Nature structural biology *5*, 765-769.

Puri, N., and Roche, P.A. (2006). Ternary SNARE Complexes Are Enriched in Lipid Rafts during Mast Cell Exocytosis. Traffic *7*, 1482-1494.

Reim, K., Wegmeyer, H., Brandstatter, J.H., Xue, M., Rosenmund, C., Dresbach, T., Hofmann, K., and Brose, N. (2005). Structurally and functionally unique complexins at retinal ribbon synapses. J Cell Biol *169*, 669-680.

Rickman, C., Hu, K., Carroll, J., and Davletov, B. (2005). Self-assembly of SNARE fusion

proteins into star-shaped oligomers. The Biochemical journal *388*, 75-79.

Sanderfoot, A.A., Kovaleva, V., Bassham, D.C., and Raikhel, N.V. (2001). Interactions between syntaxins identify at least five SNARE complexes within the Golgi/prevacuolar system of the Arabidopsis cell. Mol Biol Cell *12*, 3733-3743.

Schaub, J.R., Lu, X., Doneske, B., Shin, Y.K., and McNew, J.A. (2006). Hemifusion arrest by complexin is relieved by Ca2+-synaptotagmin I. Nature structural & molecular biology *13*, 748-750.

Sudhof, T.C. (2002). Synaptotagmins: why so many? J Biol Chem *277*, 7629-7632.

Sutton, R.B., Fasshauer, D., Jahn, R., and Brunger, A.T. (1998). Crystal structure of a SNARE complex involved in synaptic exocytosis at 2.4 A resolution. Nature *395*, 347-353.

Takahashi, S., Yamamoto, H., Matsuda, Z., Ogawa, M., Yagyu, K., Taniguchi, T., Miyata, T., Kaba, H., Higuchi, T., Okutani, F.*, et al.* (1995). Identification of two highly homologous presynaptic proteins distinctly localized at the dendritic and somatic synapses. FEBS letters *368*, 455-460.

Tang, J., Maximov, A., Shin, O.H., Dai, H., Rizo, J., and Sudhof, T.C. (2006). A complexin/synaptotagmin 1 switch controls fast synaptic vesicle exocytosis. Cell *126*, 1175-1187.

Tokumaru, H., Umayahara, K., Pellegrini, L.L., Ishizuka, T., Saisu, H., Betz, H., Augustine, G.J., and Abe, T. (2001). SNARE complex oligomerization by synaphin/complexin is

essential for synaptic vesicle exocytosis. Cell *104*, 421-432.

Tucker, W.C., Weber, T., and Chapman, E.R. (2004). Reconstitution of Ca2+-regulated membrane fusion by synaptotagmin and SNAREs. Science *304*, 435-438.

Weber, T., Zemelman, B.V., McNew, J.A., Westermann, B., Gmachl, M., Parlati, F., Sollner, T.H., and Rothman, J.E. (1998). SNAREpins: minimal machinery for membrane fusion. Cell *92*, 759-772.

Wedemeyer, J., Tsai, M., and Galli, S.J. (2000). Roles of mast cells and basophils in innate and acquired immunity. Current opinion in immunology *12*, 624-631.

Xu, Y., Zhang, F., Su, Z., McNew, J.A., and Shin, Y.K. (2005). Hemifusion in SNARE-mediated membrane fusion. Nature structural & molecular biology *12*, 417-422.

Yoon, T.Y., Okumus, B., Zhang, F., Shin, Y.K., Ha, T. (2006). Multiple intermediates in single SNARE-induced membrane fusion. Proceedings of the National Academy of Sciences of the United States of America, In press.

ACKNOWLEDGEMENTS

I would like to take this opportunity to express my thanks to those who helped me with various aspects of conducting research and the writing of this thesis. First and foremost, Dr. Yeon-Kyun Shin for his guidance, patience and support throughout my research and the thesis writing. His insights and words of encouragement have often inspired me and renewed my hopes for completing my graduate education. I would also like to thank my committee members for their efforts and contributions to this work: Dr. Herbert Fromm, Dr. Richard Honzatko, Dr. Amy Andreotti and Dr. Diane Bassham.

I also want to thank the research team in Dr. Shin's lab: Dr. Chang Sup Kim, Dr. Dae-Hyuk Kweon, Dr. Soo-Min Lee, Dr. Fan Zhang, Yinghui Zhang, Yibin Xu, Zengliu Su, Jiansong Tong, Xiaobing Lu, Bin Lu, for their help during my research in Iowa State University.

Most importantly, I want to thank my family, my mother, Wentuan Yu, and my wife, Wuyan Zhang, for their unwavering encouragement and complete support throughout my education. My success is theirs and they deserve my sincerest gratitude.